

**DIRECTED ORTHO METALATION – BORONATION
SUZUKI-MIYaura CROSS COUPLING LEADING TO
SYNTHESIS OF AZAFLUORENOL CORE LIQUID
CRYSTALS**

by

Ping-Shan Lai

A thesis submitted to the Department of Chemistry
in conformity with the requirement for
the degree of Master of Science

Queen's University
Kingston, Ontario, Canada

July, 2007

Copyright © Ping-Shan (Sunny) Lai, 2007

ABSTRACT

The synthesis of chiral fluorenol crystal materials employing directed ortho metalation (*DoM*) combined with directed remote metalation (*DreM*) and Suzuki-Miyaura Coupling was previously reported by McCubbin, Snieckus and Lemieux.ref? This study reported that certain fluorenol derivatives form a chiral smectic C phase (SmC^*) with a spontaneous polarization (P_s) that is amplified by intermolecular hydrogen bonding. Dilution and deuterium exchange experiments suggest that antiparallel hydrogen bonded dimer formation increases the rotational bias about the director that is thought to induce the P_s .needs definition The research reported in this thesis is concerned with an investigation on the effects of hydrogen bonds on the P_s of the liquid crystal by the variation of core structure, particularly the substitution of one aryl ring to pyridinyl ring.

An efficient synthesis of liquid crystals (LC) **1.14** and **2.22** by Directed *ortho* Metalation-boronation, Suzuki-Miyaura Cross Coupling reaction accompanied with Directed remote metalation was achieved. Compound **1.14** was found to be not useful as a LC material because it was unstable in the air and underwent rapid oxidation to give **2.22** upon heating. Thus, this project was focused on the preliminary study on mesophase characterization of **1.14** and **2.22**. The results (**Table 2.3**) show both **1.14** and **2.22** formed SmC phases, but only **1.14** showed smectic A (SmA) mesophase and only **2.22** showed nematic (N) mesophase cooling from isotropic liquid phase. The increase in temperature range of smectic phases for the azafluorenol **1.14** is expected because intermolecular hydrogen bonding between the hydroxyl group and aza group as shown by **Figure 1.21** may play a role to stabilize the formation of smectic (Sm) phase.

ACKNOWLEDGEMENTS

I would like to take this opportunity to show my gratitude to my supervisors, teachers, friends Victor Snieckus and Bob Lemieux. Both of them have been extremely kind and patient. To Bob, I want to say thank you for all your supports over the last three years and your care for leading me to the entrée of field of the liquid crystals. To Vic, I am really honored to have you as my teacher from my fourth year of undergraduate and subsequently a critical but helpful supervisor in my master program. You are always pushing me to the limit and the best I can be as a chemist, and I can say I've grown to be ready for the next stage of my life from your ever lasting energy to guide me. Thank you both, I will always remember you.

I am also grateful to all members of the Snieckus and Lemieux groups, past and present, for helpful advice and for making my time in both groups enjoyable. Special thanks to Wei Gan, Yigang Zhao, Ying Xin Liu, Li Li, Jian Xin Wang and Zhong Dong Zhao providing an additional friendship outside of the laboratory works. I like to thank Adam McCubbin, even though he is long gone before I started, always point me several tips in making reactions more successful. To my recent roommate, Syed Hussain, I like to thank him for his funny company. I also like to thank Dan Wang for her extra care for me over the last month when I faced some difficulties in completing my thesis.

Finally and most importantly, I would like to thank my parents to indulge me for letting me make the choice of my life – pursue my passion in organic chemistry and to support me throughout the years I returned to Queen's from another discipline quite different from organic chemistry.

STATEMENT OF CO-AUTHORSHIP AND ORIGINALITY

The work presented in this thesis was conducted by the author under the supervision of Professor R. P. Lemieux and Professor V. Snieckus in the Department of Chemistry at Queen's University. The mesophases formed by compounds **2.22** and **1.14** were characterized by polarized microscopy and differential scanning calorimetry.

The following is a list of new compounds prepared using new methodology in the course of this work: **1.14, 2.9, 2.11, 2.12, 2.13, 2.18, 2.19, 2.20, 2.22, 2.23, 2.24**.

The following is a list of known compounds prepared using new methodology or existing methods in the course of this work: **2.3, 2.4, 2.5, 2.6, 2.21**.

TABLE OF CONTENTS

ABSTRACT.....	ii
STATEMENT OF CO-AUTHORSHIP AND ORIGINALITY	iv
TABLE OF CONTENTS.....	v
CHAPTER 1 – INTRODUCTION	1
1.1. Liquid Crystals.....	1
1.1.1. Liquid Crystal Phases and Their Properties.....	1
1.1.2. Chiral Liquid Crystals.....	7
1.1.3. Hydrogen Bonding in Calamitic Liquid Crystal Phases.....	13
1.1.4. Liquid Crystals Containing Fluorenone Core Structures.....	15
1.1.5. Mesogen Design Considerations and Outline of Research.....	18
1.2. Synthetic Methodology	19
1.2.1. The Directed ortho Metalation (DoM) Reaction	19
1.2.1.1. The Mechanism of the DoM Reaction.....	22
1.2.2. The DoM Boronation Suzuki-Miyaura Cross Coupling Reaction.....	36
1.2.2.1. Mechanism of Suzuki-Miyaura Cross Coupling Reaction	36
1.2.2.2. Practical Aspects of the DoM – Suzuki Cross Coupling Reaction: Characterization of boronic acids, Catalyst / Ligands, Bases and Solvents	41
1.2.3. The Directed Remote Metalation (DreM) Reaction	48
1.2.4. The Synthesis of Azafluorenones	57
1.2.4.1. Radical Approaches	59
1.2.4.2. Indanone Approaches	61
1.2.4.3. Friedel Craft and Anionic Friedel Crafts Approaches	66
CHAPTER 2 – THE SYNTHESIS AND CHARACTERIZATION OF A NEW AZAFLUORENONE AND AZAFLUORENOL LIQUID CRYSTALS.....	68
2.1. Synthesis of Azafluorenone Enantiomers.....	68
2.2. Mesophase Characterization of 2.22 and 1.14	77
CHAPTER 3 SUMMARY AND CONCLUSIONS.....	80
3.1. Summary	80
3.2. Conclusions and Future Work	81
CHAPTER 4 EXPERIMENTAL SECTION.....	82

4.1. General Methods.....	82
4.2. Materials	83
4.3 Experimental Procedures	83
REFERENCES	93
APPENDICES	103
Appendix 1. ¹ H NMR for 2.9, 2.11, 2.13, 2.18, 2.19, 2.20, 2.22, 1.14	103
Appendix 2. HPLC Traces of 2.23	113

List of Figures

Figure 1.1. Structural representation of calamitic, discotic and polycatenar mesogens.	3
Figure 1.2. Characterization of three LC mesophases.	3
Figure 1.3. Schlieren texture of nematic LC	4
Figure 1.4. Photomicrographs of typical (a) SmA and (b) SmC textures.....	5
Figure 1.5. Representation of the McMillan model.....	5
Figure 1.6. Representation of the Wulff model.	6
Figure 1.7. Representation of the Durand model.....	7
Figure 1.8. Schematic representation of the SmC* phase without surface alignment and as a surfaces-stabilized FLC.	8
Figure 1.9. Zigzag binding site according to Boulder model.....	9
Figure 1.10. Conformational analysis of a (S)-2-octyloxy side chain and prediction of the resulting sign of PS. A side-on view along the polar axis is shown on the right. An end-on view is shown as a Newmann projection along the C2-C3 bond axis of the 2- octyloxy side-chain on the left.....	10
Figure 1.11. Rotation of the core of 1.3 about the two ester CO bonds in the zig-zag conformation.....	11
Figure 1.12. Liquid crystal host structures and phase transition temperatures in °C.....	12
Figure 1.13. Model for chirality transfer via core-core interactions.....	13
Figure 1.14. Chiral distortion of the SmC binding site.....	13
Figure 1.15. Two modes of hydrogen in liquid crystals: (a) head-to head and (b)lateral modes.....	14
Figure 1.16. First studies of Fluorene and fluorenone LCs.	15
Figure 1.17. Symmetrical Mesomorphic 2,7-dialkylfluorenone and mesomorphism (R = C ₁₀ H ₂₁).	15
Figure 1.18. Type I ferroelectric fluorene and fluorenone LC.....	16
Figure 1.19. Fluorenone and Type II ferroelectric fluorenol LC.....	17
Figure 1.20. (R)-3 dimer formed by the hydrogen bonds.	18
Figure 1.21. Proposed network of azafluorenol mesogens.....	19
Figure 1.23. Proposed Free energy diagram of the benzylic lithiation of urea 1.32	27
Figure 1.24. Naturally occurring 4-azafluorenones.	58

Figure 2.1. Photomicrograph of 2.22 in the N phase at 160 °C	78
Figure 2.2. Photomicrograph of 2.22 in the SmC phase at 159 °C	79
Figure 2.3. Photomicrograph of 1.14 in the SmA phase at 178 °C	79
Figure 2.4. Photomicrograph of 1.14 in the SmC phase at 141 °C	80
Figure 2.5. Differential Scanning Calorimetry of 2.22	80

Abbreviations

δ	chemical shift
η	rotational viscosity
θ	tilt angle
δ_p	polarization power
τ_r	ferroelectric switching time
9-BBN	9-borabicyclo[3.3.1]nonane
Ac	acetyl
Ar	aryl
bipy	2,2'-bipyridine
Bu	butyl
CIPE	complex induced proximity effect
CSP	chiral stationary phase
d	doublet
DCC	1,3-dicyclohexylcarbodiimide
de	diastereomeric excess
DIAD	diisopropylazodicarboxylate
DIPA	<i>N,N</i>-diisopropylamine
DMAP	<i>N,N</i>-4-dimethylaminopyridine
DME	dimethoxyethane
DMF	<i>N,N</i>-dimethylformamide
DMG	directed metalation group
DOBAMBC	decyloxybenzylidene <i>p</i>'-amino 2-chlorophenyl cinnamate

DoM	directed <i>ortho</i> metalation
DreM	directed remote metalation
DSC	differential scanning calorimetry
E	electric field
E⁺	electrophile
EDG	electron donating group
ee	enantiomeric excess
EI	electron impact
Et	ethyl
EWG	electron withdrawing group
FLC	ferroelectric liquid crystal
FT	Fourier transform
GC	gas chromatography
HMPA	hexamethylphosphoramide
HRMS	high resolution mass spectrum
Hz	Hertz
I	isotropic liquid
<i>i</i>-Pr	Isopropyl
IR	Infrared
KEM	kinetically enhanced metalation
KIE	kinetic isotope effect
L	ligand
LC	liquid crystal

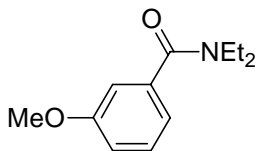
LCD	liquid crystal display
LDA	lithium diisopropylamide
LG	leaving group
LRMS	Low resolution mass spectrometry
LUMO	lowest unoccupied molecular orbital
m	multiplet
<i>m</i>CPBA	meta-chloroperbenzoic acid
Me	methyl
mmol	millimole
MOM	methoxymethyl
MS	mass spectrum
Ms	methanesulfonyl
mw	microwaves
N	nematic phase
n	director
NMR	nuclear magnetic resonance
NR	no reaction
P₀	reduced polarization
PCC	pyridiniumchlorochromate
PG	protecting group
Ph	phenyl
PPA	polyphosphoric acid
P_s	spontaneous polarization

s	singlet
SmA	smectic A phase
SmC	smectic C phase
SmC*	chiral smectic phase
SmX	unidentified smectic phase
SSFLC	surface stabilized ferroelectric liquid crystal
t	triplet
TBAF	tetrabutylammonium fluoride
TBS	tert-butyldimethylsilyl
T_c	critical temperature
TFAA	Trifluoroacetic anhydride
THF	tetrahydrofuran
TMEDA	<i>N,N,N',N'</i>-tetramethylethylenediamine
TMS	trimethylsilyl
X_{FLL}	fluorenol mole fraction
z	layer normal

List of Experimental Procedures

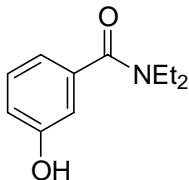
***N,N*-diethyl-3-methoxybenzamide (2.3).**

83



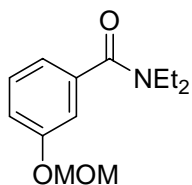
***N,N*-Diethyl-3-hydroxybenzamide (2.4).**

83



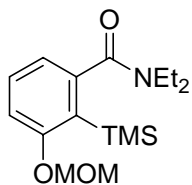
***N,N*-Diethyl-3-methoxymethoxybenzamide (2.5)**

84



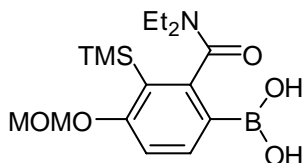
***N,N*-Diethyl-3-methoxymethoxy-2-trimethylsilylbenzamide (2.6)**

84



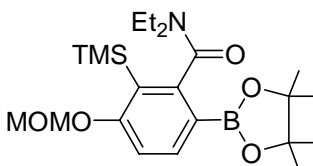
2-(*N,N*-Diethylcarboxamido)-4-methoxymethoxy-3-trimethylsilylphenyl boronic acid

85



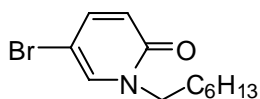
2-(*N,N*-Diethylcarbamoyl)-4-methoxymethoxy-3-trimethylsilylphenyl boronic acid pinacol ester (2.9)

86



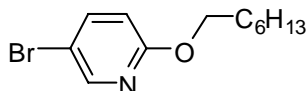
5-bromo-1-heptylpyridin-2(1H)-one (2.12)

86



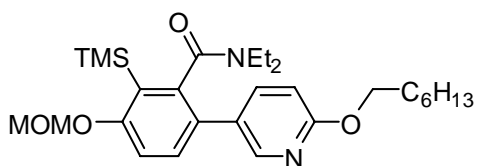
5-Bromo-2-heptyloxy pyridine (2.11)

87



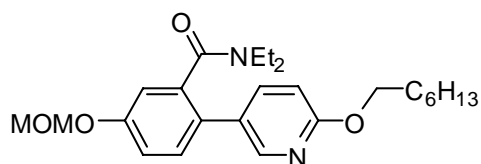
N,N-diethyl-6-(6-(heptyloxy)pyridin-3-yl)-3-(methoxymethoxy)-2-(trimethylsilyl)benzamide (2.13)

87



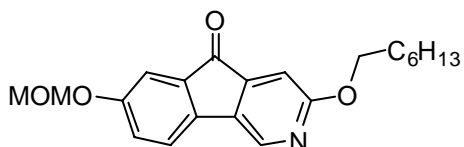
N,N-diethyl-2-(6-(heptyloxy)pyridin-3-yl)-5-(methoxymethoxy)-benzamide (2.18)

88



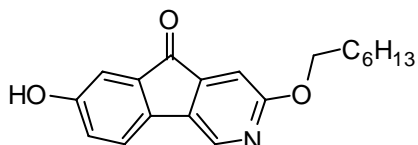
7-Methoxymethoxy-2-(2-octyloxy)-3-azafluoren-9-one (2.19)

89



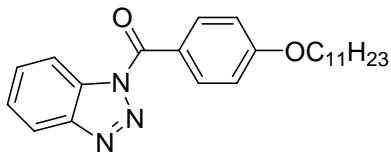
3-(Heptyloxy)-7-hydroxy-5H-indeno[1,2-c]pyridin-5-one (2.20)

90



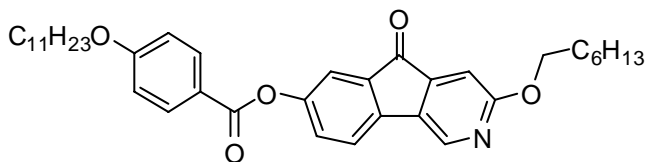
1-(4-Undecyloxybenzoyl)benzotriazole (2.21).

90



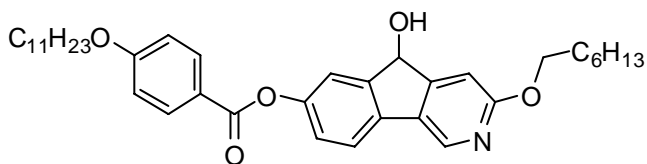
7-(Heptyloxy)-2-((undecyloxybenzoyl)oxy)-6-azafluoren-9-one (2.22)

91



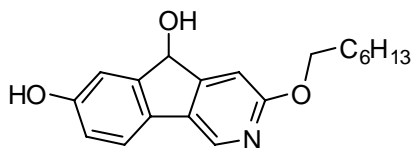
7-(Heptyloxy)-2-((undecyloxybenzoyl)oxy)-3-azafluoren-9-ol (1.14)

92



2-Hydroxy-7-(heptoxy)-3-azafluoren-9-ol (2.23).

92



CHAPTER 1 – INTRODUCTION

1.1. Liquid Crystals

1.1.1. Liquid Crystal Phases and Their Properties

Matter that we commonly perceive fall into three general categories – gas, liquid and solid. In the gas phase, the constituent atoms or molecules move freely, with no forces keeping them together or pushing them apart. Unconstrained gases do not take up a fixed volume; they flow from one point to the next, and do not return to their former configuration after deformation. Like gases, liquids can also flow but are fixed into a specific shape in a container. In contrast, solids do not fit to the volume of the container but tend to retain their volumes and shapes.¹ However, there are substances that do not belong to any of these categories, and early investigators began to question the possibility of finding fourth or even fifth states of matters.

In late 19th century, the Austrian botanist Friedrich Reinitzer² observed two melting points in samples of cholesteryl benzoate on heating. Cholesteryl benzoate melted from a solid to a cloudy liquid at 146 °C, and then turned into a clear liquid at 178 °C. More interestingly, Reinitzer noted that the bright blue-violet color of cholesteryl benzoate appeared on cooling from 179 °C until the sample crystallized. Reinitzer did not understand this observation and sent the sample to a German physicist Otto Lehmann. Lehmann described the bright-colored characteristics of cholesteryl benzoate on cooling as resulting from the long axes of the molecules orienting in one direction.³ The phase of this substance was first referred as soft crystal, but because this material exhibited the properties of both liquids and solids, this material was later given the name “Liquid Crystal” (LC).

A substance, like cholesteryl benzoate, which has one or more phases (mesophase) between isotropic liquid and crystalline solid is a LC. The ΔH of transition from Cr \rightarrow LC is 95 – 245 J/g higher than that of LC \rightarrow L, which indicates that LC exhibits some degree of orders since more energy is required to break the interaction between LC and Cr, but the phase is more liquid than crystalline in nature. In addition, liquid is said to be isotropic because properties of liquids are uniformly equivalent throughout the liquid phase. On the other hand, the LC is anisotropic because properties measured in different directions are not equivalent. Polarized microscopy has been one of key methods to determine the properties of LC. When polarized light is used on a LC sample, distinguishable patterns of mesophases can be displayed as a result of refractive index anisotropy or birefringence. Birefringence is an intrinsic property of LC that rotates the path of polarized light propagating through a sample of LC.

There are two main classifications of liquid crystals, lyotropic and thermotropic LCs. Formation and stability of lyotropic LC's mesophases are a function of solvation. By comparison, thermotropic LCs form mesophases as a function of temperature. There are three general classes of molecules forming thermotropic LC mesogens: calamitic LC, formed by rod-like molecules; discotic phase, formed by disk-shaped molecules; and polycatenar phases, formed by board-like molecules which can be regarded as the intermediate between calamitic LC and discotic LC.

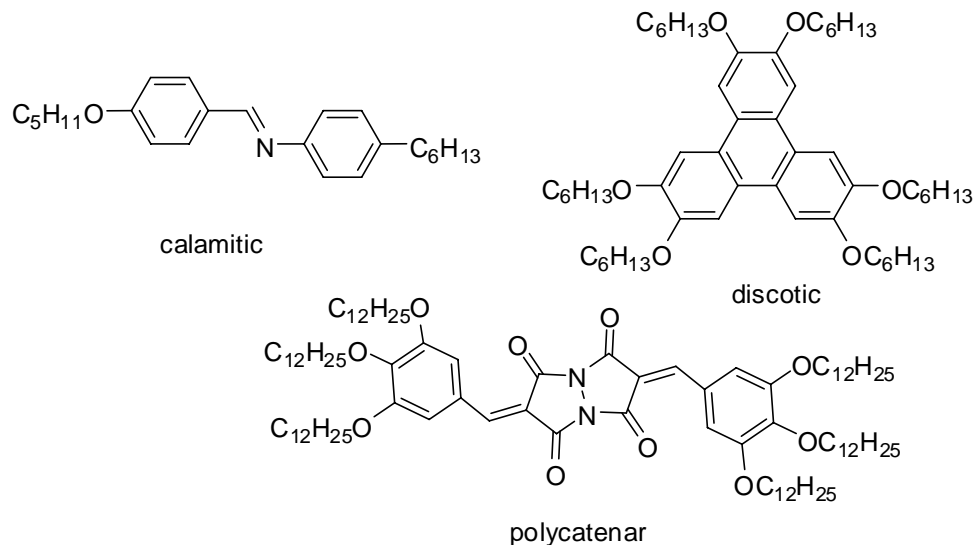


Figure 1.1. Structural representation of calamitic, discotic and polycatenar mesogens.

The focus of this thesis is on the synthesis of calamitic mesogens and the study on their formation of LC phases. Often, the ordering of calamitic LC can be dictated by the design of LC structures with attribution that favor the formation of one or more type of mesophases. The most common mesophases are the nematic (N), smectic A (SmA) and smectic C (SmC) phases, which differ in the degrees of their orientation and translational orders.

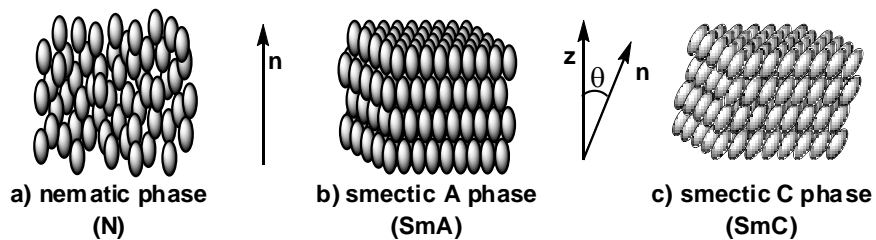


Figure 1.2. Characterization of three LC mesophases.

Rod shape like molecules with elongated tails (mesogens) are ordered with three molecular axes uniformly aligned along a director (n) in nematic phase without any

translational order. As a result, it is usually observed in the transition prior to liquid upon heating, or in the first phase observed upon cooling from the isotropic liquid phase. In the nematic phase, the texture viewed under polarized microscope exhibits point defects and extinction brushes forming the so called “Schlieren” texture (see **Figure 1.3**).

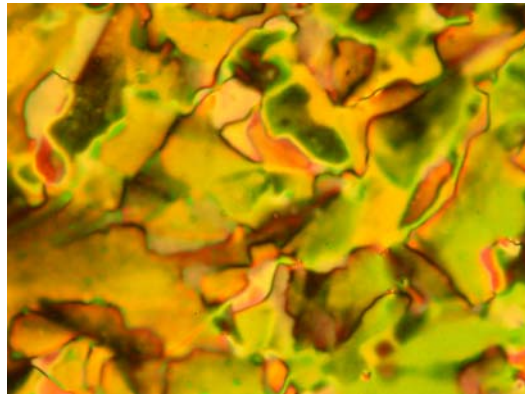


Figure 1.3. Schlieren texture of nematic LC

On further cooling before the nematic phase, smectic phases, including SmA and/or SmC phases, may form as a function of temperature. In the SmA phase, the molecules are aligned along a director (n) and exhibit short - range translational order without packing order. Focal conic (fan) textures are usually the patterns observed for SmA liquid crystals under polarized microscope. At the same time, the fan textures coexist with dark regions called homeotropic regions because the molecules are oriented perpendicular to the glass slides and therefore exhibit no birefringence.

The SmC phase differs from SmA in that the mesogens are uniformly tilted at an angle θ relative to layer normal, n . In general, the tilt angle increases with decreasing temperature. On cooling, the fan texture of the SmA phase turns into a “broken fan” texture in the SmC phase, and the homeotropic regions turn into Schlieren textures.

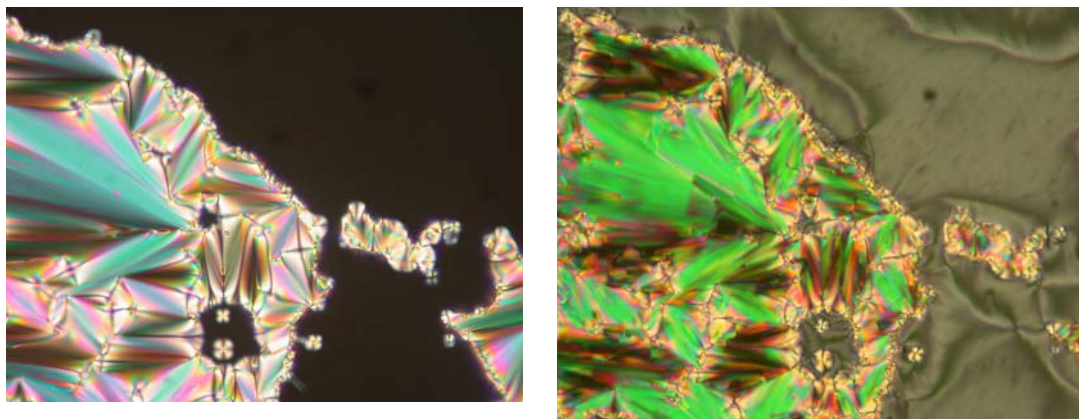


Figure 1.4. Photomicrographs of typical (a) SmA and (b) SmC textures.

There are several models to account for the tilt of the SmC phase which were proposed by McMillan, Wulff and Durand. In 1973, McMillan⁴ suggested that a torque can be produced upon a decrease in molecular rotation on cooling from SmA to SmC phase leading to the tilt observed due to coupling of outboard dipoles from polar functional groups (**Figure 1.5**).

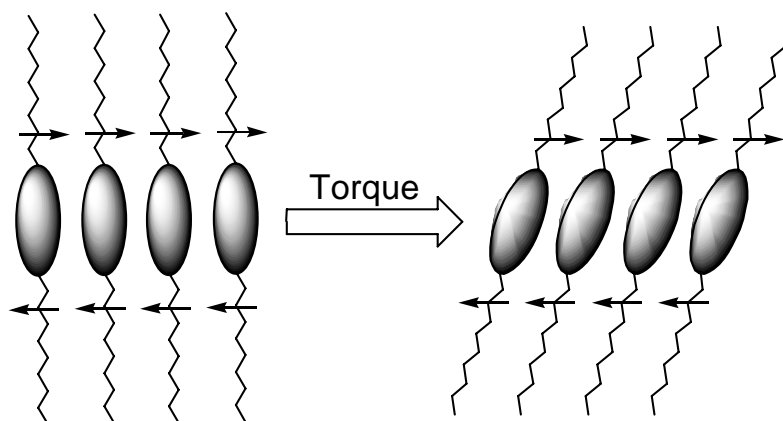


Figure 1.5. Representation of the McMillan model.

The zig-zag model was proposed by Wulff,⁵ who postulated that packing forces of calamitic molecules favor a tilted lamellar structure at lower temperature as molecular

rotation about n shows that atoms and molecules adopt a zig-zag conformation in their half extended form (**Figure 1.6**).

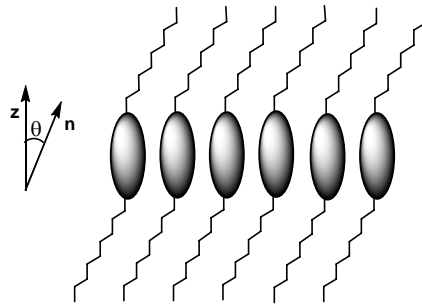


Figure 1.6. Representation of the Wulff model.

Through a comparative study of tilt angles measured by polarized microscopy and powder X-ray crystallography, Durand and Bartolino⁶ adapted the zig-zag conformation of SmC mesogens, but, unlike Wulff's model, they suggested that the cores of SmC mesogens are more tilted than the side chains. Optical tilt angle was depicted to be larger than steric tilt angle which is consolidated with their theory of molecular tilt in the SmC phase (**Figure 1.7**).

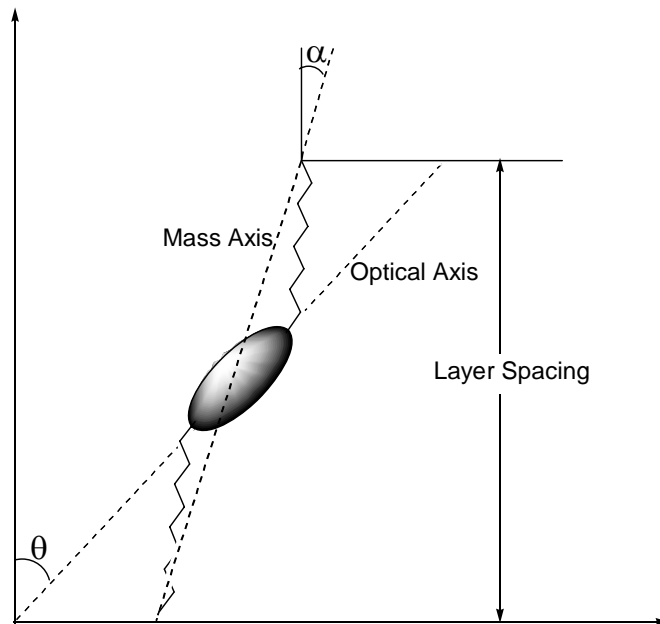


Figure 1.7. Representation of the Durand model.

The liquid nature of LC allows easy processing into thin films with the retention of optical properties. Since birefringence is a function of the angle formed by plane-polarized light and the director n , this property has been applied to produce ON/OFF light shutters by electrically switching the LC film between two different molecular orientations relative to crossed polarizers. Most LC applications are based on this simple concept of an ON/OFF light shutter. Although nematic LC constitute the major component of commercial LCD applications, chiral SmC (SmC^*) LC have significantly potentiality in the next generation of LCD devices because they can be switched ON and OFF about 10^3 times faster than nematic LC systems.

1.1.2. Chiral Liquid Crystals

If the SmC phase consists of chiral, non-racemic molecules, a bulk electrical polarization referred to as the spontaneous polarization (P_s) is present in the absence of any electrical field; these materials are ferroelectric. However, in the absence of external constraints, the SmC^* phase forms a macroscopic helical structure in which the P_s of vector rotates from one layer to the next relative to the helical axis and averages out to zero over a full helical pitch.

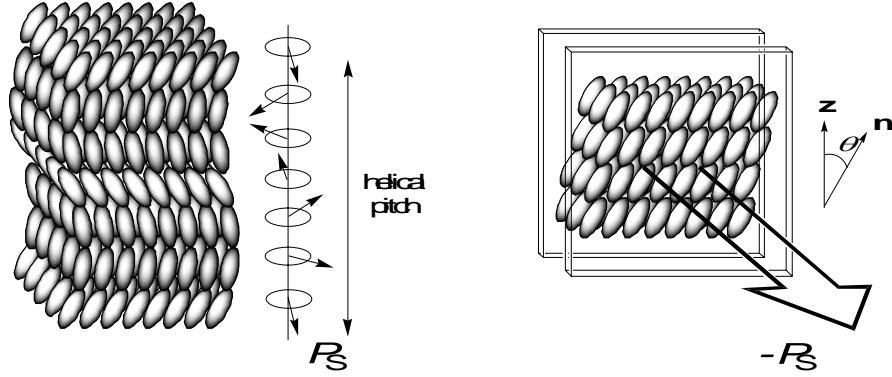


Figure 1.8. Schematic representation of the SmC* phase without surface alignment and as a surfaces-stabilized FLC.

In 1980, Clark and Lagerwall⁷ showed that the helical structure of a SmC* liquid crystal film on the order of a few micron thickness rubbed polyimide between the glass slides to give a *surface-stabilized ferroelectric liquid crystal* (SSFLC) with a net spontaneous polarization oriented perpendicular to the glass plates. The molecular orientation of SmC* mesogens can be switched by applying an electric field across the film, thus resulting in ON/OFF light shutter between crossed polarizer. For a SSFLC to be useful or commercialized, it must be composed of a mixture of a chiral dopant with high polarization power and an achiral host with low viscosity and wide SmC temperature range. The polarization power is a measure of the propensity of a chiral dopant to induce a spontaneous polarization according to equation 1, where x_d is the mole fraction of the chiral dopant and P_0 is the normalized spontaneous polarization adjusted for variation in tilt angle according to equation 2.

$$\delta = \left(\frac{dP_0(x_d)}{dx_d} \right)_{x_d \rightarrow 0} \quad (1)$$

$$P_0 = P_s / \sin\theta \quad (2)$$

The ferroelectric polarization of tilted chiral smectic phases is a manifestation of molecular chirality occurring in an ordered liquid. The Boulder model was developed to achieve a basic understanding of the origins of the ferroelectric polarization in chiral smectic C phases and to predict the sign and magnitude of P_s . The Boulder model proposed by Walba⁸ was useful for understanding the polar order of conventional chiral dopants or mesogens with chiral side-chains such as (*S*)-2-octyloxy side-chain. The rotational order of molecules in the SmC* C phase is modeled by a mean field potential (binding site) that has the shape of a bent cylinder (**Fig. 1.9**)

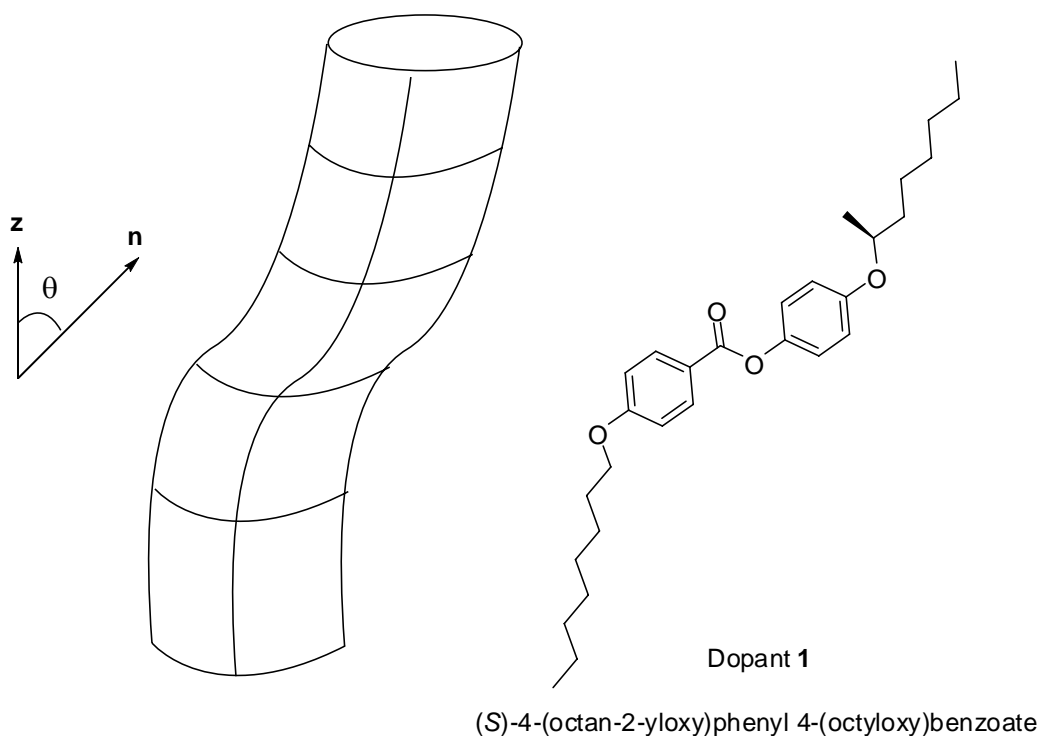


Figure 1.9. Zigzag binding site according to Boulder model.

According to the Boulder model, spontaneous polarization results from an orientational bias of molecular dipoles imposed by the steric coupling between polar functional groups and adjacent stereogenic centres. For example, in the dopant **1**, the conformational analysis about the C2-C3 bond of the polar (*S*)-2-octyloxy side-chain

revealed three staggered conformations corresponding to different orientation of the alkoxy groups relative to the polar axis. There are only two conformers (A and B) shown in **Fig. 1.10** because the dipole moments of third one lies with tilt plane and does not contribute Ps; conformer A and B by have the alkoxy dipole along the polar axis in opposite directions. Due to reduced hindrance of the anti-relationship between the methyl group and C₅H₁₁, conformer A is favored over B, and thus the Ps induced is negative.⁹ This model is consistent with the experimental results.

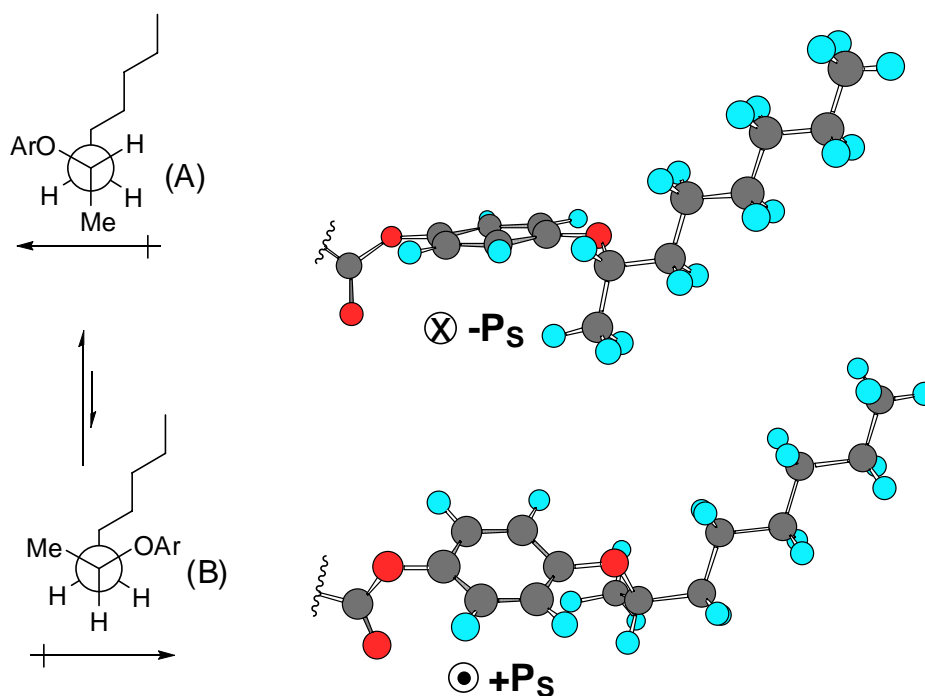


Figure 1.10. Conformational analysis of a (S)-2-octyloxy side chain and prediction of the resulting sign of PS. A side-on view along the polar axis is shown on the right. An end-on view is shown as a Newmann projection along the C2-C3 bond axis of the 2-octyloxy side-chain on the left.

The Boulder model can be generally applied to explain the origin of Ps of dopants with chiral side chains. Such dopants have polarization powers that are generally sensitive to the structure of the achiral SmC host because of the high degree of conformational disorder in the side chain region of the SmC layer. On the other hand, the

polarization power of a dopant with a chiral core (Type II) often varies with the host structure, which cannot be accounted for in its original form.

The behavior of Type II dopants was investigated in studies of SmC chiral dopant with atropisomeric biphenyl cores.¹⁰ AM1 calculations predicted that, in the zigzag conformation, rotation of the biphenyl core about the two ester CO bonds results in four energy minima. Two of the minima correspond to conformations in which the transverse dipole of the core lies in the tilt plane and thus would not be expected to contribute to P_S . The conformations that correspond to the other two minima, A and B which would be expected to contribute equally to P_S but in opposite directions, are shown in **Fig. 1.11**. Calculations predict that conformer A is favoured over the conformer B by about 1.0 kcal/mol.

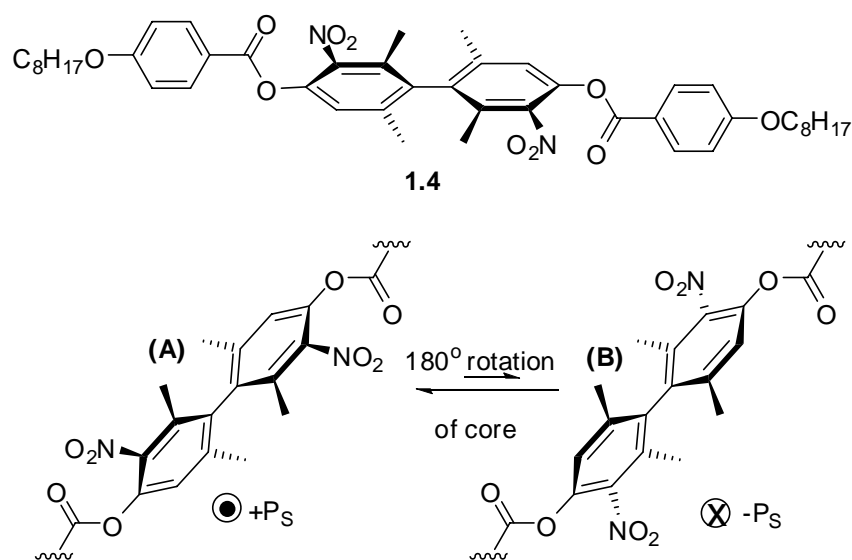


Figure 1.11. Rotation of the core of **1.4** about the two ester CO bonds in the zig-zag conformation.

A significant polarization was observed with atropisomer **1.4**, the polarization power being highly dependant on the nature of the host. Four SmC hosts (see **Fig. 1.12**)

were examined. The polarization power of **1.4** is 1738 nC/cm² when it is doped with the phenyl- pyrimidine host, **PhP1**. Lower polarization powers were obtained when **1.4** was doped with other hosts. For instance, **1.4** in a phenylbenzoate host **PhB** has a polarization power of less than 30 nC/cm².

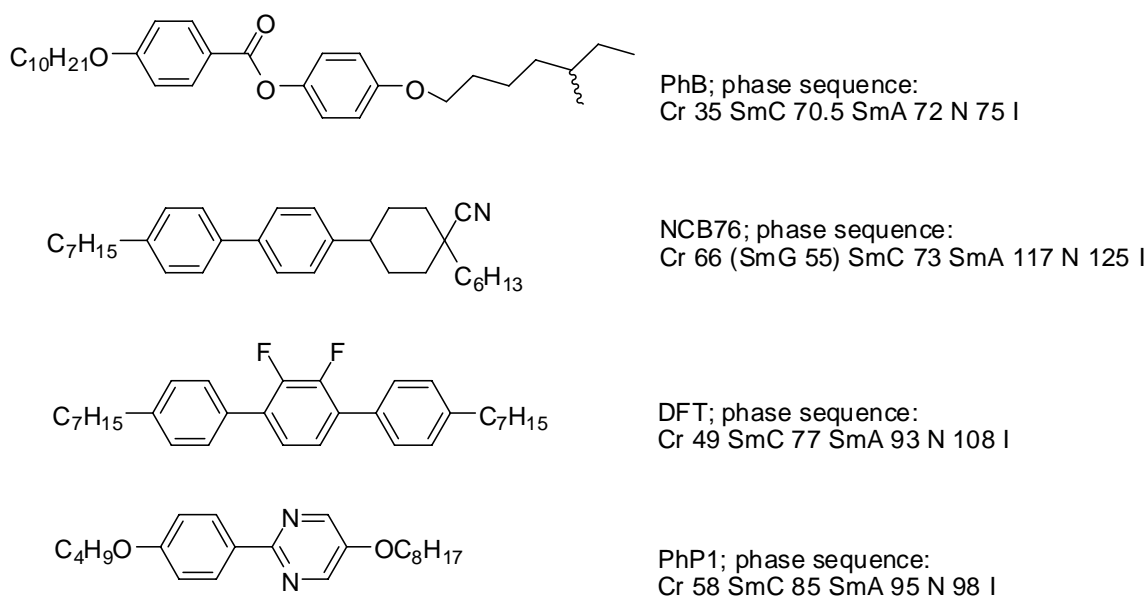


Figure 1.12. Liquid crystal host structures and phase transition temperatures in °C.

The host dependence of the polarization power is thought to be a function of the complementarity of the core structures of the dopant and the host to undergo chirality transfer. This led to the Chirality Transfer Feedback (CTF) model developed by Lemieux¹¹ and coworkers. As a result of intermolecular chirality transfer, the binding site topography is thought to be distorted asymmetrically, which may contribute to higher polar ordering of the dopant by causing a shift in the conformational equilibrium of the atropisomeric core with respect to the α -ester side chains. Unlike classical host-guest chemistry, the host, together with the dopant, plays an active role in this feedback mechanism to amplify the polarization power. Lemieux suggests that this model and the

Boulder model are not mutually exclusive to account for the type II host effect which may be the consequence of differences in the intrinsic topography of the SmC binding site and/or degree of distortion of the binding site.

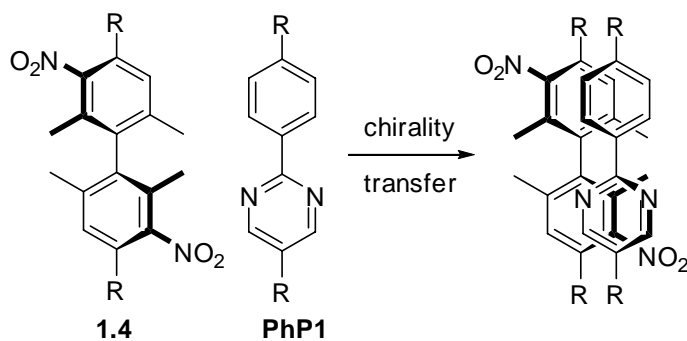


Figure 1.13. Model for chirality transfer via core-core interactions.

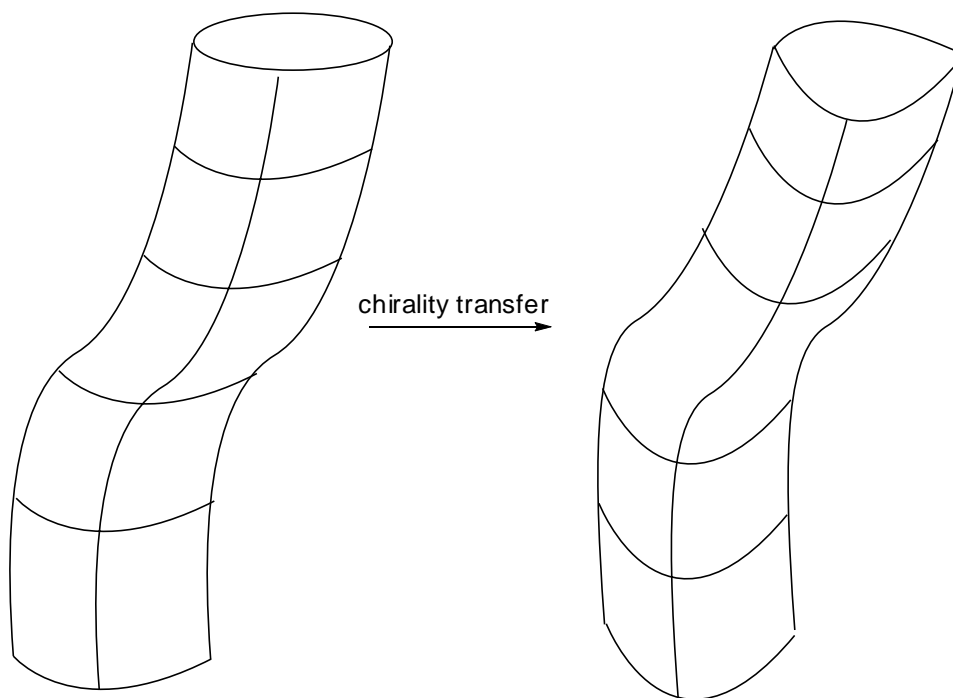


Figure 1.14. Chiral distortion of the SmC binding site.

1.1.3. Hydrogen Bonding in Calamitic Liquid Crystal Phases

In the condensed state, molecules aggregate with other molecules to form materials with interesting properties through intermolecular interactions such as hydrogen bonding, π - π stacking, and van der Waal forces. Favourable intermolecular interactions, such as π - π stacking as well as hydrogen bonding may also drive microphase segregation. For example, conformationally rigid aromatic cores tend to self-associate rather than mixing with parafinic conformationally flexible side-chains. Because of their stability (bonding energy of 10-50 kJ/mol) and directionality ($X^{\delta-}\cdots H^{\delta+}$) hydrogen bonds are an important feature to promote self-assembly into LC phases. Hydrogen bonding has been exploited in promoting LC phase formation in two important ways. The first involves the self-assembly of complementary structures (which may or may not be mesogenic themselves) into rod-like supramolecular structures that exhibit mesogenicity (**Figure 1.15(a)**).¹² The second involves lateral hydrogen bonding that enhances translational ordering and thus promotes the formation of smectic phases (**Figure 1.15(b)**).

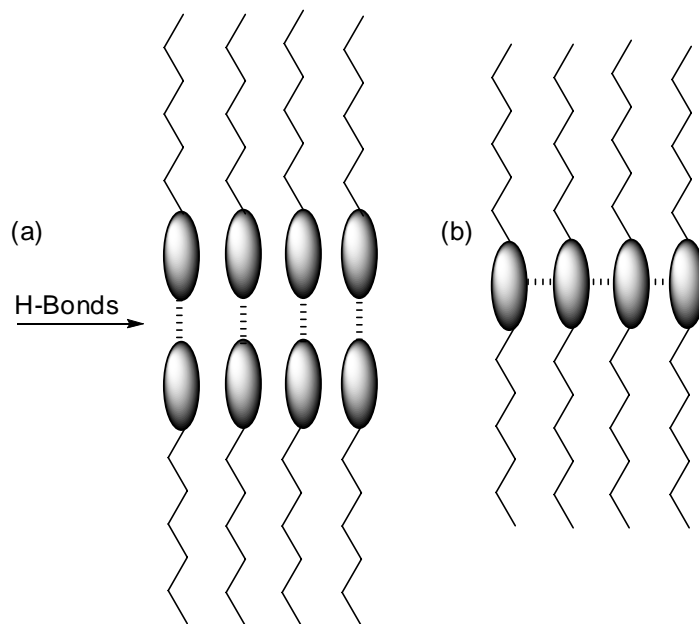


Figure 1.15. Two modes of hydrogen in liquid crystals: (a) head-to head and (b)lateral modes.

1.1.4. Liquid Crystals Containing Fluorene Core Structures

In 1955, Gray and coworkers¹³ reported the first liquid crystal containing fluorene and fluorenone cores, the mono-substituted **1.5** and symmetrically disubstituted **1.6** which form nematic and smectic phase. In addition, the fluorenes **1.7** were shown to form a broad smectic phase but the fluorenones **1.8a** and **1.8b** were found not to be mesogenic.

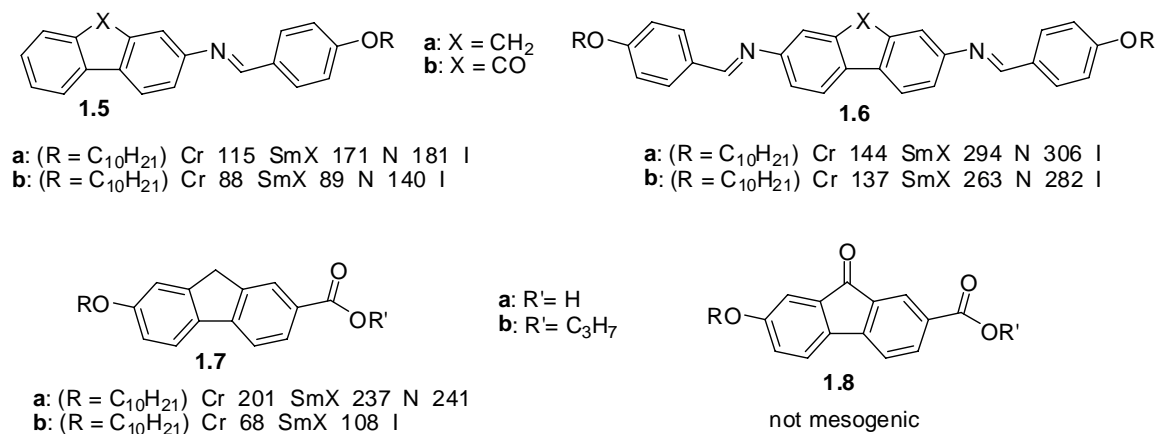


Figure 1.16. First studies of Fluorene and fluorenone LCs.

In 2002, a series of symmetrical 2,7-dialkylfluorenones (**1.9**, **Fig. 1.17**) were investigated by Ivanov¹⁴ who showed that fluorenones with alkyl chain lengths between C₅ and C₁₄ form only SmC phases with a broad range of up to 39 °K. The iso-pentyl derivative has no LC properties due to the lateral bulk of the branched side chains. From IR studies, π - π stacking force in these molecules with fluorenone cores were suggested to be an important factor in the crystal formation but maybe less so in the LC phase.

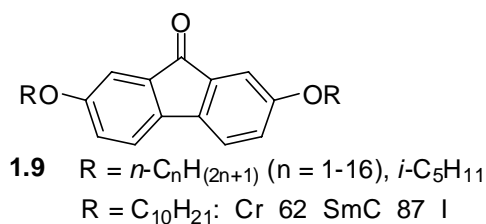


Figure 1.17. Symmetrical Mesomorphic 2,7-dialkylfluorenone and mesomorphism (R = C₁₀H₂₁).

Type I ferroelectric LCs with fluorenone cores and one stereo polar unit on the side chain were reported by Takatoh¹⁵ and coworkers in late 1980's and in 1990. In general, the mesomorphism of these compounds confirmed earlier studies. However, it was noted that the fluorenones have lower clearing points than those reported for the fluorene analogues, probably due to the lateral bulk of carbonyl groups. SmA phase formation is favored in compounds containing fluorene cores and SmC phase formation is promoted in compounds containing polar fluorenone cores. Spontaneous polarization of fluorenone **1.11b** was measured at $T-T_C = -10$ °K to be 50 nC/cm^2 , which is higher than that reported for the fluorene derivatives **1.11a** (30 nC/cm^2). This was rationalized based on the higher tilt angle of the fluorenones in the SmC^* phase, which causes a more hindered rotation of the molecules about their long axes and increased polar order.

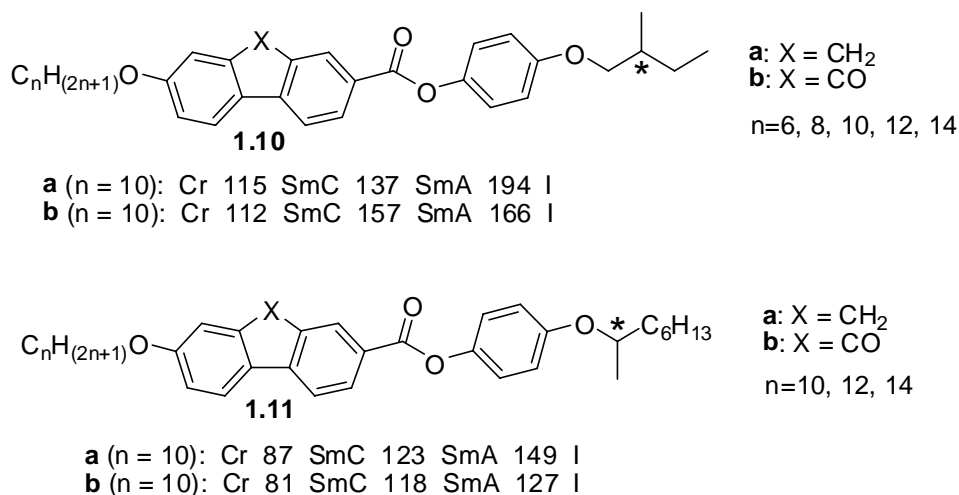


Figure 1.18. Type I ferroelectric fluorene and fluorenone LC.

Recently, Lemieux and McCubbin¹⁶ reported the type II SmC^* LC with a chiral fluorenol core. The chiral fluorenol mesogen (*R*)-2-(1-octyloxy)-7-((4-undecyloxybenzoyl)oxy)fluoren-9-ol(*R*)-**3** was synthesized using a combined directed

metalation-cross coupling strategy. The SmC* LC phase exhibited by the fluorenol mesogen is more stable than its corresponding fluorenone precursor, and has a wider temperature range which may be attributed to intermolecular hydrogen bonding.

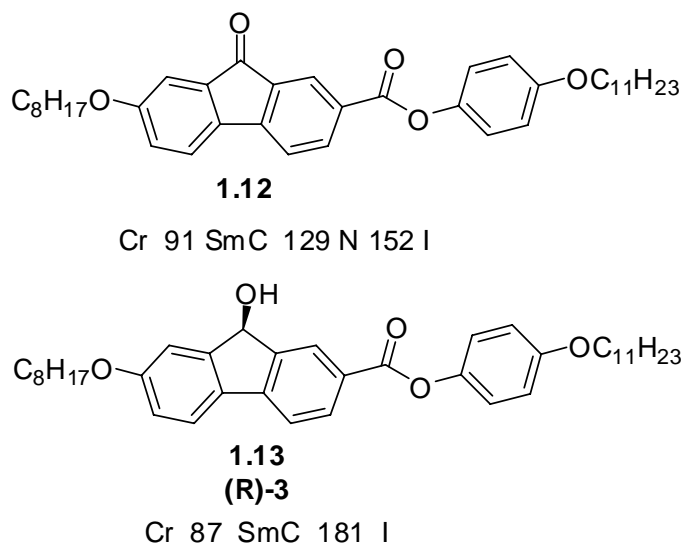


Figure 1.19. Fluorenone and Type II ferroelectric fluorenol LC.

The spontaneous polarization (P_s) and tilt angle were measured as a function of temperature for (*R*)-**3** as a surface-stabilized FLC. The P_s of (*R*)-**3** at 10 °K below the SmC*-I phase transition temperature was found to be -10.7 nC/cm^2 , corresponding to a reduced polarization (P_o) of -20.2 nC/cm^2 . Dilution experiment by mixing a series of structurally similar mesogens that cannot form hydrogen bonds with (*R*)-**3** and deuterium exchange experiments provided evidence that the fluorenol, (*R*)-**3**, forms a dimeric structure via hydrogen bonding. The structure of the fluorenol causes a subtle orientational bias that results in the observed polarization. The dilution studies suggest that no polarization would be observed in the absence of dimerization. Therefore, the role of hydrogen bonding in self assembly to enhance polar order in a ferroelectric liquid crystal was confirmed.

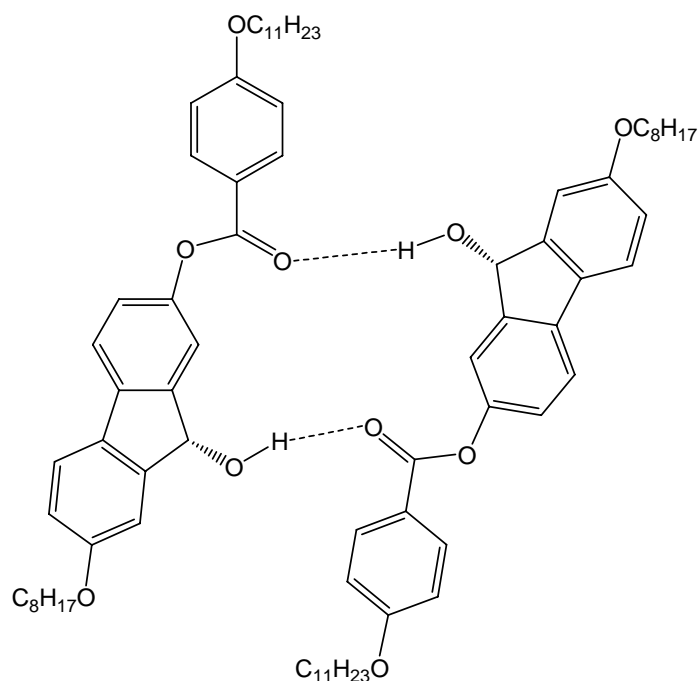


Figure 1.20. (R)-3 dimer formed by the hydrogen bonds.

1.1.5. Mesogen Design Considerations and Outline of Research

As described above, intermolecular hydrogen bonding can be important in the formation of liquid crystal phases and in defining their bulk properties. Most of the studies today have focused on the effect of hydrogen bonding in stabilizing mesophase formation. The incorporation of hydrogen bonding groups in the stereo polar unit is beginning to be explored but knowledge on this effect is still limited. In theory, SmC* mesogens with functionalities were capable of forming a stronger hydrogen bonding interaction such as OH-N. Thus an azafluoreneol may form polar hydrogen bond networks which force the mesogen transverse dipole moment to orient in a specific direction along the polar axis to enhance the polar order. The goal of this research was therefore to design and synthesize a system in which the aza moiety can be included into the core of

an LC mesogen and the obvious choice, from the previous work in the Lemieux laboratories, was an azafluorenol derivative (**Fig. 1.21**).

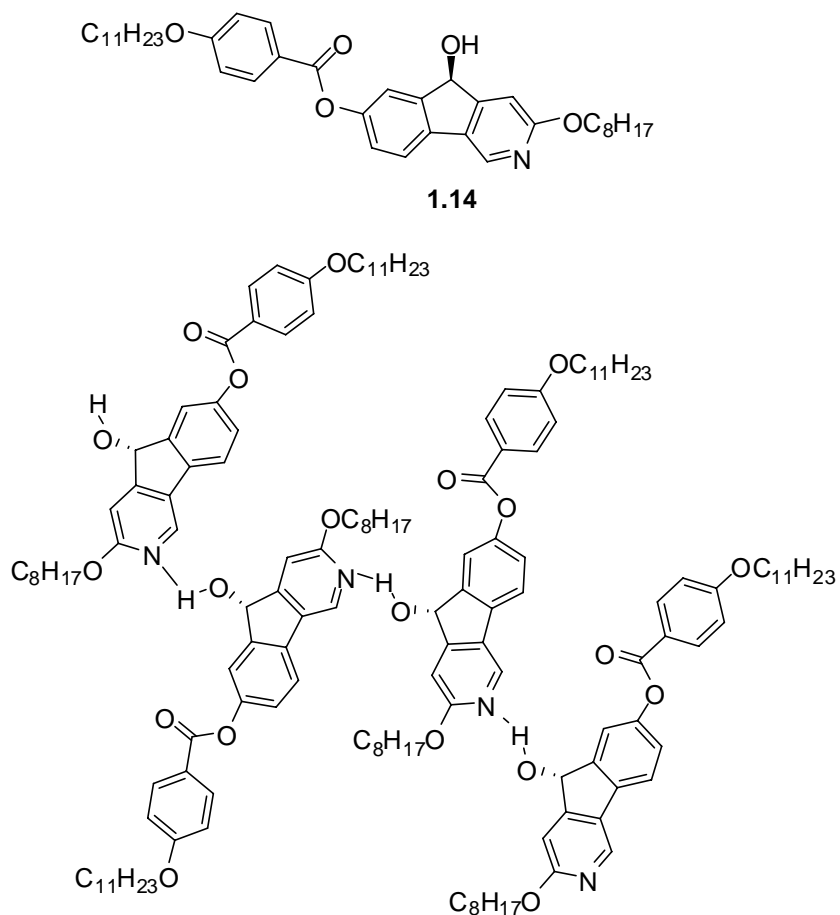


Figure 1.21. Proposed network of azafluorenol mesogens.

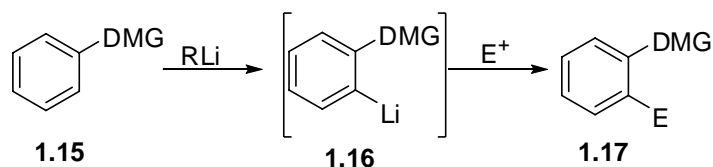
It was envisaged that such chiral azafluorenol mesogens can be constructed from the corresponding azafluorenone whose synthesis could be achieved based on Directed *ortho* metalation (DoM), Pd catalyzed Suzuki-Miyaura cross coupling and directed remote metalation (DreM) chemistry.

1.2. Synthetic Methodology

1.2.1. The Directed *ortho* Metalation (DoM) Reaction

In view of the presence of aromatic and heteroaromatic moieties in natural products, pharmaceuticals and agrochemicals, the development of efficient synthetic methods for these classes of molecules is a significant component of organic synthesis. Electrophilic aromatic substitution (EAS) is undisputably the traditional pedagogy of aromatic chemistry for the preparation of polysubstituted aryl rings.^{17,18} Although the practical aspects of EAS have helped chemists in planning the synthesis of various aromatics, harsh conditions and formation of mixtures of positional isomers handicap EAS tactic to a great extent. The regioselective preparation of polysubstituted and usefully functionalized aromatics and heteroaromatics is a significant area of continuing investigation. Over the past two decades, the directed *ortho* metalation (DoM) has evolved into a reliable and useful method for the synthesis of contiguously substituted aromatic molecules of value in both small and large-scale synthetic programs.¹⁹⁻²¹

The *ortho* deprotonation of dibenzofuran by MeLi and CO₂ addition to yield 4-dibenzofurancarboxylic acid constitutes the first DoM reaction discovered by Gilman^{22,23} over 60 years ago. However, its potential was not realized until the 1970s when alkyllithiums were commercially available due to their large-scale use in anionic polymerization chemistry²⁴ and the publication of an insightful, comprehensive review by Gschwend and Rodriguez.¹⁹ The DoM reaction is simplistically depicted in **Scheme 1.1**. The reaction involves the deprotonation by an alkyl lithium base *ortho* to a heteroatom containing directed metalation group (DMG) **1.15**. Subsequently, the resulting anionic intermediate **1.16** undergoes reaction with an electrophile to afford a 1,2-disubstituted aromatics **1.17**.



Scheme 1.1.

The reaction is proposed to proceed by the involvement of the DMG in coordination or inductive fashion effecting the *ortho* metalation process. Many DMGs have been developed over the years. Although the mechanistic details of the DoM reaction have not been fully elucidated due to its complexity, it is generally agreed that a good DMG contains sites for coordination for an alkyllithium, and must not be prone to nucleophilic attack by a strong base. Therefore, factors like steric hindrance and charge deactivation are invoked to design a reasonably good DMG. The seminal work of Hauser in the mid-1960s provided amide and sulfonamide as DMGs; in the ensuing years, a useful armament of DMGs have accumulated for deployment in DoM chemistry warfare (**Table 1.1**). These DMGs may be generally organized into two classes – carbon based and heteroatom based. The oxazoline DMG of Meyers and Gschwend is an example of a carbon-based DMG which, after serving its purpose in DoM chemistry, may be hydrolyzed to give a carboxylic acid derivative. The *N,N*-diethyl carboxamide invented by Beak stands as a powerful carbon-based DMG which has enjoyed considerable use as a conduit for the synthesis of the polycyclic aromatics. The *O*-carbamate discovered in the Snieckus laboratories shows extraordinary *ortho* directing strength but the reaction must be carried at very low temperature in order to avoid the *ortho*-Fries rearrangement.²⁵ The *O*-sulfamate, more recently developed in the Snieckus group²⁶ is another appealing DMG that not only functions as a DMG but also exhibits facile transition metal catalyzed Kumada-Corriu cross coupling characteristics.

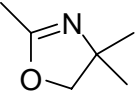
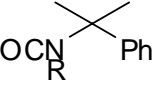
Carbon Based DMGs			Heteroatom Based DMGs	
CON-R	Hauser,	1964	SO ₂ NR ₂	Hauser, 1969
	Meyers Gschwend,	1975	N-Boc N-CO <i>t</i> Bu	Gschwend, 1979 Muchowski, 1989
CONEt ₂	Beak,	1977	OSO ₂ NR ₂	Snieckus, 2003
	Snieckus,	2001	OCONEt ₂	Snieckus, 1983
			OP(O)NEt ₂	Snieckus, 2003
			OCH ₂ CH ₃	Christensen, 1975
			P(O) <i>t</i> Bu ₂	Snieckus, 1998

Table 1.1.

The hierarchy of DMG efficiency was established by the combined efforts of many laboratories. Competition studies comparing two DMGs were initialized by Slocum and coworkers on OMe as anchoring DMG, extended by Beak, Meyers and Snieckus on 4-CONEt₂, oxazoline and OCONEt₂ as anchoring groups respectively to compose the current picture.²⁷

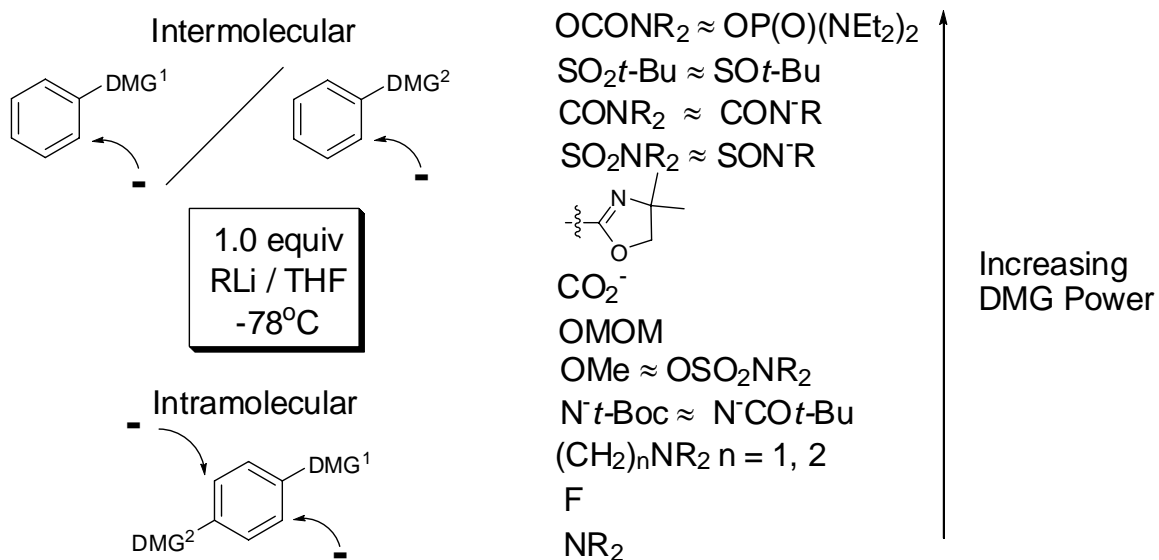
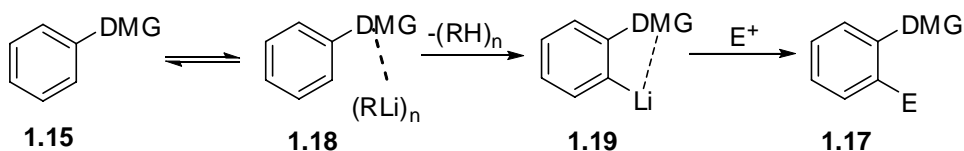


Figure 1.22. Hierarchy of DMGs.

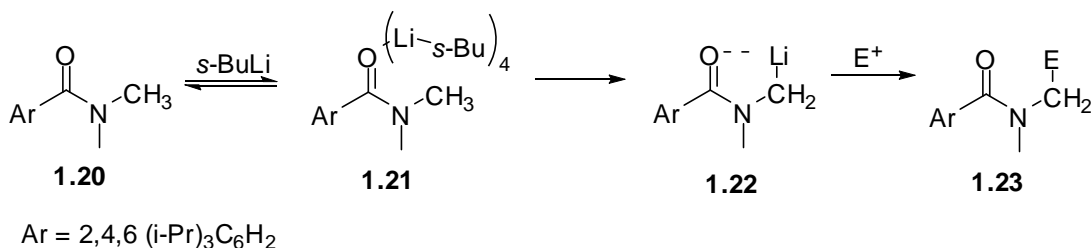
1.2.1.1. The Mechanism of the DoM Reaction

“All of these new organotransition-metal chemistry at the end of 1950s had been discovered by empirical methods and nothing was known about the chemistry involved. I decided to begin my new project by trying to determine the mechanism of one of these important reactions in the hope that this knowledge would suggest new chemistry to study.” (Professor Richard Heck).²⁸ Mechanistic understanding of new reactions leads to appreciation of their potential and application. Twelve years after the discovery of the DoM reaction,²² Roberts and Curtin^{29,30} proposed that the reaction proceeds by butyllithium precoordination with the methoxy function in anisole, and this proposal has become the basis of rationalization of the regioselectivity of the DoM reaction. In contrast to the simplistic view (**Scheme 1.1**), the mechanism of DoM reaction is complicated and remains a controversial subject. Three mechanistic formalisms, the complex induced proximity effect (CIPE), the kinetically enhanced metalation (KEM) and the inductive effect have been proposed as mechanistic rationalizations of the DoM reaction and these will now be discussed.

Evidence for the precoordination of alkyllithium to the DMG was first secured by Beak and Meyers who studied the α -deprotonation of amides and formamides **1.20**,³¹ using stop-flow FT-IR spectroscopy. These studies showed that a precoordinated complex, **1.18** is on the path of the reaction prior to α -lithiation **1.19** thus suggesting a two step mechanism and resulting in the coining of the Complex Induced Proximity Effect (CIPE) as the key component of the DoM reaction.

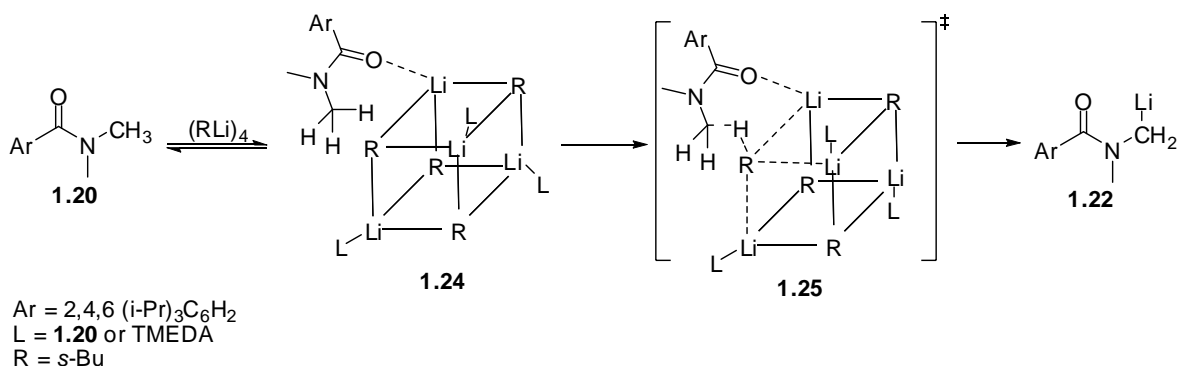


Scheme 1.2.



Scheme 1.3.

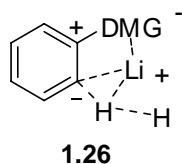
Lithiated products (**1.24**, **1.25** and **1.22**) of dimethyl carboxamide **1.20**, formed from treatment of *s*-BuLi in cyclohexane at room temperature, were directly observed by stopped-flow IR spectroscopy.³² Kinetic studies led to the hypothesis that the complexed *s*-BuLi tetramer **1.24** was formed in rapid equilibrium with **1.20** followed by α proton transfer from the *N*-methyl via a transition state **1.25** to give **1.22**. It was shown that the *s*-BuLi tetramer structure is maintained upon addition of TMEDA.³³ Interestingly, this observation is in contrast with the dogma that TMEDA promotes deprotonation by breaking the lithiating aggregates. It is argued that TMEDA binding to the lithium assists the release of the incipient carbanion in the transition state **1.25**.



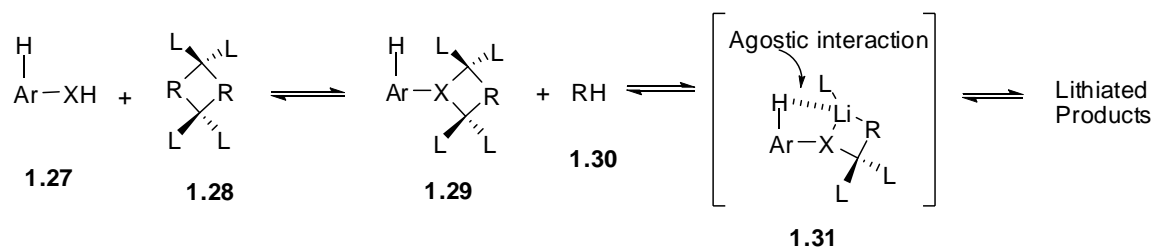
Scheme 1.4.

The CIPE concept is used to rationalize the regioselectivity in the DoM reaction. In 1989, Schleyer pointed out that the complexation should proceed more slowly if the free energy (ΔH) of complexation has to be overcome. Therefore, low reactivity would be

expected, but this does not agree with the experiment observations.³⁴ The mechanism of the DoM reaction may be inadequately presented by CIPE.³² Using a series of *ab initio* computations, Schleyer and Homme³⁴ postulated a “Kinetic Enhanced Metalation” as a feasible one-step DoM reaction mechanism in which complexation and proton abstraction occurred simultaneously.³⁵ In this model, the transition state is stabilized by two effects – a favorable charges distribution and a shorter distance of Li-DMG (DMG = alkoxy and F as electronegative groups) in forming the partial bond in the transition state **1.26**, which account for the rate enhancement of the reaction and a large KIE. In addition, Saa’s results^{36,37} also supports this model with the observation of agostic metal hydrogen interactions by ⁶Li, ¹H-HOESY NMR (**Scheme 1.6**).



Scheme 1.5.

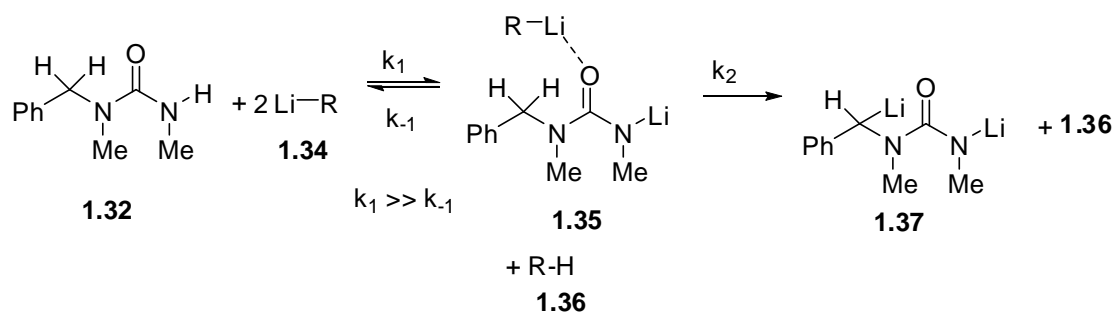
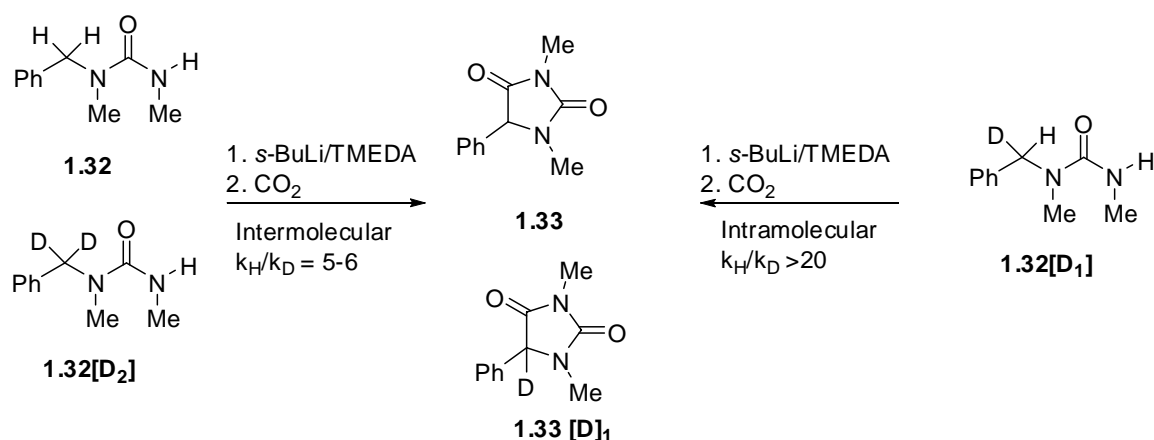


Ar = phenyl, naphthyl
X = O, CONMe

Scheme 1.6.

The two step CIPE process has been demonstrated through inter- and intra-molecular protium/deuterium isotope effect studies.³⁸ In the directed lithiation study of urea **1.32**, the ratio of **1.33/1.33[d₁]** was measured to estimate the experimental isotope effect and provided the following values: $k_H/k_{Dintermolec} = 5-6$ and $k_H/k_{Dintramolec} > 20$. The

k_H/k_D ratios were estimated by determining the product ratios of undeuteriated vs. deuteriated **1.33** after treatment of **1.32**, **1.32[D₁]**, **1.32[D₂]** with *s*-BuLi/TMEDA followed by deuterium work-up. If the reaction proceeds through a single step, the ratio of **1.33** to **1.33[D₁]** would be determined solely by the primary isotope effect in both the intramolecular and intermolecular experiment. Thus, a similar value for k_H/k_D would be obtained in both cases. On this basis, Beak and coworkers argued that a one-step mechanism can be safely excluded and a mechanism consisting of at least two steps is required. Lithiation of urea **1.32** was further proposed to proceed through largely irreversible complexation followed by a slow deprotonation which can be depicted in **Scheme 1.7** and free energy diagram of **Figure 1.23** respectively.



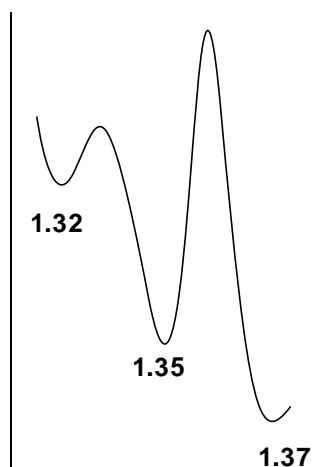
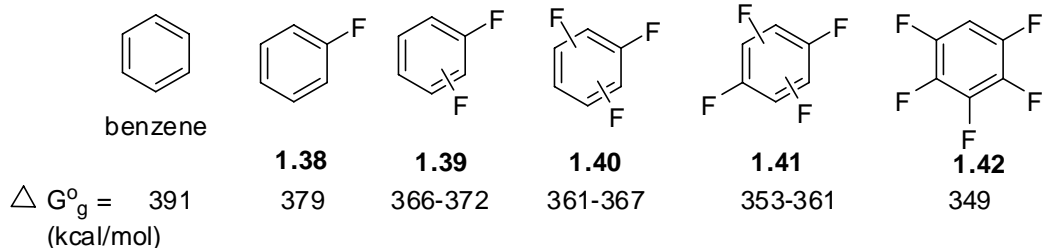


Figure 1.23. Proposed reaction profile of the benzylic lithiation of urea **1.32**.

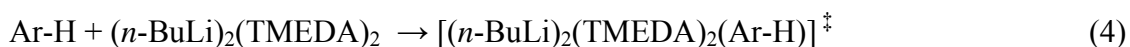
In a study of additivity of substituent effects in a fluoroarene series, the gas phase acidities (free energies of deprotonation, ΔG°_g) of fluorinated arenes (**1.38-1.42**) were obtained by determining the ion concentration by cyclotron mass spectrometry.³⁹ Using these results and the results derived from base catalyzed isotope exchange reaction, Schlosser and coworkers⁴⁰ were able to demonstrate the increasing acidity of the proton next to the fluorine for each addition of fluorine into the benzene. These results paralleled the diminishing pKa values of each addition of fluorine in the series of fluoro-substituted acetic acids (pKa (CH₂FCOOH - CH₃COOH) = -2.2; pKa (CHF₂COOH - CH₂FCOOH) = -1.7; pKa (CF₃COOH - CHF₂COOH) = -1.1).⁴¹ Isotope effect studies in the regioselectivity of metalation of the substituted fluorinated benzene by potassium amide in liquid ammonia⁴² or by lithium cyclohexylamide in cyclohexane⁴³ also echo the relative strength of gas phase acidities of various substituted fluorinated benzenes measured by Schlosser and coworkers.⁴⁰ Thus, inductive effect was also rationalized as one of the major mechanisms operated for DoM.



Scheme 1.8.

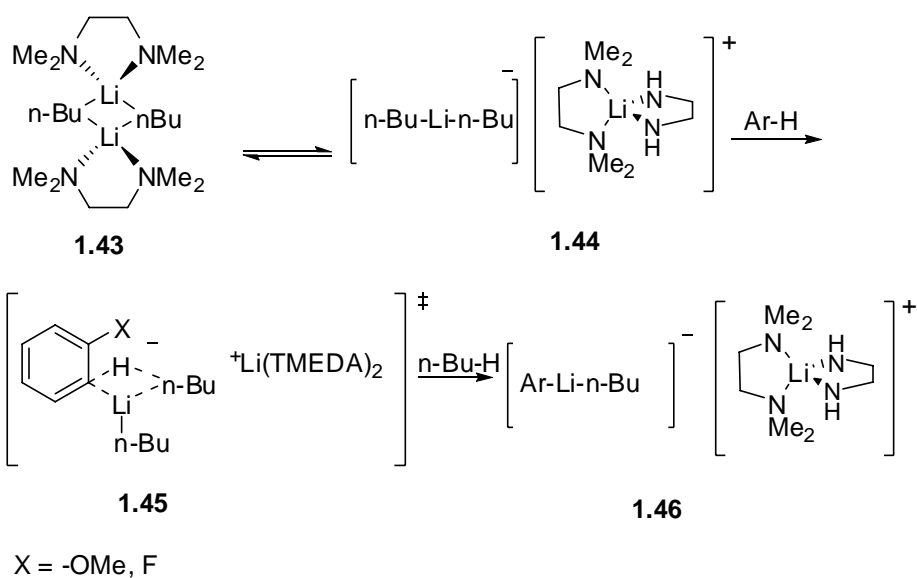
On the basis of comprehensive kinetic and *ab initio* calculation studies, Collum⁴⁴ concluded that the inductive mechanism is operative in the cases of anisole, resorcinol (1,3-dimethoxybenzene), methoxymethoxybenzene, fluorobenzene, *m*-difluorobenzene, and (2-dimethylamino)ethoxybenzene. Kinetic studies showed that the rate depends on the first order of both [arene] and [BuLi], but is independent of the [TMEDA]. The idealized rate law and generalized mechanism are shown by eqs 3 and 4. Rate laws were found to be substrate independent for all cases. Probable rate-limiting transition structures of stoichiometry [(*n*-BuLi)₂(TMEDA)₂(Ar-H)][‡] are consistent with the triple ion mechanism first presented by Fuoss in 1933, relevant here to describe the DoM reaction.⁴⁵

$$-d[\text{Ar-H}]/dt = k' [\text{ArH}]^1 [\text{BuLi}]^1 [\text{TMEDA}]^0 \quad (3)$$



Collum proposed that TMEDA-Li dimer **1.43** (**Scheme 1.9**) exists in equilibrium with **1.44**, but addition of arene (Ar-H) bearing weakly coordinating group leads to the irreversible transformation to the lithiated species **1.46** via a triple ion transition state, **1.45** which is consistent with the determined rate law eqn 4. In view of their similarity to other main group “ate” complexes, triple ions should show high basicities and nucleophilicities toward the lower pK_a hydrogen *ortho* to heteroatom groups in the aryls. *Ab initio* calculations were carried out to assess relative activation enthalpies (ΔH^\ddagger) of

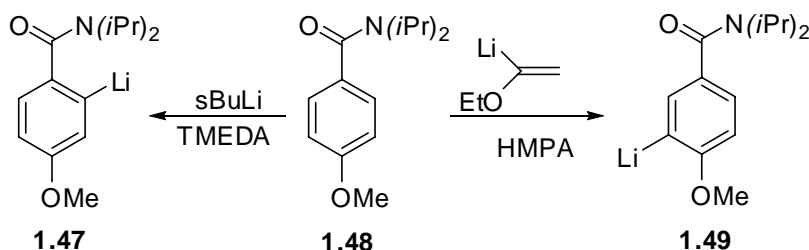
different substrates using a CIPE based model and triple ion based model, respectively. On the basis of computational data for the different oriented conformers, the lithiations of aryls bearing methoxy and fluorine groups were interpreted as likely to proceed by a triple ion mechanism rather than by a CIPE mechanism. This interpretation that OMe and F-substituted aromatics undergo DoM owing to the inductive effects of the substituents is in agreement with the observations of Shimano and Meyers which will now be discussed.



Scheme 1.9.

In 1994,⁴⁶ Shimano and Meyers reported that the lithiation of **1.48** with *s*-BuLi·TMEDA furnished **1.47** but that the lithiation of **1.48** with α -ethoxyvinyl lithium (EVL)·hexamethylphosphamide (HMPA) afforded **1.49** as evidenced by MeI quench experiments. The results were initially rationalized by consideration of steric effects created by a large cluster of yet undetermined stoichiometry involving both EVL and HMPA which prevented formation of the **1.47** species. A more recent proposal by Beak and Snieckus²⁷ attributes these observations to the reduction of the ability of the amide to

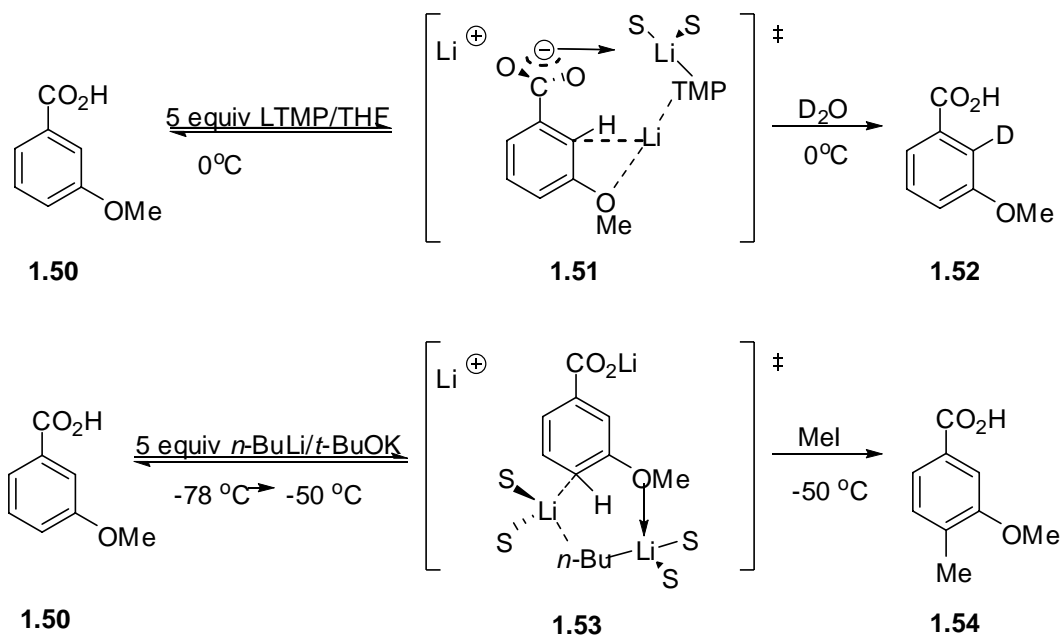
coordinate with EVL·HMPA. In general, carboxamide acts as a DMG through coordination with the lithium bases; whereas OMe exerts its directing ability mainly through an inductive effect and partly through oxygen coordination.²⁰ As a result, lithiation of **1.48** using *s*-BuLi·TMEDA occurs *ortho* to the diisopropyl carboxamide owing to the CIPE. On the other hand, a CIPE is not involved in the lithiation of **1.48** using EVL·HMPA because complexation between carboxamide and EVL is undermined.



Scheme 1.10.

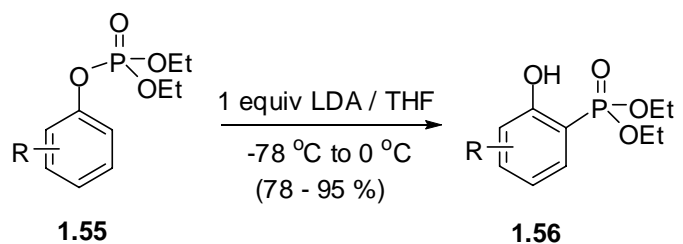
As a further contribution to the DoM mechanism, Mortier investigated the metalation of *meta*-anisic acid as a function of base.⁴⁷ Thus, treatment of *m*-anisic acid with lithium 2,2,6,6-tetramethyl piperidide (LTMP) followed by addition of D₂O yielded 2-d *m*-anisic acid, **1.52** (**Scheme 1.11**) only, whereas treatment with the Schlosser-Lohmann base (*n*-BuLi/*t*-BuOK) followed by addition of MeI yielded 4-methyl *m*-anisic acid, **1.54** (80%) as a major product with a mixture of 2-methyl *m*-anisic acid (9%) and 6-methyl *m*-anisic acid (11%) as byproducts. Mortier concluded that lithiation by LTMP is thermodynamically controlled and anion species (**1.51**) generated at the 2-position is stabilized by resonance from the contribution of CO₂⁻ and inductive effect of OMe. In contrast, the stronger the Schlosser-Lohmann base is not influenced significantly by the directing ability of CO₂⁻. It exhibits non-selective deprotonation at 2-, 4-, and 6- positions of **1.50** but the 4-C-H bond is the more inductively activated aromatic position due to

being present next to the most electronegative heteroatom (i.e. OMe) and thus the C-anion is preferentially formed under the kinetically controlled conditions.



Scheme 1.11

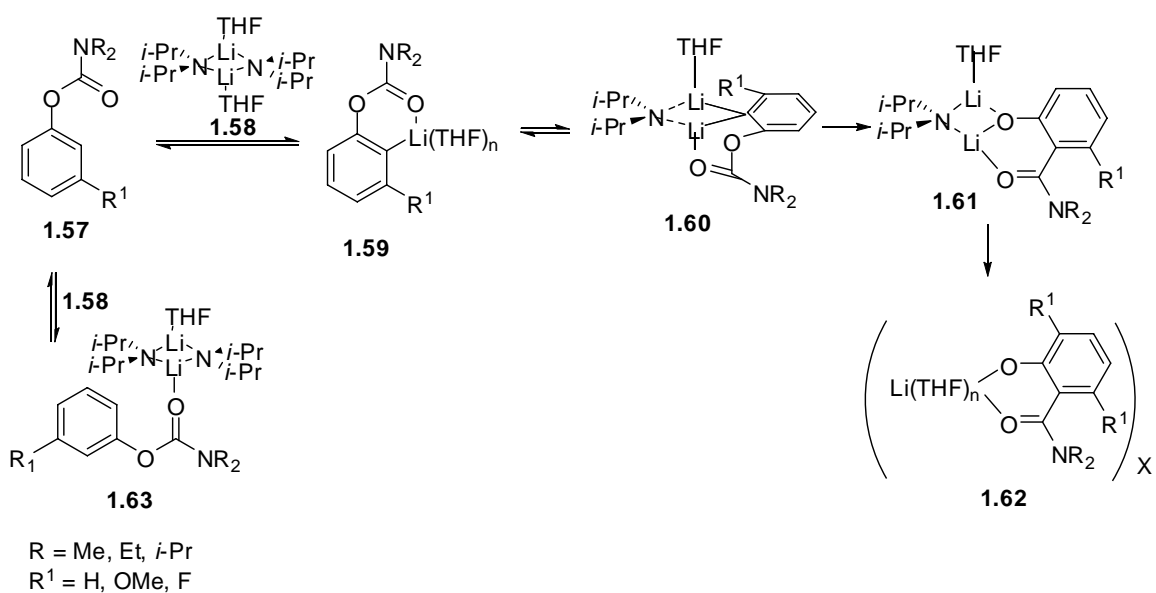
Mechanistic evidence for the DoM reaction has also accumulated from studies on the anionic Fries rearrangement which can be thought as an extension of DoM reaction. In 1981, Melvin⁴⁸ found that treatment of **1.55** with LDA led to the formation of **1.56** in 78 to 95% yields (**Scheme 1.12**). The same reaction was also observed in the aryls bearing phosphodiamidate.⁴⁹



R = 3-OMe, 4-OMe, 5-OMe, 3,5-OMe

Scheme 1.12

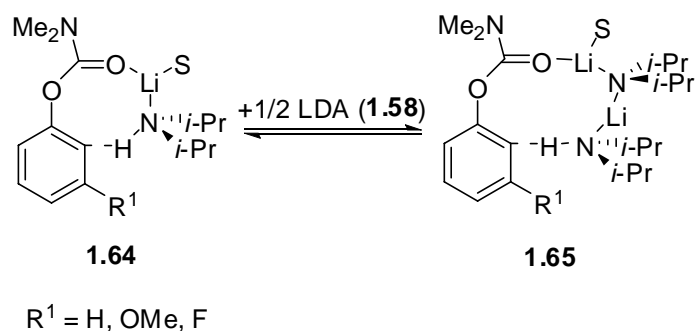
In 1983, Sibi and Snieckus²⁵ observed a similar anionic rearrangement of aryl *O*-carbamates. This type of reaction, for which the term anionic *ortho* Fries rearrangement was subsequently coined and which has been cultivated in large part by Snieckus and coworkers has gradually received attentive interest from the pharmaceutical industry.⁵⁰ Recently, mechanistic studies of lithiation of aryl *O*-carbamates, **1.57** by Singh and Collum⁵¹ suggest that *ortho* lithiation rather than the anionic Fries rearrangement is the rate determining step based on the large KIE ($k_H/k_D = 16$) and the lack of effect on rate when diisopropylamine is added to the reaction. ⁶Li and ¹⁵N NMR spectroscopy revealed the presence of an LDA dimer, LDA dimer-arene complexes, and aryllithium monomer LDA-aryllithium mixed dimers, and a LDA-lithium phenolate mixed dimer along the reaction pathway (**Scheme 1.13**).



Scheme 1.13

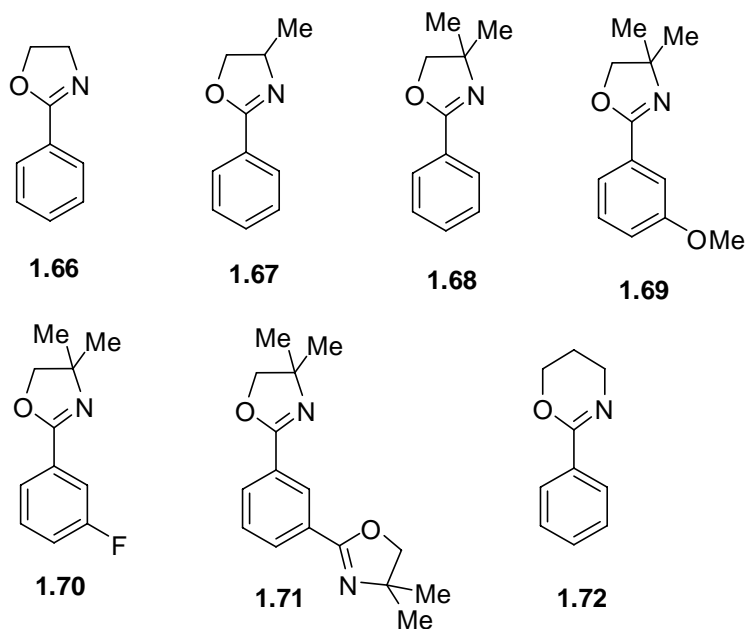
Detailed rate studies of the reaction of **1.57** with LDA, corroborated by density functional theory (DFT) calculations, suggests that *ortho* lithiation proceeds through **1.64**,

a monosolvated monomer transition state. In contrast, in poorly solvating solvents such as toluene, metalation proceeds through a monosolvated dimer **1.65** transition structure. *Ortho* lithiation is accelerated by the presence of *meta* electron withdrawing groups, e.g. $R^1 = F$. Furthermore, the need of excess LDA is suggested to break the mixed aggregate of **1.58** which may cause autoinhibition of the lithium base and thereby prevent successful metalation.



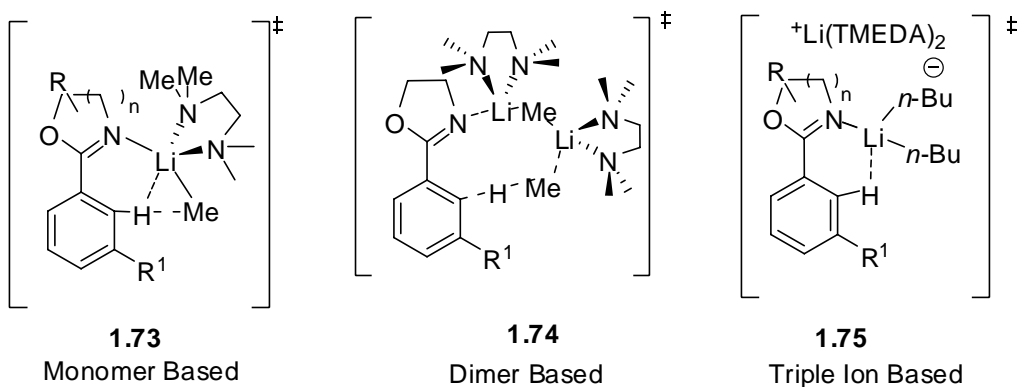
Scheme 1.14

Most recently, Chadwick and Collum investigated the the lithiation reaction of aryl oxazolines (**Scheme 1.15**).⁵²



Scheme 1.15

The studies yielded similar results to those observed for aryl *O*-carbamates in that the rate determining step involves proton transfer ($k_H/k_D = 22 - 32$), coordination of aryl oxazolines and bases (*n*-BuLi or MeLi)/0.5-5 M TMEDA in pentane stabilize the transition state but appear not to activate the *ortho*-hydrogen through an inductive effect, and the presence of *meta*- electron withdrawing groups (OMe, F) also accelerate *ortho*-lithiation. Three transition states, monomer-based (**1.73**), dimer based (**1.74**) and triple-ion based (**1.75**) were proposed to rationalize the DoM reaction of aryl oxazolines.



Scheme 1.16

In another study, Sammakia and Latham⁵³ proposed from the ratio of electrophile incorporation onto ferrocene bearing the oxazoline group that *s*-BuLi/THF-induced DoM of aryl oxazoline proceeds via *N*-rather than an *O*-directed mechanism. Collum's DFT calculations⁵² implicate subtle differences between the *N*-lithiation and *O*-lithiation in both the dimer vs the triple-ion mechanism. The monomer-based metalation shows a high preference for *N*- over *O*-directed metalation and a high sensitivity to a steric effect. Furthermore, DFT calculations indicate that the dimer based metalation is disfavored by $\Delta H > 40$ kcal/mol compared to the monomer based metalation. In the triple ion based model, *ortho*-lithiation of **1.69** was significantly stabilized by the *syn*-methoxy

orientation towards the oxazoline. This result may be questioned on the basis of the expected steric effect of the OMe group syn-oriented with respect to the oxazoline ring. However, the destabilizing effect by the deposit of the electron lone pair of oxygen of anti-oriented methoxy group in **1.69** to the already electron rich triple ion transitional structure offers a rationalization of the results derived from the computation. In addition, although the metalation of the *meta*-fluoro aryloxazoline (**1.70**) was too fast to be studied, its calculated ΔG^\ddagger was found to be >4 kcal/mol lower than that of the corresponding meta-OMe derivative (**1.69**). The facile metalation of *m*-fluoroaryloxazoline **1.70** was attributed to not only the inductive effect of the F-substituent but also to its weak coordinating ability. In the case of the aryl dioxazoline (**1.71**), the cooperative effect of two DMGs appears to be manifested in the substantial increase of the rate of reaction (about 100 times faster than that of **1.68**). The conclusion of this study on aryloxazolines is nothing more than giving substance to what chemists have qualitatively proposed previously: DMGs can exert their effects on the *D*_oM reaction through coordination with the lithium base or by inductively acidifying the proton *ortho* to the electron negative groups such as OMe and F.

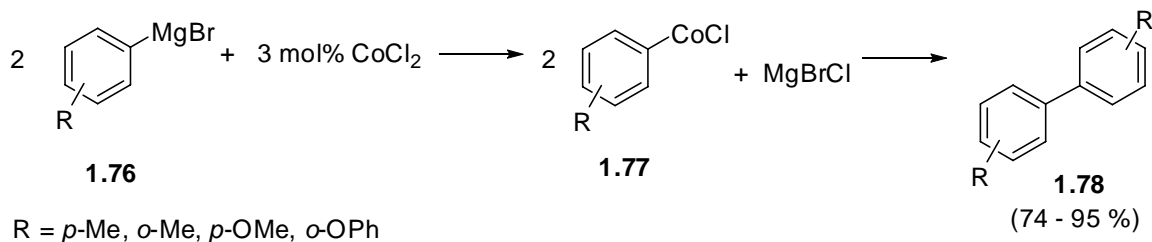
Since 1939,^{54,23,29} evidence has accumulated to support CIPE and inductive effects but less so in support of KEM as the mechanistic rationalization for the *D*_oM reaction. However, the *D*_oM mechanism may vary as a function of conditions, i.e. solvents, bases, as well as the nature of the DMGs. What is probably clear is that electro negative atom containing DMGs i.e. OMe or F, under standard metalation conditions may exert their directing effects through an inductive effect and that *O*-carbamate and carboxamide DMGs, bearing a site for coordinating with metals may proceed by a CIPE

mechanism mainly. At the risk of stating the obvious, the rate law of DoM does not provide the structure of the transition state, but the stoichiometry has shed light on the possible structure of the transitional state, studies which have been largely explored by the Collum group^{44,51,52,55} using experimental and computational approaches. However, calculations are not to be taken easily without the backing of empirical experimental results. Not when all these are certified and considered, the mechanism of the DoM still remains elusive and disputable.

1.2.2. The DoM Boronation Suzuki-Miyaura Cross Coupling Reaction

1.2.2.1. Mechanism of Suzuki-Miyaura Cross Coupling Reaction

In the context of modern synthetic organic chemistry, the aryl-aryl transition metal - catalyzed cross coupling reaction has become the master piece over the past three decades, with the name reactions of Kumada-Corriu-Tamao,^{56,57} Negishi,⁵⁸ Migita-Stille,⁵⁹ Hiyama^{60,61} and Suzuki-Miyaura⁶² for magnesium, zinc, tin, silicon, and boron as the catalytic active metal species respectively being readily recognized by the synthetic community (**Table 1.2**). The current status owes its origin in the discovery of Kharasch who, in 1941 first employed Grignard reagents **1.76** and cobaltous chloride as the co-catalyst to achieve the homo coupling of aryls (**Scheme 1.17**) to yield the biaryls **1.78**.⁶³



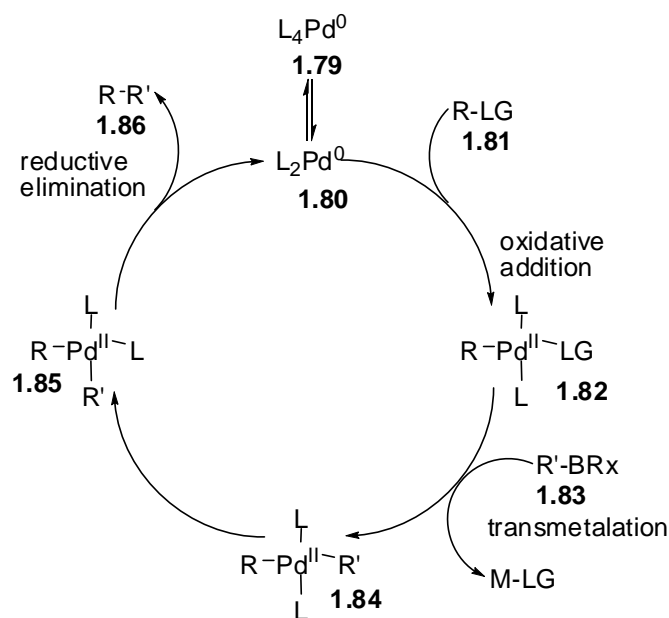
Scheme 1.17

It was not until the 1970 when Kumada⁵⁷ and Corriu⁵⁶ independently reported the Ni-catalyzed cross coupling of Grignard reagents with vinyl or aryl halides, which marked the beginning of the development of the transition metal catalyzed aryl-aryl cross coupling reaction. An analogous zinc cross coupling reaction, discovered by Negishi, shows tolerance for a variety of substrate functional groups because organozincs are less nucleophilic than their magnesium analogs. Organomagnesium and organozinc compounds are nevertheless unstable for prolonged periods of time. In contrast, organostannes and organoborons are stable in air and water and can be stored on the shelf for extensive time without serious degradation. In addition to these established cross coupling reactions, the Hiyama silicon-based cross coupling, which is of more recent origin, is primed for further exploration and requires new convenient methodology for the preparation of organosilane starting materials. These cross coupling reactions are summarized in **Table 1.2**.^{56,57,64-71}

Ar ¹ Met	+	Ar ² LG	$\xrightarrow{\text{NiL}_n \text{ or PdL}_n}$	Ar ¹ - Ar ²	
Met		LG	Investigator	Yr	Refs
MgX		hal, OTf	Corriu Kumada	1972	56-57
ZnX		hal, OTf	Negishi	1976-77	58, 64
B(OH) ₂		Br, I, OTf	Suzuki	1979	66
BF ₃ K		Br, I	Batey Molander	2001-02	67
SnR ₃		hal OTf	Migita, Stille	1977-78	68
SiRF ₂		I	Hiyama	1989	69
SiR ₂ OH		I	Denmark Mori	1999	70, 71

Table 1.2

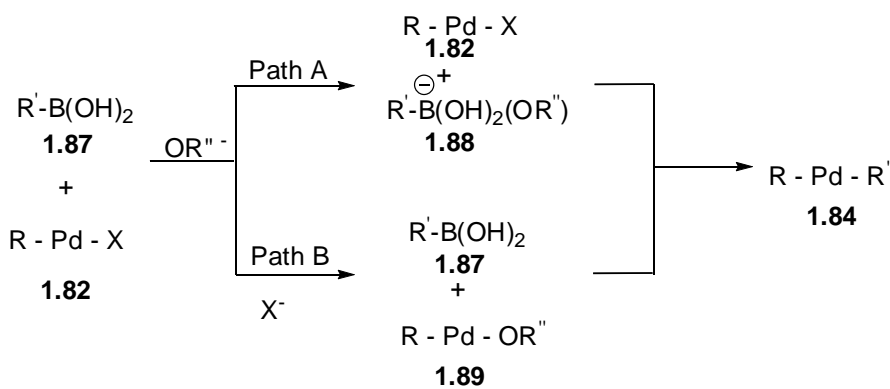
The Suzuki-Miyaura cross coupling reaction has been developed into a general process for a wide range of selective carbon-carbon formations. Because of environmental friendliness, tolerance to many different functional groups, stability toward air and oxygen, and convenience for preparation of organoboron compounds, much attention has recently been focused on the Suzuki Miyaura cross coupling protocol.⁶⁵ Furthermore, in spite of the broad synthetic application, the mechanism of the Pd catalyzed Suzuki-Miyaura reaction is poorly understood. The currently given mechanism involves the standard scheme of oxidative addition, transmetalation, and reductive elimination (**Scheme 1.18**).⁷²⁻⁷⁴



Scheme 1.18

Pre-catalyst **1.79** first undergoes ligand dissociation to form **1.80** which is believed to be the active catalyst on the basis of kinetic, and 1H and ^{31}P NMR spectroscopic studies.^{75,76} Then the Pd (0) active catalyst undergoes oxidative insertion to form **1.82**. Although reactions vary with the type of substrates that are added, oxidative addition is normally the rate - determining step of the catalytic cycle.^{65,77} A kinetic study

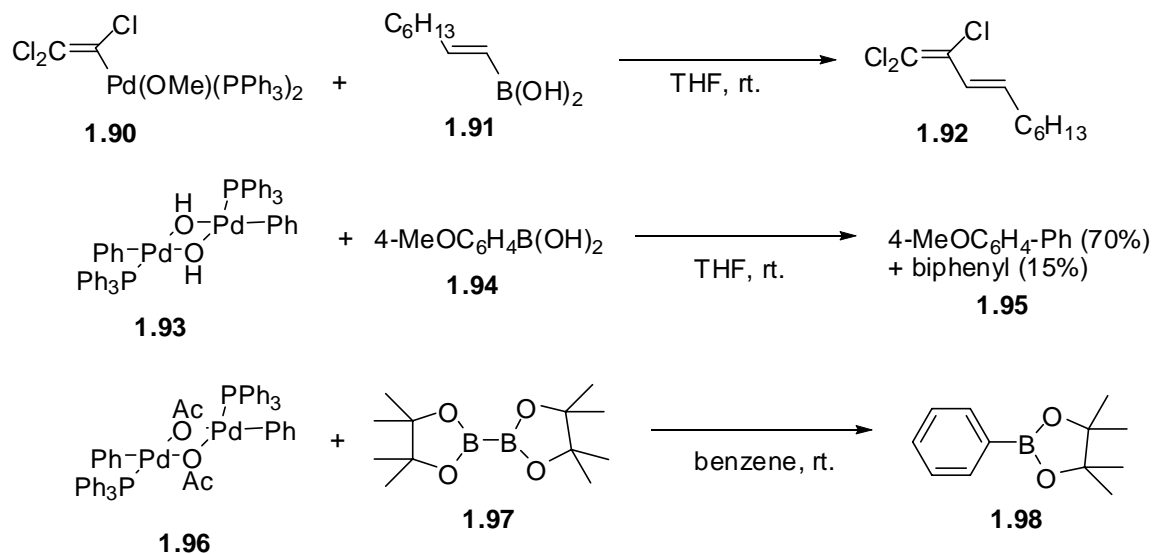
on the Ni (0) and Pd (0) - catalyzed reaction⁷⁸ suggested that the mechanism of the oxidative addition of aryl iodide to [PdL₂] **1.80** can be related to aromatic nucleophilic substitution since the rate of the reaction is accelerated for aryl halides containing electron withdrawing substituents. The reactivity of halides or leaving groups decreases in the order of I > OTf > Br >> Cl, >>> F.^{75,79,80} Subsequently, transmetallation from **1.83** to the Pd (II) **1.82** is proposed to occur to yield **1.84**. The use of base is obligatory for the Suzuki-Miyaura cross coupling reaction in order to critically increase reactivity of the transmetallation step. Nevertheless, the transmetalation is poorly understood. In 2002, Miyaura proposed two possible simplistic pathways (**Scheme 1.19**) of base-assisted transmetallation derived from the available information.⁸¹ In path A, nucleophilic addition of OR''⁻ to boronic acid **1.87** gives the ate complex **1.88** which, upon transmetallation, leads to **1.84**. In path B, nucleophilic substitution of X⁻ with OR''⁻ gives **1.89** which, being more electron rich than **1.82**, readily undergoes transmetallation to provide **1.84**.



Scheme 1.19

Although there is no direct evidence to support path A via **1.88**, ate complexes such as [RC≡CBR₃]₂Li,⁸² R₄B⁻Li,⁶⁵ [ArBR₃]₂Li,⁶⁵ Ph₄B⁻Na,^{83,84} [R₃BO-Me]⁻Na,⁸⁵ [ArB(R)(OR)₂]₂Li,⁸⁶ and [ArBF₃]⁻K⁸⁷ are well known and have been used in Pd and Ni-

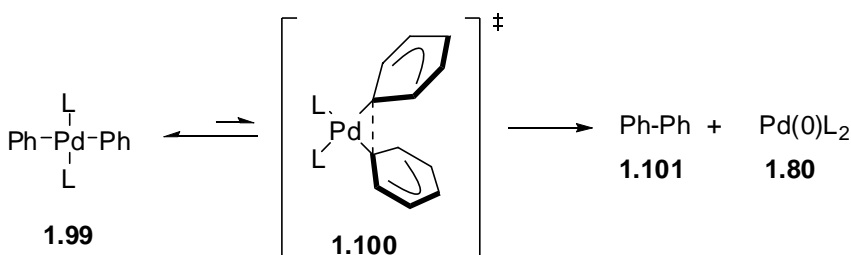
catalyzed cross coupling reactions. On the other hand, path B is supported by studies in which the “oxidative addition” type methoxo,⁸⁸ hydroxo,⁸⁹ and (acetoxo)palladium (II) complexes⁸⁸ undergo cross coupling upon treatment with an organoboron compounds (**Scheme 1.20**). However, on the basis of computational studies using ONIOM and DFT methods, Maseras and coworkers⁹⁰ concluded that path B can be safely excluded because of the many unreasonably high energy complexes in this path. In addition, oxopalladium complexes, e.g., **1.90** were suggested to be generated from oxidative insertion of Pd(0) to R-(OR’’) bond rather from nucleophilic replacement of **1.82** by OR’’⁻. In other words, bases exert their effects to enhance the rate of the Suzuki-Miyaura cross coupling reaction most likely by increasing the nucleophilicity of the borane (R-B(OR)₂) via borate formation.^{90,91}



Scheme 1.20.

Although many studies have been devoted into the investigation of oxidative addition, relatively fewer studies have been carried to discover the mechanism of reductive elimination. Nevertheless, the *trans* to *cis* isomerization from **1.84** to **1.85** was

repeatedly proposed to occur prior to reductive elimination.^{65,92} In 1989, a study by Stang and Kowalski⁹³ suggested that *cis*-isomerization was taken effects through dissociation of trans isomer **1.84**. The facts of addition of PPh₃ that would inhibit the cross coupling of two organo groups in the isolated **1.84** Pt analogue complex and would slightly enhance the rate of cross coupling of two organo groups in the isolated **1.85** Pt analogue complex indicate that the ligands in trans-isomer must undergo dissociation as the rate limiting step which could be impeded by the addition of PPh₃. In addition, cross coupling of two organo groups in *cis*-isomer **1.85** would probably involve concerted reductive elimination from activated complex **1.100**. Thus, in the context of transitional metal catalyzed cross coupling reaction, it was proposed that reductive elimination would follow the pathway as illustrated in Scheme **1.21** where **1.99** would isomerizes to *cis*-like complex **1.100** that would immediately give the cross coupling biphenyl **1.101** after the reductive elimination of two cross coupling partners from the catalytic cycle accompanied with regeneration of Pd(0)L₂ **1.80**.^{94,93}

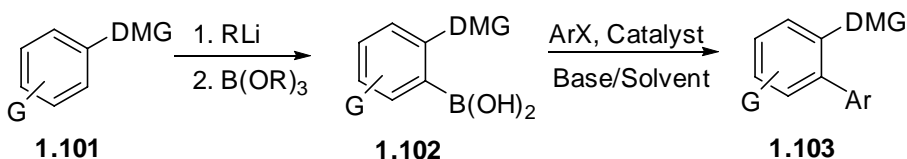


Scheme 1.21.

1.2.2.2. Practical Aspects of the DoM – Suzuki Cross Coupling Reaction: Characterization of Boronic Acids, Catalyst / Ligands, Bases and Solvents

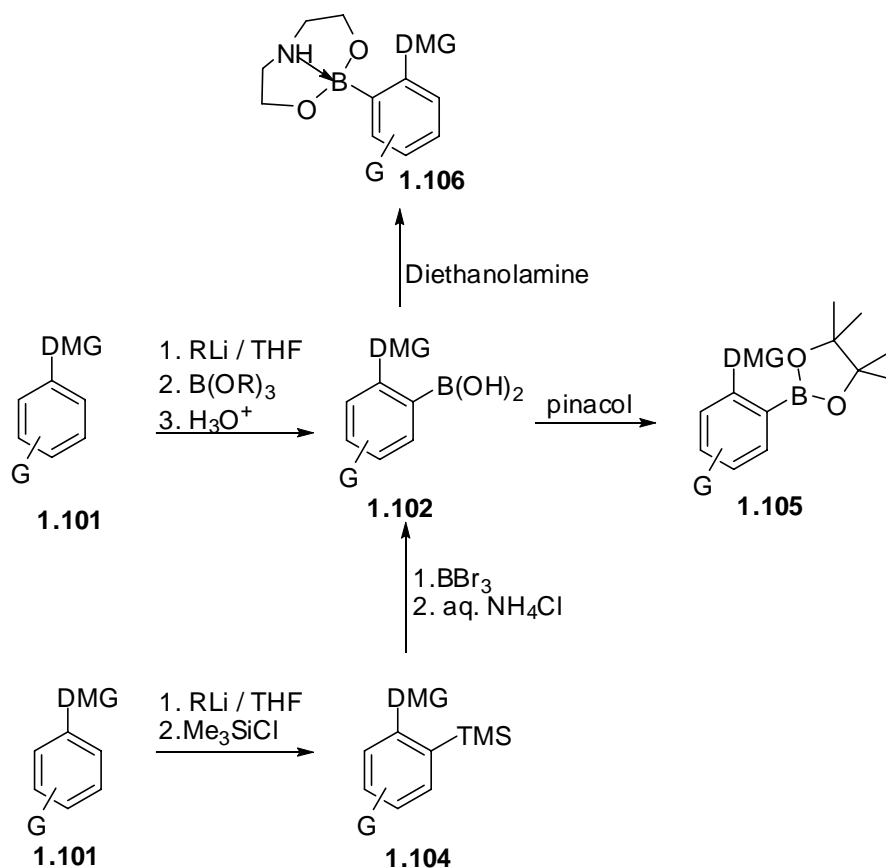
The synthesis of arylboron compounds may be achieved by three general strategies: transmetalation,^{67,95-98} cross coupling⁹⁹⁻¹⁰¹ and aromatic C-H borylation.¹⁰²⁻¹⁰⁴

Among these, transmetallation offers the most straightforward method for preparing arylboron compounds because the requisite organometallic reagent is easily available.¹⁰⁵ Connecting transmetallation to DoM for Li-B exchange was first demonstrated in 1985¹⁰⁶ to provide assured regiochemistry for the Suzuki-Miyaura cross coupling, a reaction which has seen subsequent broad application (**Scheme 1.22**).¹⁰⁷



Scheme 1.22.

CONR_2 ,¹⁰⁸ OCONR_2 ,¹⁰⁹ OMe ,¹¹⁰ OMOM ,¹¹¹ SO_2NEt_2 ,¹¹² OSO_2NEt_2 ,²⁶ and NHCOR ¹¹³ have been employed as DMGs in the DoM reaction to construct *ortho*-functionalized arylboronic compounds via direct Li-B exchange or *ipso*-borodesilylation of aryl silane **1.104** prepared by Li-Si exchange (**Scheme 1.23**).¹¹⁴ Following treatment of **1.102** with pinacol and diethanolamine would afford the pinacol boronate **1.105** and arylborocane **1.106** respectively.



Scheme 1.23.

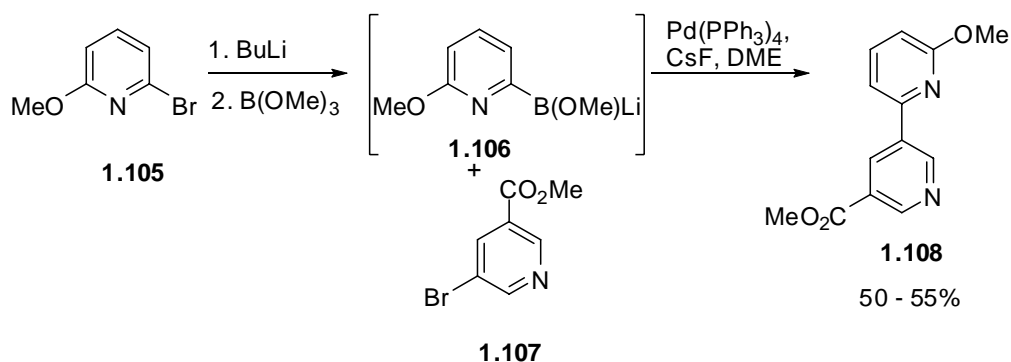
The reaction of an aryllithium (or arylmagnesium)²⁶ with B(OR)_3 leads to the initial formation of a relatively unstable $\text{ArB(OR)}_3\text{Li}$ in equilibrium with ArB(OR)_2 and ROLi .⁹⁵ This sometimes leads to the formation of undesirable di-, tri-, or tetraorganoborates.⁹⁵ Based on yields and cleanliness of reaction triisopropyl borane is the best available borane reagent for the formation of $\text{ArB(OR)}_3\text{Li}$ without production of other organoborates and thereby leads smoothly to ArB(OH)_2 by hydrolysis upon treatment of acid.^{95,115} Nevertheless, after recrystallization, NMR spectroscopy of selected cases in CDCl_3 has shown two pairs of signals corresponding to a boronic acid and a boroxine, a mixture of boronate oligomers.¹¹⁶ For the purpose of purification and obtaining a crystalline highly stable boronic acid derivative, the diethanolamine adducts

are recommended and have been prepared.^{117,118} In addition, bulky pinacolato boronates may have sufficient stability for chromatographic purification and GC analysis.⁹⁶ While pinacolato boronates participate broadly in Suzuki reactions,^{119,120} the corresponding diethanolamine adducts require an *N*-substituent and Pd-Cu cocatalyst for successful reactions or reconversion to the respective boronic acids.^{121,122}

In the quest of using these organo boron compounds in cross coupling reactions, the nature of Pd catalysts, bases, and solvents must be taken into consideration.⁶⁵ Transition metal (Pd, Pt,¹²³ and Ni¹²⁴) catalysts have been developed to tune for the optimum efficiency of Suzuki-Miyaura cross coupling reaction. Pd(PPh₃)₄ has been so frequently used that it has become a “standard catalyst” and is found to be effective in many of cross-coupling reactions.⁶⁵ Nevertheless, in some cases, especially cross couplings of sterically hindered aryl boronic acids or aryl chlorides bearing electron donating groups, the reactions catalyzed by Pd(PPh₃)₄ are dramatically attenuated.¹²⁵ As a result, much research have been devoted into the development of ligands for a number of Pd (II) catalyst precursors, e.g., Pd(OAc)₂, PdCl₂, Pd₂dba₃ and PdCl₂(dppf).¹²⁶ Perusal of the literature (see also **Scheme 1.25** and **Table 1.3**) shows that P(*t*Bu)₃ and S-Phos championed by Fu¹²⁷ and Buchwald¹²⁸ respectively, are efficacious, versatile phosphine ligands that significantly improve the reactivity of *in situ* generated Pd(0) catalysts. (1,3-Diisopropylimidazol-2-ylidene)(3-chloropyridyl)palladium (II) dichloride (PEPPSI) is a *N*-heterocycle carbene-Pd complex ligand that is receiving increased attention due to advantage of low loading making it appealing for industrial use.¹²⁹

The mild base Na₂CO₃ is effective in a wide range of cross coupling reactions of arylboronic acids. Tests of reactivity of bases^{130,131} in the cross coupling of

mesitylboronic acid with iodobenzene was carried out to show the following order of reactivity: TIOH > Ba(OH)₂ > Tl₂CO₃ > NaOH > Cs₂CO₃, K₃PO₄ > Na₂CO₃ > NaHCO₃. The bases Na₂CO₃, Cs₂CO₃, K₃PO₄, NaOH, Ba(OH)₂ and TIOH are usually suitable for aryl-aryl cross coupling reactions in mixed organic-aqueous media (H₂O/toluene,¹³² H₂O/DME,¹³³ H₂O/dioxane¹³⁴ and H₂O/THF¹³⁵). The higher reactivity and lower toxicity of Ba(OH)₂ base makes it a more favourable base than TIOH, especially for the synthesis of sterically hindered tri-*ortho*-substituted biaryls.^{136,137} However, protodeboronation can be a serious problem for more electron poor aryl boronic acids such as 3-formyl-2-thiopheneboronic acid¹³⁸ and bis(thiophene)boronic acids.¹³⁹ In addition, 2-pyridylboronic acid provides no coupling products most likely due to rapid protodeboronation.¹⁴⁰ To overcome this problem, an ate complex **1.106** (Scheme 1.24) was generated *in situ* directly from **1.105** and its cross coupling with **1.107** to furnish the bipyridine derivatives **1.108** was achieved in modest yield.¹⁴⁰ To circumvent the problem of competitive protodeboronation, K₃PO₄·H₂O,¹²⁴ CsF¹⁴¹ and NEt₃¹⁴¹ are often employed in non-aqueous media (i.e THF, DME and DMF).

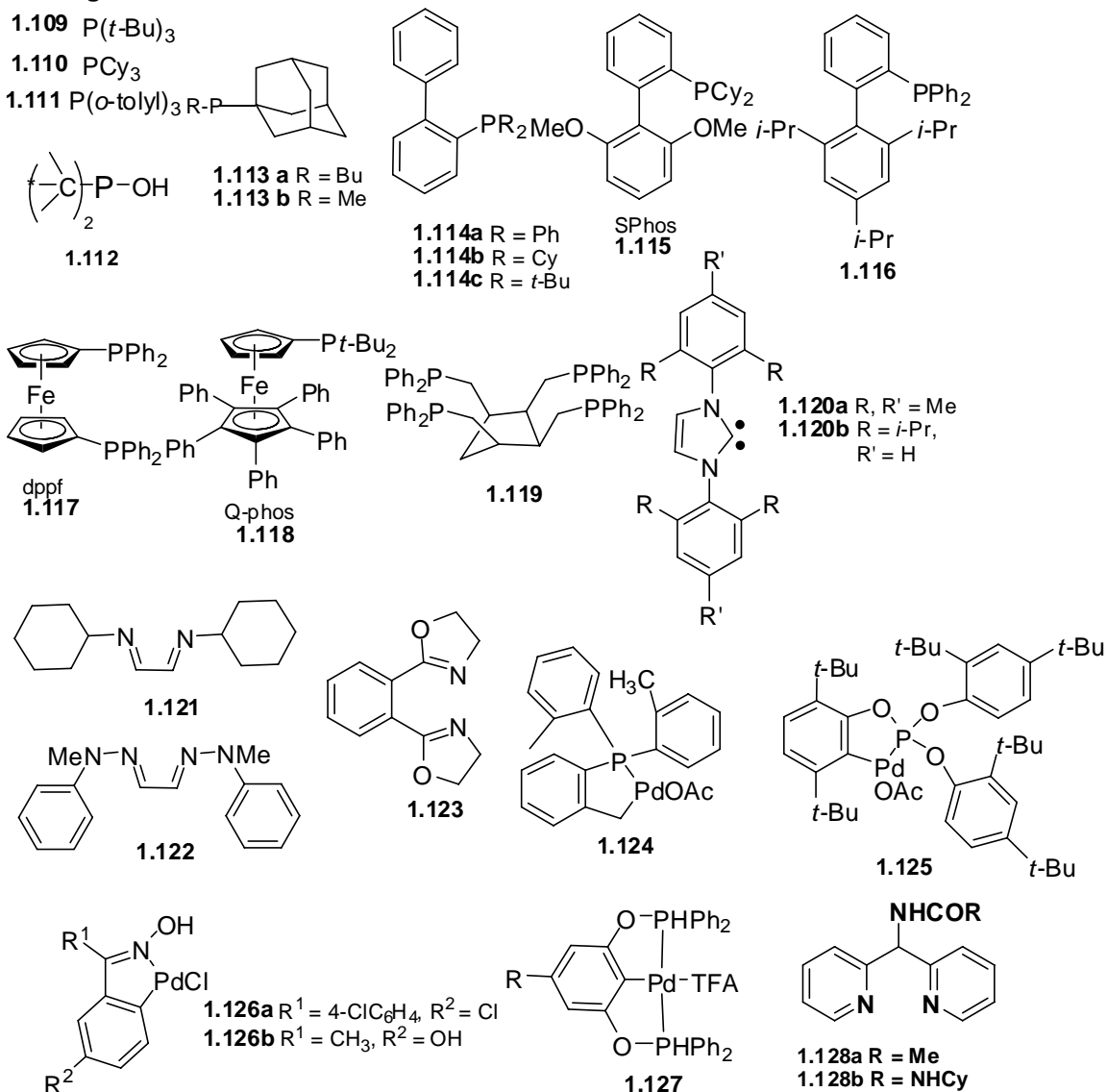


Scheme 1.24.

Pd Catalyst: Pd(PPh₃)₄, Pd(OAc)₂, Pd₂(dba)₃, PdCl₂(dppf), Pd(PPh₃)₂Cl₂, Pd(acac)₂

Ni Catalyst: NiCl₂(PPh₃)₂, NiCl₂(dppf)

Ligand Structure:



Scheme 1.25.

Suzuki-Miyaura cross coupling reaction, over more than two decades of continuing efforts, has become a widely practiced and useful method to construct Sp² C-Sp² C bonds of various substrates. Many of these conditions were developed to advance this technique. Perusal of literature revealed that conditions of this methodology vary

with bases, solvents, temperature, catalysts and ligands of which some examples were provided here in **Table 1.3** for the purpose of demonstration and discussion invoked in previous paragraphs.

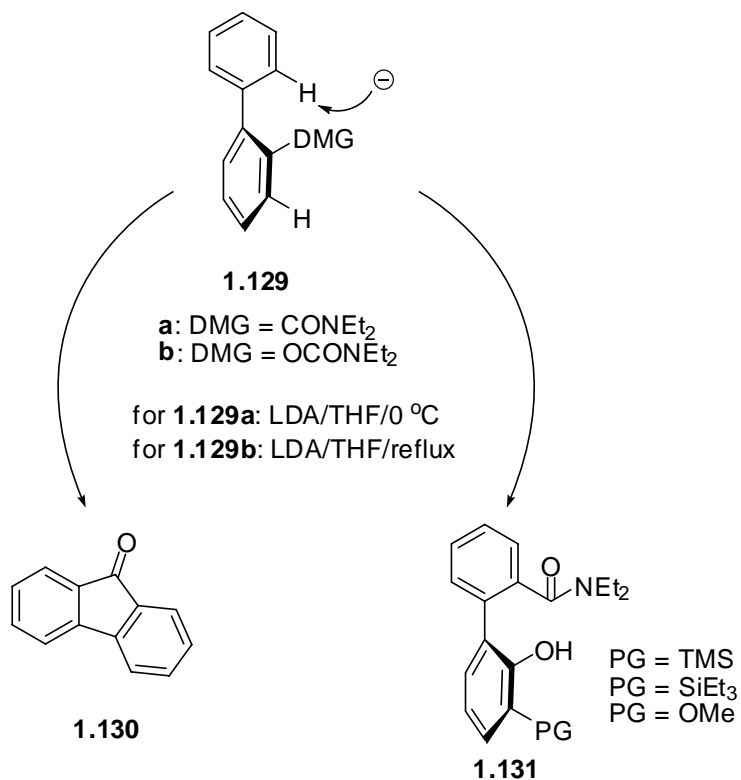
#	Bases	Solvents	Temp. (^o C)	Catalysts	Ligand	Ref.
1	Na ₂ CO ₃	Tol-MeOH-H ₂ O	80	Pd ₂ (dba) ₃	1.111	142
2	Na ₂ CO ₃	MeOH-H ₂ O	reflux	Pd(PPh ₃) ₄	—	143 144
3	Na ₂ CO ₃	toluene-H ₂ O	reflux	Pd(PPh ₃) ₄	—	145 146 147
4	Na ₂ CO ₃	1,4-dioxane	reflux	Pd(PPh ₃) ₂ Cl ₂	—	148
5	NaOH	Benzene-THF	65	Pd(PPh ₃) ₄	—	149
6	NaOH	Toluene-H ₂ O	99	Pd(PPh ₃) ₄	—	132
7	NaHCO ₃	DME-H ₂ O	80	Pd(PPh ₃) ₄	—	150
8	NaHCO ₃	DMF-H ₂ O	50	Pd(PPh ₃) ₄	—	151
9	K ₃ PO ₄	10:1 Tol:H ₂ O	100	Pd(OAc) ₂	1.115	128
10	K ₃ PO ₄	<i>n</i> -butanol	90-100	Pd ₂ (dba) ₃	1.115	128
11	K ₃ PO ₄	Toluene	80 – 100	Pd ₂ (dba) ₃	1.114b	125
12	K ₃ PO ₄	<i>n</i> H ₂ O, dioxane	80	NiCl ₂ dppf	—	152
13	K ₃ PO ₄	<i>n</i> H ₂ O, toluene	80	NiCl ₂ (PPh ₃) ₂	1.117	153
14	K ₃ PO ₄	<i>n</i> H ₂ O, toluene	80	NiCl ₂ (PPh ₃) ₂	1.117	154
15	K ₂ CO ₃	Bu ₄ NBr-H ₂ O	70	Pd(OAc) ₂	—	155
16	K ₂ CO ₃	THF/DME/ H ₂ O	80	PdCl ₂ (dppf)	—	156
17	KF	THF	r.t.	Pd ₂ (dba) ₃	1.109	127
18	KF	THF	r.t./100	Pd ₂ (dba) ₃	1.118	157
19	KOH	MeOH/H ₂ O	60	Pd(OAc) ₂	1.128b	158
20	Cs ₂ CO ₃	Dioxane	80	Pd ₂ (dba) ₃	1.120a	159 160
21	Cs ₂ CO ₃	Dioxane	r.t	Pd ₂ (dba) ₃	1.109	161 127
22	CsF	DME	85	Pd(PPh ₃) ₄	—	162
23	TIOEt	THF-H ₂ O	r.t.	PdCl ₂ (dppf)	AsPh ₃	163

#	Bases	Solvents	Temp. (°C)	Catalysts	Ligand	Ref.
24	TIOH	THF-H ₂ O	r.t.	PdCl ₂ (dppf)	AsPh ₃	164 165
25	Ag ₂ O- K ₂ CO ₃	Toluene	100	Pd(OAc) ₂	PPh ₃	166
26	Et ₃ N	<i>n</i> -PrOH-H ₂ O	reflux	PdCl ₂ (dppf)	—	167 168

Table 1.3.

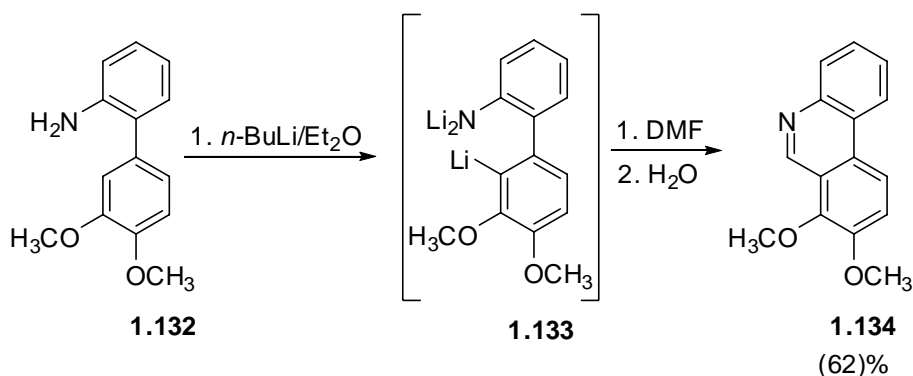
1.2.3. The Directed Remote Metalation (DreM) Reaction

The discovery of the remote ring regioselective deprotonation of biaryl amide¹⁶⁹ and *O*-carbamate^{170,171} derivatives has led to the development of a general strategy, referred to as the Directed remote Metalation (DreM) reaction, for the synthesis of fluorenones and more highly substituted biaryl amides respectively (**Scheme 1.26**).

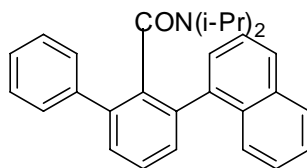


Scheme 1.26.

The earliest reported case of DreM in the context of biaryl system was provided by Narahimhan and Chandrachud¹⁷² in the synthesis of 7,8-dimethoxy phenanthridine **1.134** (Scheme 1.27). Thus, treatment of **1.132** with *n*-BuLi followed by DMF quench was reported to lead to **1.134** proceeding via the lithiated intermediate **1.133**. However, Meyers¹⁷³ reported that Narahimhan's result was not reproducible. Further exploration of DreM was actually inspired by the examination of the X-ray crystallographic structure of a *m*-terphenyl **1.135**¹⁷⁴ (Scheme 1.28) and by considering the role of CIPE in the compounds bearing amide as the DMG.³¹



Scheme 1.27.

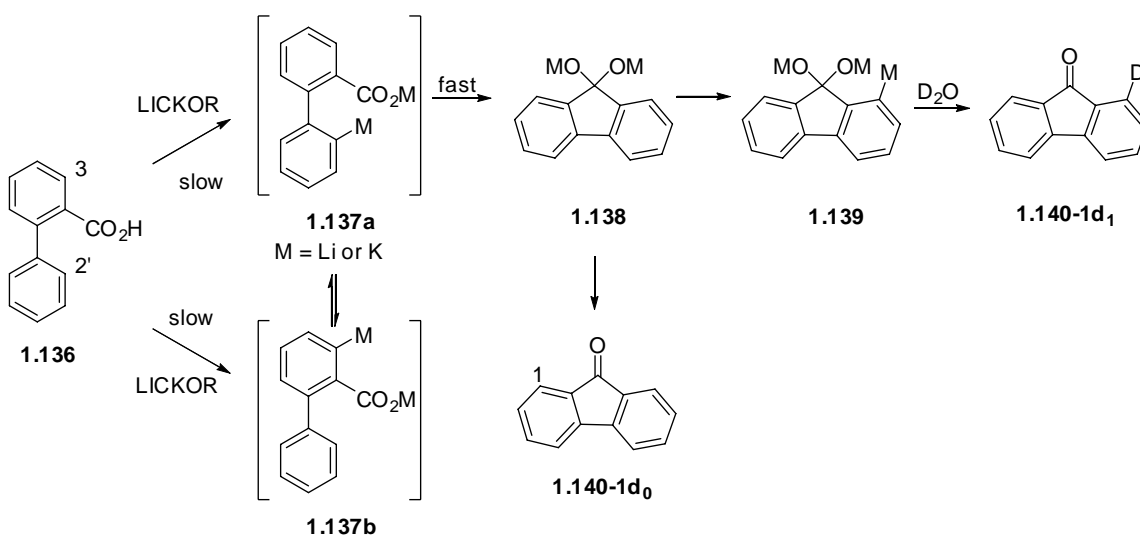


1.135

Scheme 1.28

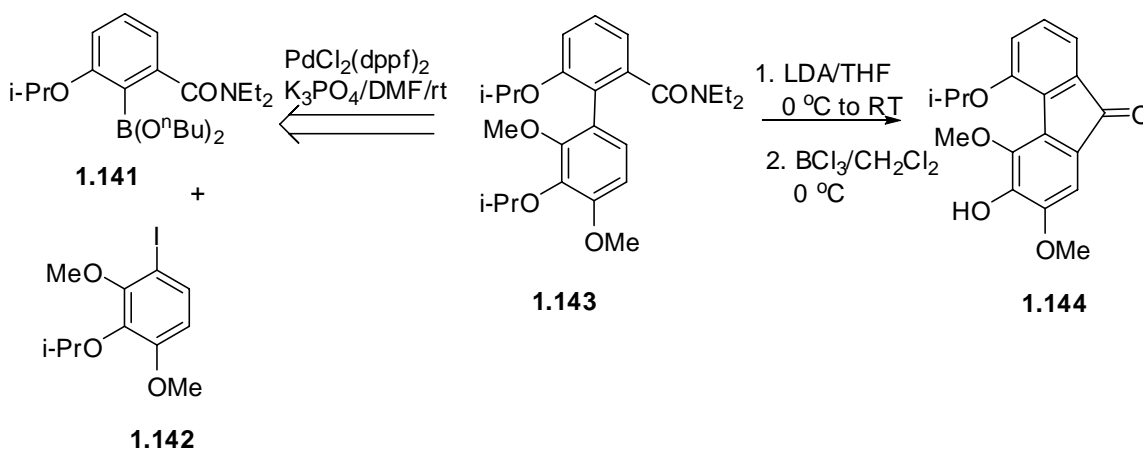
Mechanistic aspects of the DreM reaction mediated by the Lochmann-Schlosser base, LICKOR (*n*-butyllithium/*t*-BuOK) were recently examined by Mortier and Tilly.¹⁷⁵ Mechanistic evidence was obtained by studying the reaction as a function of bases, order

of base addition and duration of metalation, and interpretation of the results was based on deuterium incorporation in the observed products. Treatment of **1.136** with 3.5 equivalent of LICKOR for one hour at 60 °C followed by quench with excess D₂O at room temperature provided the fluorenone **1.140-1d₁** (41% 1d₁, 59% 1d₀) in 76% yield after separation from unreacted **1.136** (20% 3d₁, 80% 3d₀). This result suggested that metalation of 2-biphenyl carboxylic acid **1.136** with excess LICKOR could occur at the remote 2' position and / or 3 position (**Scheme 1.29**). Furthermore, **1.140-1d₁** and **1.140-1d₀** were derived from the geminal dimetalloalkoxide intermediate **1.138**, which can be completely converted to **1.139** by addition of base. Indeed, treatment of **1.135** with 5 equivalent of LICKOR for one hour prior to addition of *n*-BuLi to the reaction mixture followed by D₂O work-up furnished deuterated fluorenone **1.140-1d₁** (**100% d₁**) in 70% yield. The authors concluded that metalation of 2-biphenylcarboxylic acid in 3-position and 2'-position was assisted by pre-coordination (CIPE) of base with carboxylate, and that the dimetallo dialkoxide was the probable intermediate in order to rationalize the requirement of three equivalents of LICKOR for optimal conversion of **1.136** to **1.140**.



Scheme 1.29. Mortier's investigation on DreM mechanism of biphenyl-2-carboxylic acid.

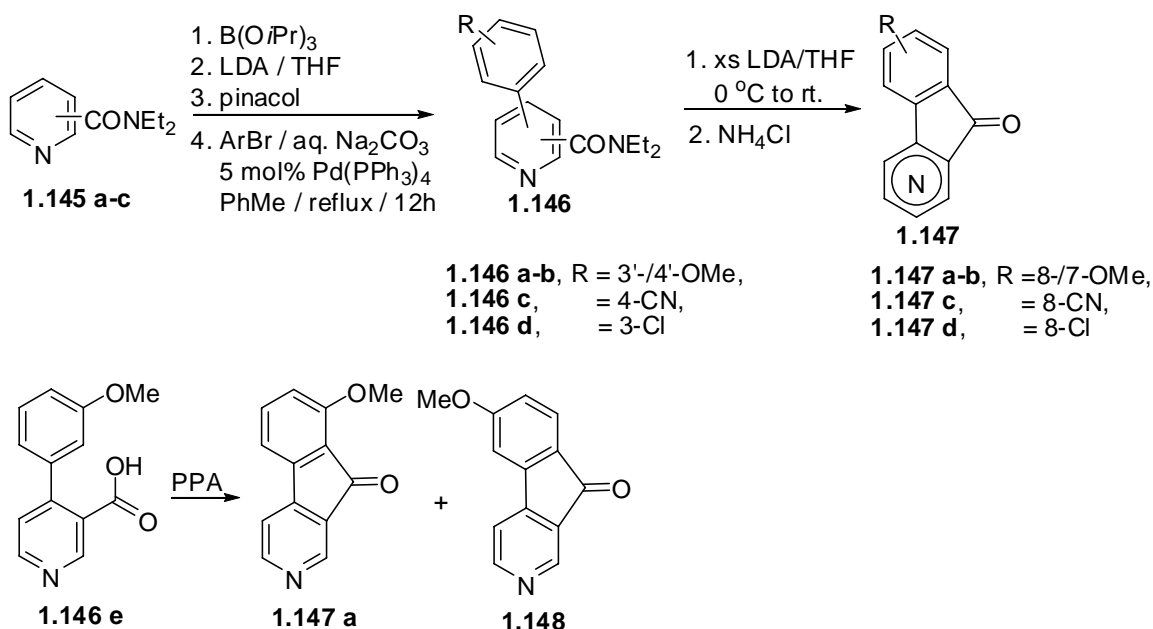
The utility of the DreM reaction was demonstrated in the total synthesis of dengibsin¹⁶⁹ and dengibsinin.¹⁷⁰ The biaryl **1.143**, available by a Suzuki-Miyaura cross coupling reaction was sequentially subjected to LDA- induced DreM-cyclization and selective deisopropylation to yield dengibsinin **1.144** in 24% overall yield over 5 steps (**Scheme 1.30**). The DreM – mediated cyclization was generalized for the synthesis of a large number of fluorenones from *m*-teraryls in the same study.¹⁷⁰ The DreM protocol was also used to synthesize fluorenone/fluorenol liquid crystal¹⁶ core structures whose properties will be discussed in Chapter 3.



Scheme 1.30.

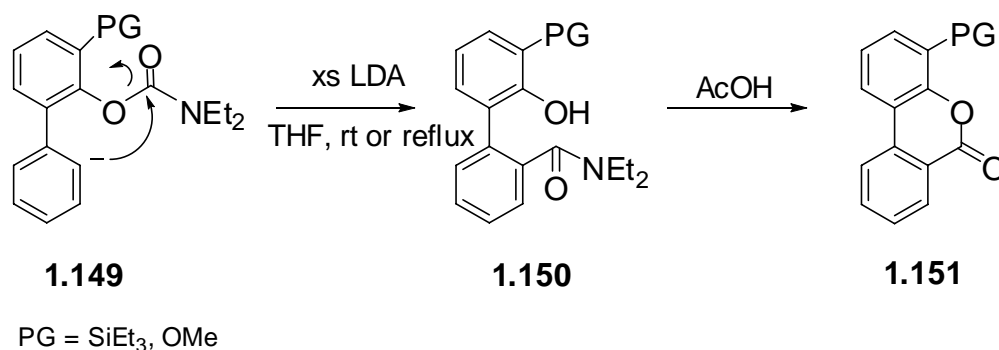
Recently, the synthesis of a selected group of azafluorenones **1.146 a-d** from the picolinamide, nicotinamide and isonicotinamides **1.145 a-c** by a one pot protocol *DoM*-boronation and Suzuki-Miyaura cross coupling reaction, followed by an DreM-cyclization step of the resulting azabiaryls **1.146 a-d** was achieved in 26 – 50% overall yields (**Scheme 1.31**).¹¹⁸ The one-pot procedure avoids the tedious isolation of the usually unstable intermediary pyridyl boronic acids,^{176,177,122} and thereby allows a straightforward access to the azafluorenone **1.147 a-d** some of which cannot be obtained

using classical Friedel-Craft cyclization technology. The DreM strategy can be regarded as an anionic Friedel-Craft equivalent which serve as a complement to the Lewis acid mediated processes. In fact, **1.146 e** was reported to afford an approximately 1:1 mixture of **1.147a** and the isomeric-6-methoxy-2-azafluorenone **1.148** (72% combined yield).¹⁷⁸



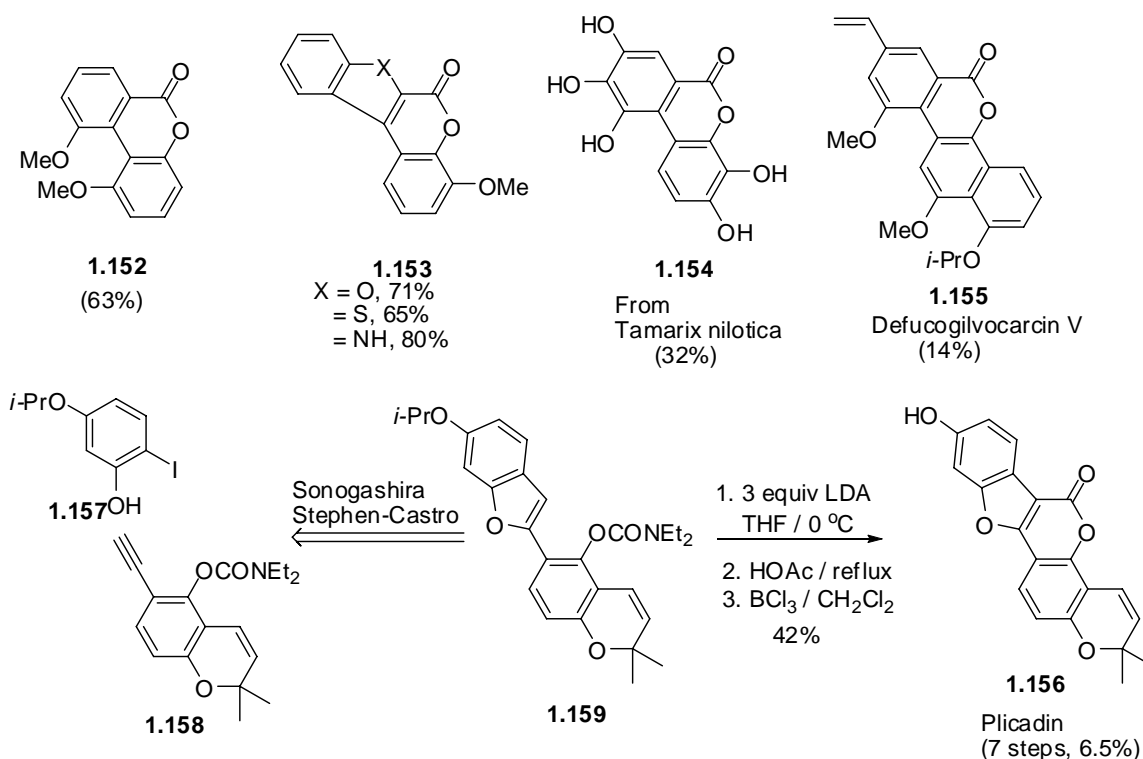
Scheme 1.31.

The anionic *ortho* Fries rearrangement of *O*-aryl carbamates to give *N,N*-diethyl-2-hydroxybenzamides was discovered in 1983.²⁵ In the biaryl 2-*O*-carbamate series **1.149** (**Scheme 1.32**), LDA-mediated *ortho* carbamoyl migration is precluded by the presence of a PG and instead the DreM – migration process is observed to furnish **1.150**. This reaction is of synthetic interest in that a) it allows a “piggy-back” approach to prepare highly hindered 2,2'-biaryls which may not be readily obtained by direct Suzuki cross coupling and b) it may be used for the construction of dibenzopyranones **1.151**.



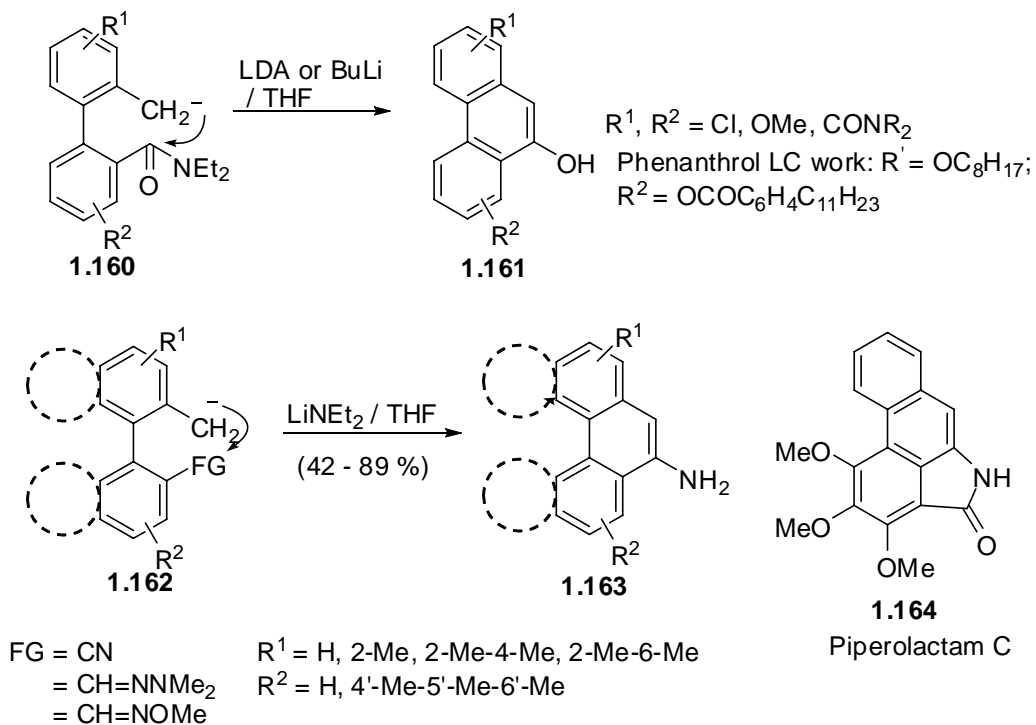
Scheme 1.32.

Illustrations of the use of the *O*-carbamoyl biaryl DreM – migration reaction in concert with DoM and cross coupling chemistry includes the synthesis of highly oxygenated dibenzopyranone such as peri-substituted **1.152**, heterocyclic analogues **1.153**¹⁷⁹ and the natural product from *Tamarix nilotica* **1.154**,¹⁷¹ defucogilvocarcin V **1.155**¹¹¹ and plicadin **1.156**.¹⁸⁰ For the latter example, a Sonogashira – Stephens-Castro reaction cascade of **1.157** (**Scheme 1.33**) with the chromene **1.158**, prepared by combined DoM - Sonogashira methodology affords **1.159**, which, after DreM - cyclization and selective deprotection leads to plicadin **1.156** in 6.5% overall yield.



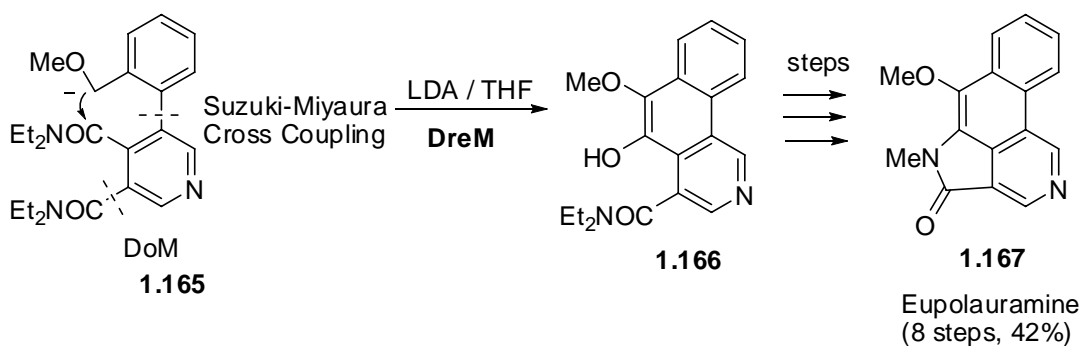
Scheme 1.33.

The DreM chemistry of substituted tolylbiaryls 2-methyl-2'-amido biaryls **1.160** provides 9-phenanthrols **1.161** with substitution patterns which are not readily prepared by conventional methodologies,¹⁸¹ e.g., electrophilic substitution,¹⁸² Pschorr reaction,¹⁸³ Mallory photocyclization¹⁸⁴ and which also usually lead to mixtures of isomers.¹⁸¹ LC with phenanthrols cores are also readily synthesized by DreM of 2-methyl-2'-amidobiaryls.¹⁸⁵ In the substituted **1.162** containing nitriles, oximes ethers and hydrazones rather than amides, the DreM reactions proceed with the deprotonation of the benzylic site followed by cyclization leads to the production of the corresponding 9-aminophenanthrene **1.163** (Scheme 1.34). Using this method, piperolactam C **1.164**,¹⁸⁶ a natural product which is believed to detoxify metabolites of aristolochic acids,¹⁸⁷ was synthesized.



Scheme 1.34.

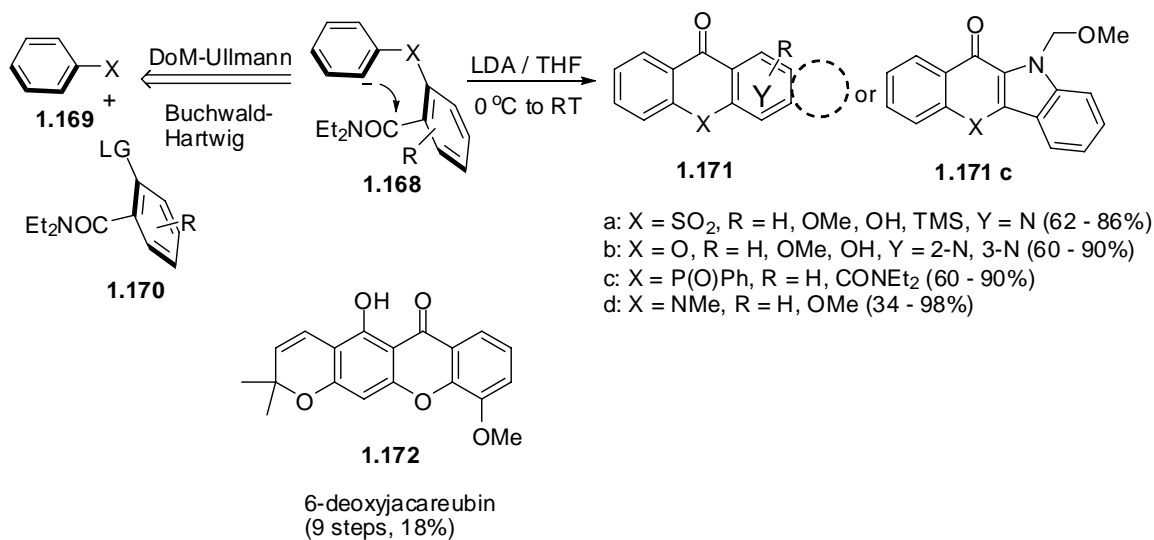
Similarly, manipulation of **1.165**, derived by a DoM-cross coupling sequence by DreM chemistry allows the efficient construction of the natural products Eupolauramine **1.167**.¹⁸⁸



Scheme 1.35.

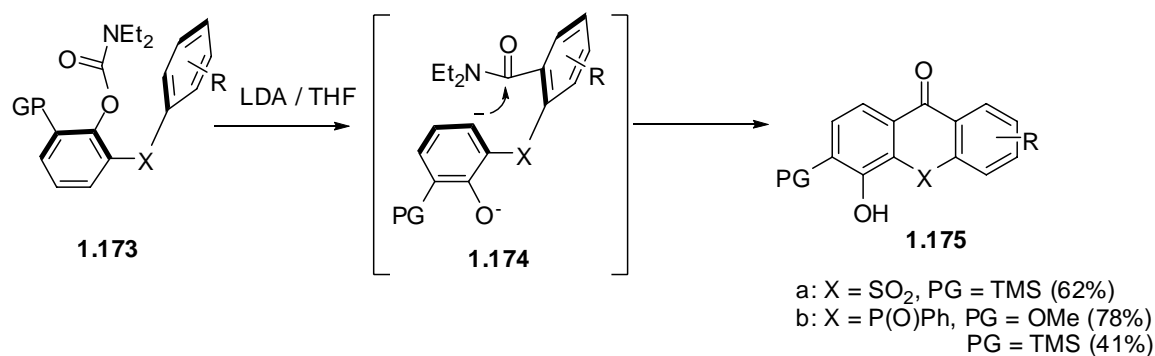
In an extension of the DoM concept, the heteroatom-bridged biaryls **1.168** carrying the diethylcarbamide or *O*-diethylcarbamate DMGs, offered by DreM reaction,

an immediate pass to general syntheses of thioxanthenes **1.171a**,¹⁸⁹ xanthenes **1.171b**,¹⁹⁰ dibenzophosphorinones **1.171c**,¹⁹¹ acridones **1.171d**,¹⁹² and oxcarbazepine,¹⁹³ a antiepileptic drug. The Ar-X-Ar moiety can be easily assembled by the DoM-Ullmann, and Buchwald-Hartwig coupling routes. This same strategy has been implemented for the construction of the 6-deoxyjacareubin **1.172**, a natural product isolated from the leaves of *Vismia latifolia*.¹⁹⁰



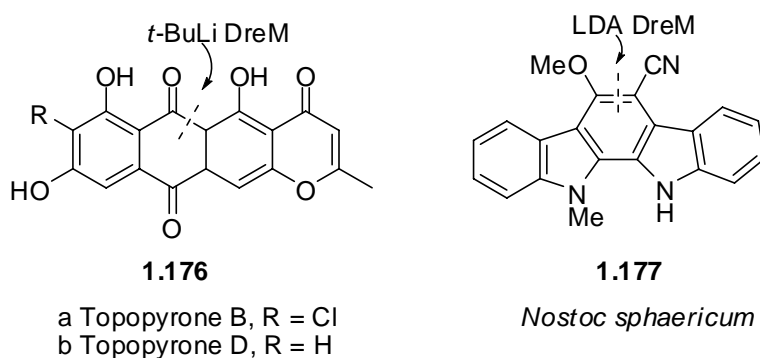
Scheme 1.36.

In similar Ar-X-Ar systems but with 2-*O*-carbamoyl groups (**1.173**, **Scheme 1.37**), anionic Fries rearrangement is avoided by *ortho*-protection to allow a remote equivalent reaction to give an intermediate **1.174** which undergoes a DreM – cyclization step to afford unusually substituted xanthenes and phosphorinones **1.175a** and **1.175b** in a one-pot process.^{189,191}



Scheme 1.37.

The considerable versatility of the DreM reaction as an alternative to the classical Friedel-Crafts cyclization is demonstrated ostensibly not only by the above examples but also in other total syntheses, e.g., topopyrone B and D¹⁹⁴ **1.176 a-b** and the unnamed indolo[2,3-*a*]carbazole alkaloid¹⁹⁵ **1.177**, a natural product which serves as potential candidate for development of antitumor agents.^{196,197}



Scheme 1.38.

1.2.4. The Synthesis of Azafluorenones

The azafluorenone core is found in an intriguing class of alkaloids, represented by onychine as one of the simplest members which has been shown to show antimicrobial activity against *Candida*, a genus of yeast that causes numerous infections (called *candidiasis* or thrush) in humans and animals.¹⁹⁸ Many 4-azafluorenone (indeno[1,2-

b]pyridine) derivatives bearing hydroxyl and / or methoxy substituents have been isolated from Nature (**Figure 1.24**).¹⁹⁹ The azafluorenone core was also shown to exhibit LC properties.²⁰⁰

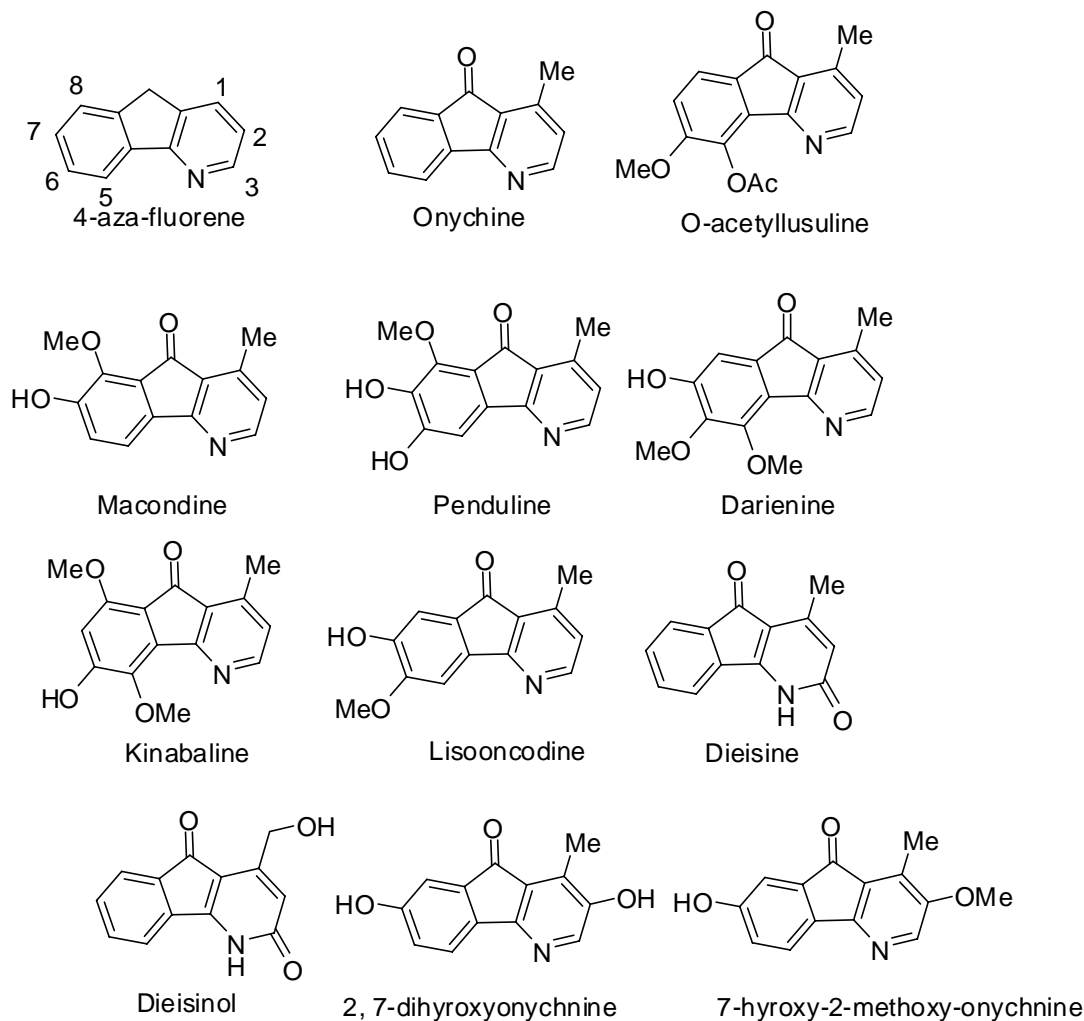
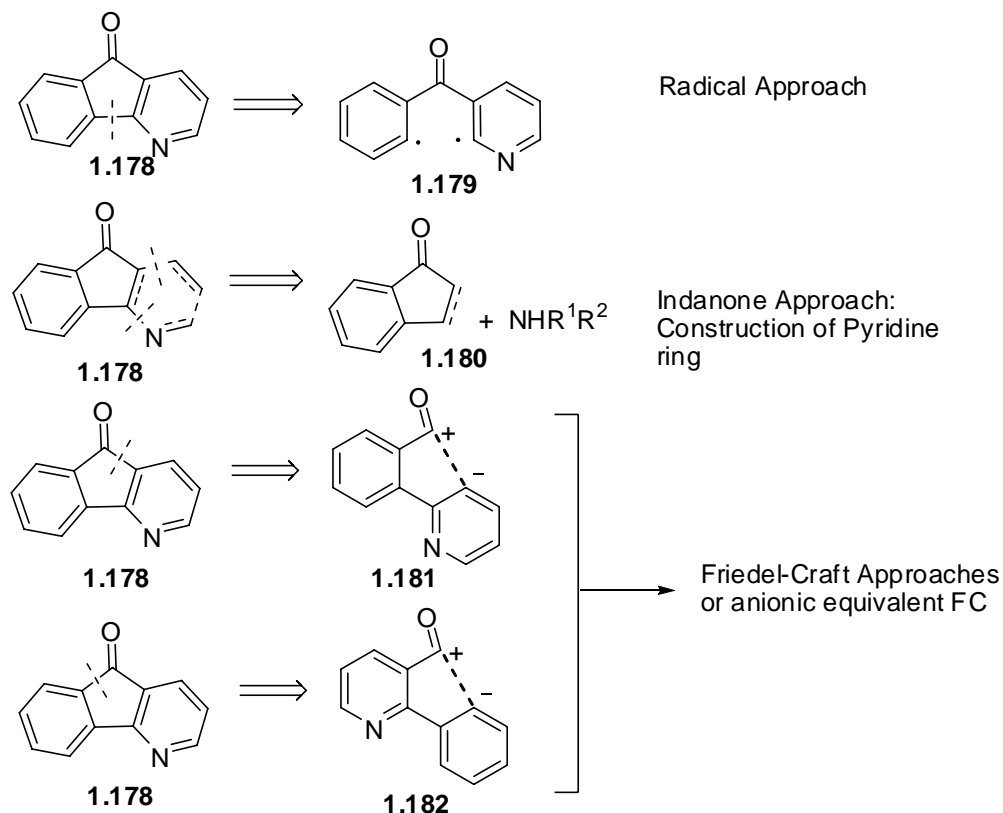


Figure 1.24. Naturally occurring 4-azafluorenones.

As a result of their unique structures and their potential antimicrobial properties, the synthesis of the azafluorenones has been an active area of investigation. Twelve selected azafluorenone syntheses will illustrate the variety of approaches. Retrosynthetic analysis based on three simple categories road map these approaches (**Scheme 1.39**). In

the radical approach, species **1.179** is generated either by thermolysis or photolysis to give the azafluorenone **1.178**. In a heteroannulation approach, the readily available indene or indanone **1.180** provides an efficient synthesis of **1.178**. The widely used cross coupling strategy is now very commonly used to prepare azabiaryls (not pyridinyl biaryls) which then allow either Friedel-Craft (FC) or anionic FC equivalent approaches to **1.178**.

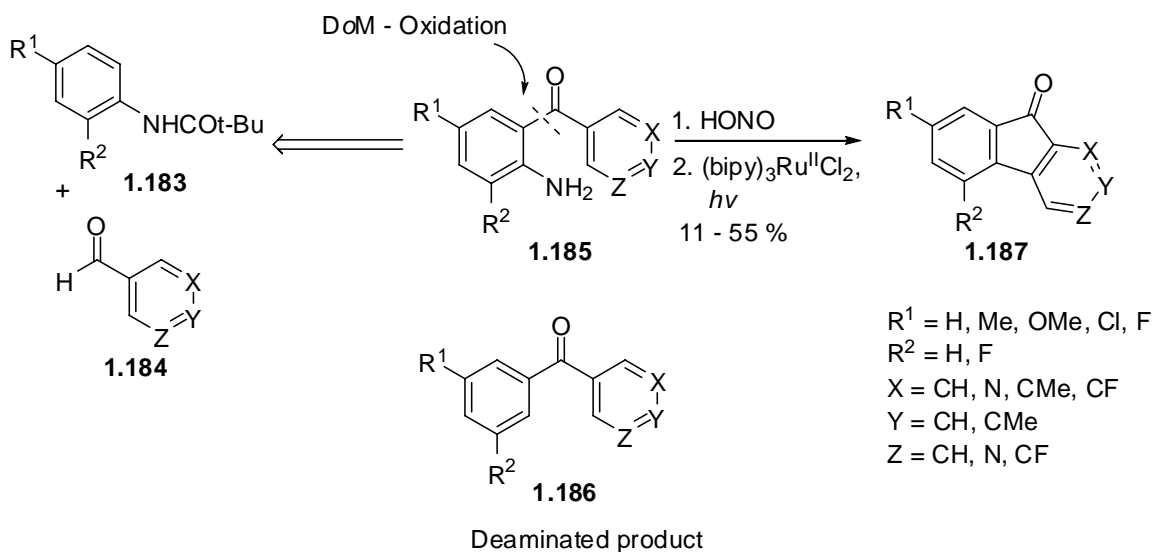


Scheme 1.39.

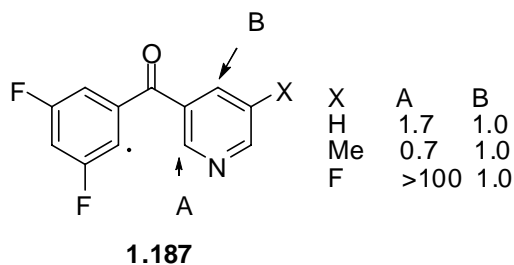
1.2.4.1. Radical Approaches

The radical approach, $\mathbf{1.179} \rightarrow \mathbf{1.178}$ may be the less favored method towards the azafluorenone nucleus because of lack of predictability in the regioselectivity and inefficiency.²⁰¹ Kyba and co-workers²⁰¹ reported the synthesis of azafluorenones **1.190** using a photochemical Pschorr cyclization, $\mathbf{1.185} \rightarrow \mathbf{1.187}$, as the key step (**Scheme 1.40**).

The intermediates **1.185** were prepared by a DoM reaction of the *N*-Boc anilines **1.183** with the aryl aldehydes **1.184**. Oxidation of the resulting alcohols gave the intermediates **1.185** which were then subjected to sequential diazotization and photolysis to furnish **1.187** in 11-55 % overall yield in the last two steps. A major problem of this approach is in the diazotization step, which leads to reductive deamination to give **1.186** as a side product (**Scheme 1.40**). Regioselectivity of the ring cyclization also varies as a function of substituents on the pyridine ring, e.g. A/B = 1.7/1.0 when X = H compared to A/B = 0.7/1.0 when X = Me (**Scheme 1.41**).

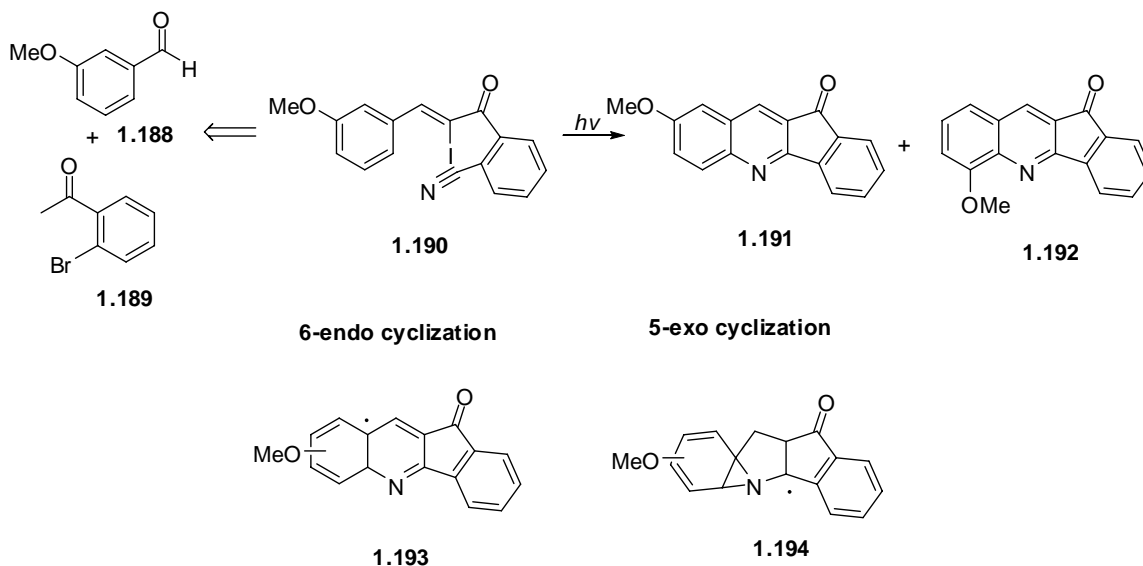


Scheme 1.40.



Scheme 1.41.

Cascade radical cyclization of **1.190**, conveniently obtained from the cross aldol reaction of 3-methoxybenzaldehyde **1.188** and 2-bromoacetophenone **1.189** followed by sequential von Braun reaction with copper cyanide and iodination, was subjected to sunlamp irradiation to give the 11*H*-indeno[1,2-*b*]quinolin-11-ones **1.191** and **1.192** in a ratio of 1: 3.2 with a 25% combined slump yield (**Scheme 1.42**).²⁰² No direct evidence for the distinct involvement of spiroindene **1.193** resulting from a 5-exo cyclization and the radical intermediate **1.194** formed by 6-endo cyclization was obtained.

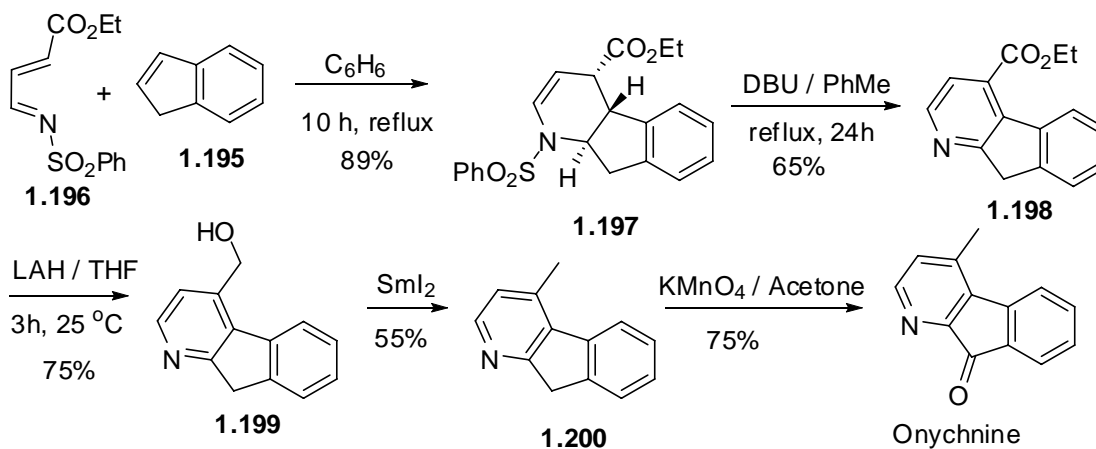


Scheme 1.42

1.2.4.2. Indanone Approaches

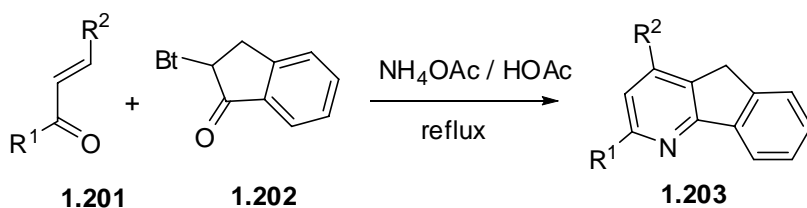
Diels-Alder, Michael addition and subsequent aza-Wittig reaction, and Friedlander approaches have been used for the construction of azafluorenones. These approaches often involve indanone or indene as the key starting materials. For instance, indene **1.195** (**Scheme 1.43**) was employed in the synthesis of onychine. Thus, Diels-Alder reaction of *N*-sulfonyl-1-aza-1,3-butadiene **1.196** with indene **1.195** afforded the intermediate **1.197** in good yield (89%). DBU assisted aromatization, **1.197** \rightarrow **1.198**,

LAH reduction, **1.198** → **1.199**, further reduction of primary alcohol of **1.199** by SmI₂, and oxidation of the resulting azafluorene **1.200** completed this route of onychine in 18 % overall yield.¹⁹⁹



Scheme 1.43.

In another study, α -benzotriazolyl indanone **1.202** (Scheme 1.45) was used in the construction of azafluorene **1.203**. This is a one pot procedure involving Michael addition, intramolecular ring annulation, and aromatization to afford **1.203 a** and **b** respectively in reasonable overall yields.²⁰³

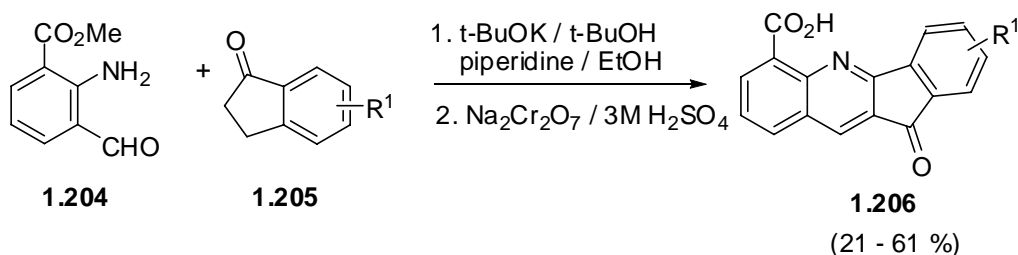


a R¹ = Ph, R² = Ph, yld = 77%
b R¹ = p-BrC₆H₄, R² = p-MeOC₆H₄, yld = 72%

Scheme 1.44.

Several potential anticancer tetracyclic quinolines **1.206** containing the azafluorenone moiety required for structure and activity relationship (SAR) studies were prepared in moderate overall yields (21 – 61%) by the Friedlander condensation of 2-

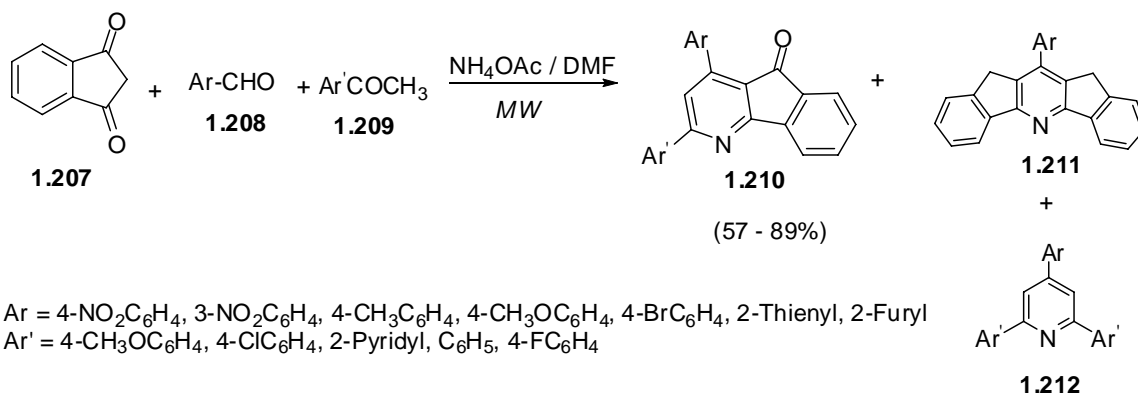
amino-3-formylbenzoate **1.204** with 1-indanones **1.205** followed by oxidation using Jones reagent.²⁰⁴



$R^1 = 4,7\text{-diMe}, 5,7\text{-diMe}, 4,7\text{-diOMe}, 5,6,7\text{-triOMe}$

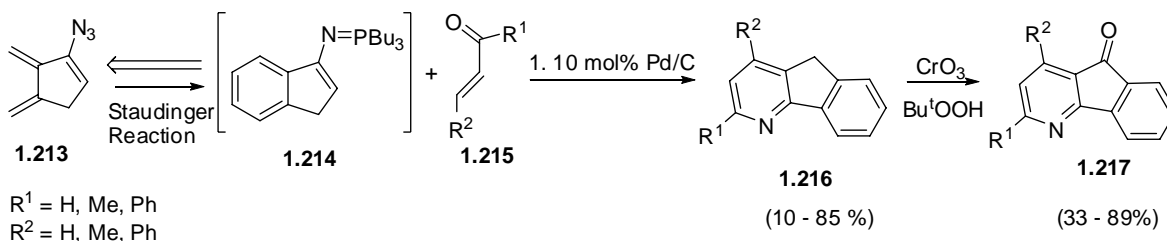
Scheme 1.45.

The synthesis of 4-azafluorenones may be accomplished by microwave assisted multi-component reaction (MCR) of 1,3-indanedione **1.207**, aryl aldehyde **1.208** and arylmethyl ketone **1.209** in the presence of ammonium acetate (**Scheme 1.46**). The study represents the renaissance of the Friedlander reaction in a more efficient manner and involving shorter reaction times. Aryl aldehydes bearing electron-withdrawing (EWGs) groups undergo reaction more rapidly than those possessing electron-donating groups (EDGs). Nevertheless, C-1 and C-3 substituted azafluorenones are available by this route. However, the utility of this developed MCR was undermined by the formation of undesired diindenone pyridine **1.211** and pyridine **1.212** products.²⁰⁵



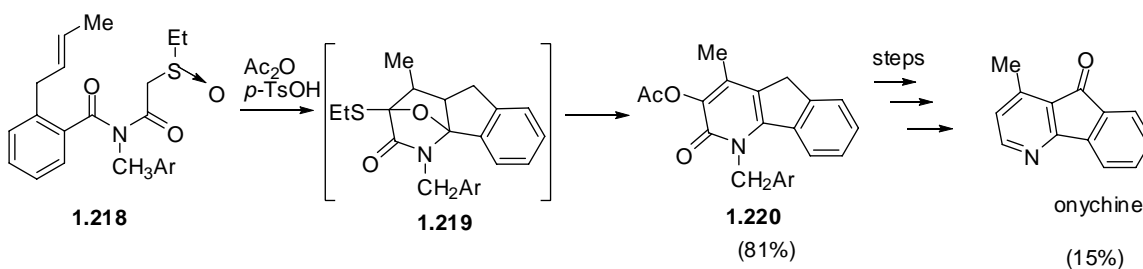
Scheme 1.46.

A less apparent way to derive a substituted azafluorenone is through an aza-Wittig reaction as reported by Nitta and co-workers.²⁰⁶ Thus, subjection of the 3-azidoindene **1.213** to the Staudinger reaction led to the (indene-3-ylimino)tributylphosphorane **1.214** which, without isolation, was treated with the α , β -unsaturated ketone **1.215** in the presence of dehydrogenating reagent (Pd/C) resulting in sequential Michael and Wittig reactions to give the azafluorene **1.216**. The azafluorenone **1.216** was prepared by oxidation of **1.217** using a Cr (VI) reagent.



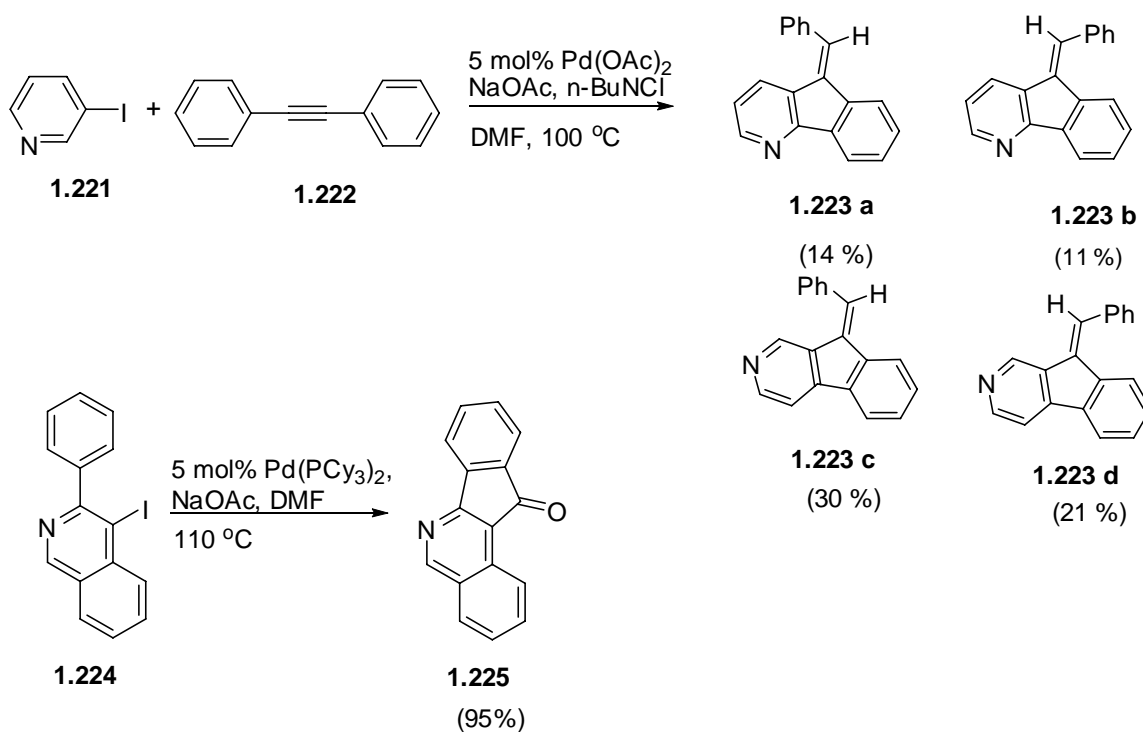
Scheme 1.47.

Padwa and coworkers²⁰⁷ also showed that the Pummerer rearrangement is a useful methodology for synthesis of various azafluorenone as well as azaanthraquinone alkaloids. In this study leading to the synthesis of onychine, imidosulfoxides **1.218** (Scheme 1.48) was subjected to Pummerer conditions triggering subsequent dipolar cycloaddition to give the pyridone intermediate **1.219**. Further manipulations led to **1.220** and hence onychine in 15 % overall yield in 9 steps.



Scheme 1.48.

Recent advance in palladium chemistry has led to the discovery and development of important cross coupling and ring annulation methods for the synthesis of carbocycles and heterocycles. Two studies related to the synthesis of azafluorenones provide examples of these modern and efficient approaches to heterocycles which involve making multiple C-C bonds consecutively. Thus, treatment of 2 equivalents of 3-iodopyridine **1.221** (Scheme 1.50) with 1 equivalent of diphenyl alkyne **1.222** under palladium (5 mol%) catalyzed conditions leads to a cascade cyclization to afford the azafluorene **1.223** in 76%.²⁰⁸ Palladium-catalysis also proved to be an efficient means to effect cyclocarbonylation of *o*-halobiaryls **1.224** leading to the construction of azafluorenone analogue **1.225** in an excellent yield.²⁰⁹ These sequences illustrate the value of Pd-catalyzed reactions which allow short syntheses of azafluorenones albeit, in the first case, with compromise in terms of selectivity and yields.

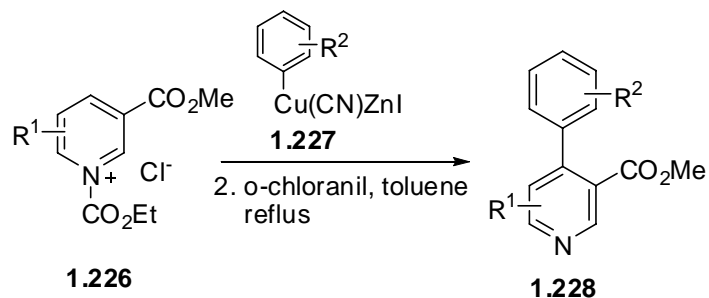


Scheme 1.49.

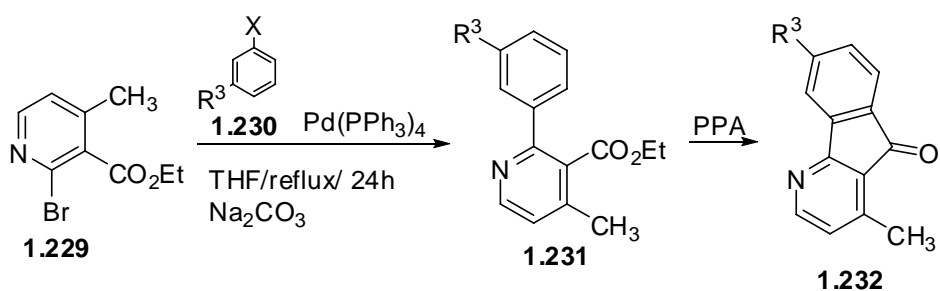
1.2.4.3. Friedel Craft and Anionic Friedel Crafts Approaches

Owing to the progressive development of cross coupling reactions,^{50,126,105} hetero-biaryls may be readily assembled using various coupling strategies. Shiao and Liu²¹⁰ demonstrated that biaryls **1.228** (Scheme 1.50) may be obtained by copper mediated nucleophilic addition of 1-ethoxycarbonyl-pyridinium chloride **1.226** with mixed copper cyanocuprate **1.227**. Suzuki-Miyaura and Stille cross coupling reactions provide reliable routes to the substituted ethyl 2-phenylnicotinate and chloro-pyridyl carboxamide **1.231**²¹¹ and **1.235** starting with **1.229** and **1.233** respectively (Scheme 1.50).²¹² The resulting pyridyl biaryls **1.231** were further cyclized by Friedel-Craft or by DreM reactions in the presence of polyphosphoric acid (PPA) and lithium tetramethyl piperidine (LTMP) respectively. These classical and anionic FC approaches may provide

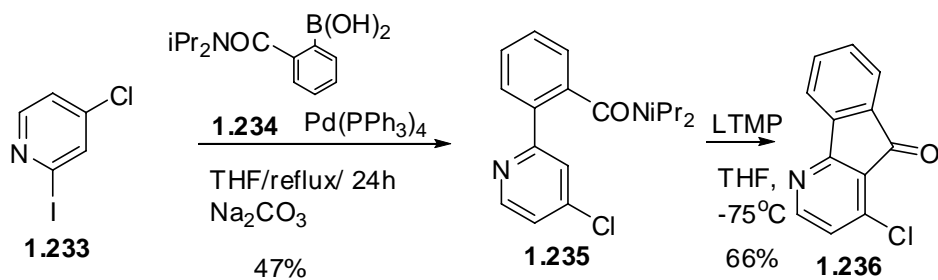
advantageous opportunity for prior functionalizing of the two aryl rings by the traditional EAS and DoM itself before subjection to the cross coupling reactions.



$\text{R}^1 = \text{H}, 5\text{-Me}, 6\text{-Me}$
 $\text{R}^2 = \text{H}, 4\text{-Me}, 2\text{-F}, 4\text{-F}, 4\text{-Cl}$ (40-61%)



a. $\text{X} = \text{B}(\text{OH})_2$, $\text{R} = \text{H}$ 58% 80%
 b. $\text{X} = \text{B}(\text{OH})_2$, $\text{R} = \text{OMe}$ 82% 80%
 c. $\text{X} = \text{SnMe}_3$, $\text{R} = \text{OMe}$ 95%

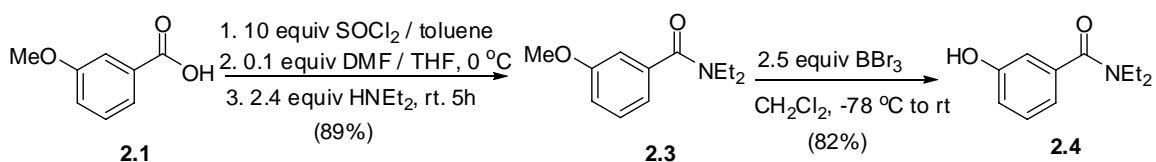


Scheme 1.50.

CHAPTER 2 – THE SYNTHESIS AND CHARACTERIZATION OF A NEW AZAFLUORENONE AND AZAFLUORENOL LIQUID CRYSTALS

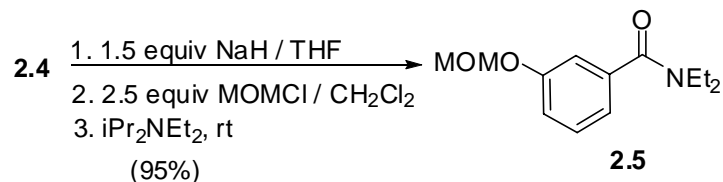
2.1. Synthesis of Azafluorenol Enantiomers

The construction of the target azafluorenol mesogen **1.14** (page 19) is based on the original synthesis of the corresponding fluorenol mesogen **1.13** both of which follows a DoM, Suzuki-Miyaura cross coupling and DreM synthetic sequence.¹⁶ The preparation of LC **1.14** is derived from the commercially available *m*-anisic acid **2.1** and 2, 5-dibromopyridine **2.2** which are envisaged as the two ends of the central connection via a Suzuki-Miyaura cross coupling step. To initiate the synthesis, the benzoic acid **2.1** was converted into the corresponding amide **2.3** which, upon BBr₃ treatment afforded the benzamide **2.4**.



Scheme 2.1

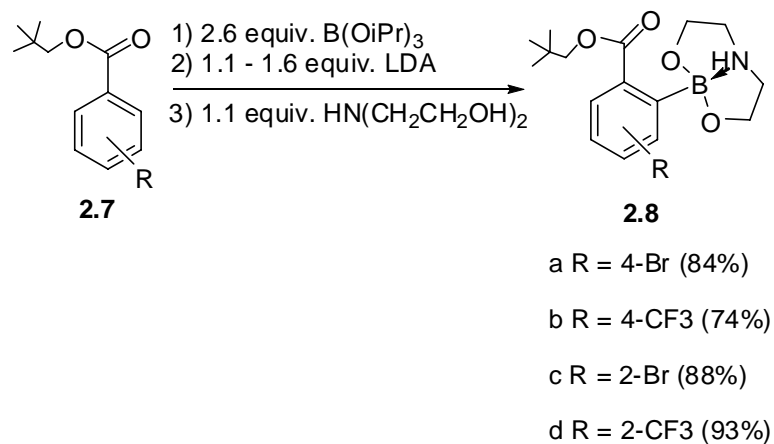
Installation of methylenemethoxy group (MOM), necessary for the differential deprotection before esterification at a later stage of the synthesis, afforded **2.5** which, upon DoM and silylation, gave **2.6**. As expected from previous results,²¹³ silylation occurred solely at C-2 without detection of alternate isomers based on the GC/MS results due to the synergy exerted by the two DMGs.^{200,214,215} Two conditions were tested to optimize the silylation process (**Scheme 2.2**), and there is a significant improvement by the condition b in comparison to the condition a. Although metalation of aromatics by LDA is expected to be reversible (LDA pK_a = 34 vs *N*, *N*-diethyl-benzamide *ortho*-H pK_a = 37.8)²¹⁶, TMSCl is an LDA-compatible *in situ* electrophile which intercepts the anionic species as soon as it is generated.²¹⁷



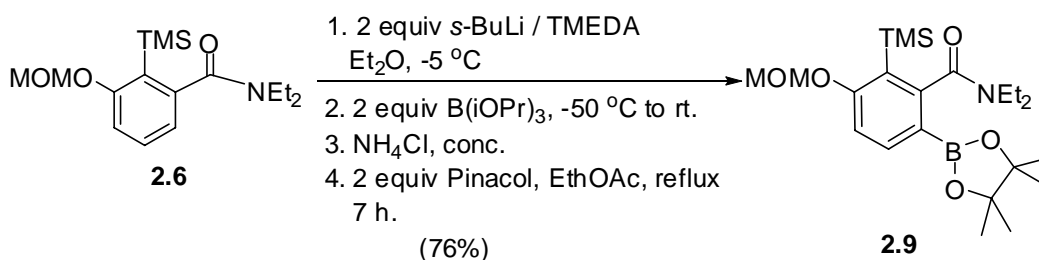
a: 1. 1.3 equiv. TMEDA / THF; 2. 1.3 equiv. *s*-BuLi. 3. 1.8 equiv. TMSCl. -78°C to rt.
 b: 1. 1.5 equiv. TMSCl; 2. 1.7 equiv. LDA / THF. -78°C to rt.

Scheme 2.2

With the most acidic site thus protected by the TMS group, metalation of **2.6** and quenching with triisopropyl borate (TIPB) followed by addition of pinacol yielded the pinacolato boronic ester **2.9**, the required intermediate for the Suzuki-Miyaura cross coupling (**Scheme 2.4**). Caron and Hawkins¹¹⁷ reported the use of TIPB as *in situ* electrophile for LDA-mediated DoM of neopentyl benzoate **2.7**, leading to *ortho*-substituted arylboronic acid derivatives **2.8** under relatively mild reaction conditions (**Scheme 2.3**). Unfortunately, application of the Hawkins conditions on **2.6** failed to deliver **2.9** presumably the result of inability of LDA to effect *ortho*-deprotonation. However, to a degree of delight, the pinacolato boronic ester **2.9** was obtained by the traditional metalation method²⁰ using *s*-BuLi / TMEDA to force complete and irreversible deprotonation followed by boronation using TIPB.



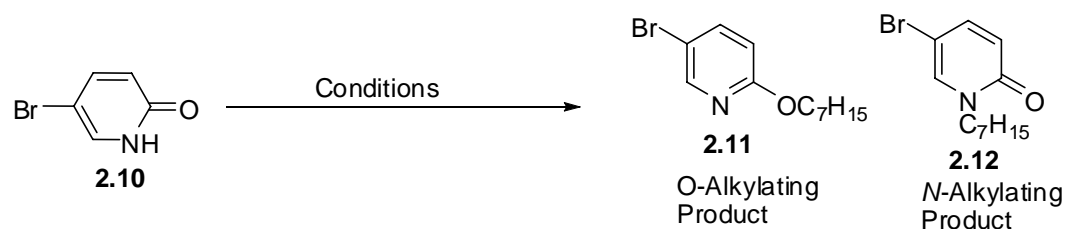
Scheme 2.3



Scheme 2.4

In the initial step for the preparation of the coupling partner 5-bromo-2-heptyloxy pyridine **2.11**, the alkylation of the ambident 5-bromopyridin-2(1H)-one **2.10** using various bases and electrophiles was studied. Using NaH as base and *n*-bromoheptane as alkylating agent led to nearly complete alkylation but in the undesirable 1.7:1 ratio of *N*- to *O*-alkylated products, **2.12**:**2.11**. With the consideration that this result may be attributed to *N*-alkylation being kinetically controlled, the employment of a weaker base, longer reaction times, and higher temperature which may favor the formation of **2.11** was tested. Thus using Hunig's base resulted in the formation of a more favorable 3:1 ratio of products **2.11**:**2.12**; however with a decreased efficiency (20 % yield). Use of the Mitsunobu reaction on **2.10** led to similar results (**2.11**:**2.12** = 1.8:1). This observation was somewhat expected based on the results of Comins and Gao²¹⁸

who showed that Mitsunobu reaction of 2-pyridone with various alkylating agents in methylene chloride afforded **2.11**:**2.12** in a ratio of 0.85 : 1. In another study, Hopkins and Jonak²¹⁹ showed that treatment of 2-pyridone with isopropyl iodide in the presence of silver carbonate in pentane led to the formation of 2-isopropoxy pyridine in quantitative yield (100%). However, when the latter conditions were applied to the reaction of **2.10** using Ag₂CO₃ and *n*-bromoheptane, only **2.10** was recovered in quantitative yield. In view of these results and the inevitability of formation of *N*- and *O*-isomeric products, **2.12** and **2.11**, a different approach to obtain the desired **2.11** isomer was considered.

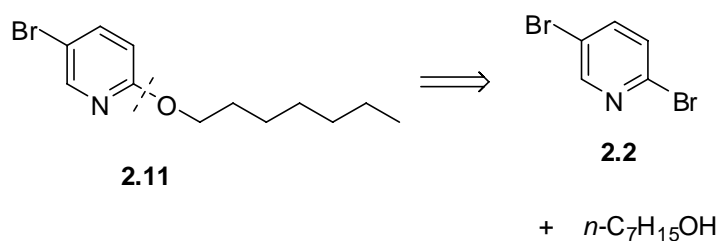


#	Conditions	2.11 + 2.12 (% yld)	O/N ratio	2.10 (% yld)
A	i) 1.2 equiv NaH / THF ii) 3.0 equiv <i>n</i> -C ₇ H ₁₅ Br, 1 h, 0°C to rt.	95	1:1.7	5
B	i) 1.1 equiv <i>n</i> -heptanol/CH ₂ Cl ₂ ii) 1.2 equiv PPh ₃ , 1.5 equiv DIAD, rt. 9h	50	1.8:1	50
C	i) 2 equiv <i>i</i> Pr ₂ NEt/CH ₂ Cl ₂ ii) 2 equiv <i>n</i> -C ₇ H ₁₅ Br, 8h, rt.	20	3:1	80
D	i) 2 equiv <i>n</i> -C ₇ H ₁₅ Br ii) 1 equiv Ag ₂ CO ₃ /heptane 69 °C, 24h	N/A	N/A	100

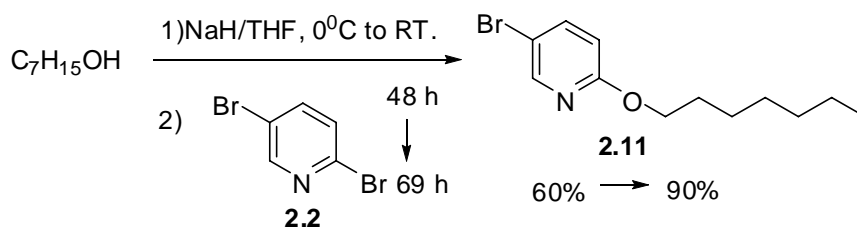
Table 2.1.

In view of the above results, an alternative approach, **2.2** → **2.11**, **Scheme 2.5** was considered based on literature precedent.²²⁰ Thus, the synthesis of 5-bromo-2-heptoxypyridine **2.11** was achieved in 60% by treatment of *n*-heptanol with NaH followed by addition 2,5-bromopyridine after stirring the reaction mixture for 48 h. The

reaction was followed by GC-MS, and a higher isolated yield (90%) was achieved when the reaction time was increased from 48 h to 69 h. The selectivity of the substitution can be explained by the withdrawing characteristics of nitrogen atom which induces the nucleophile to attack the 2-position rather than the 5-position.

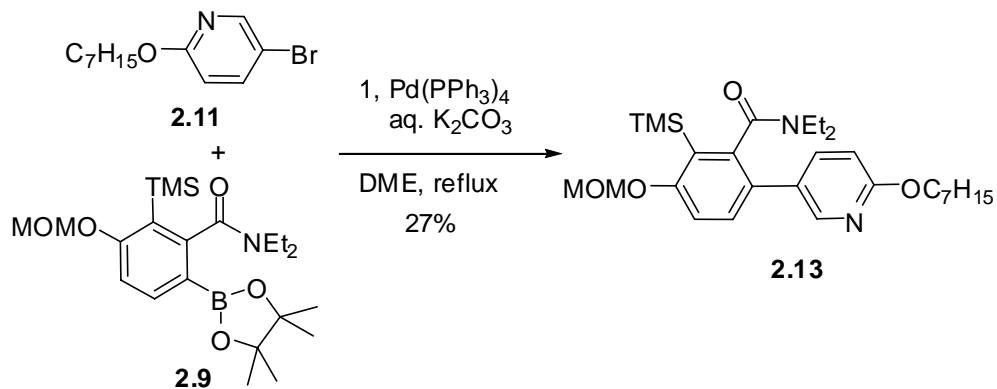


Scheme 2.5



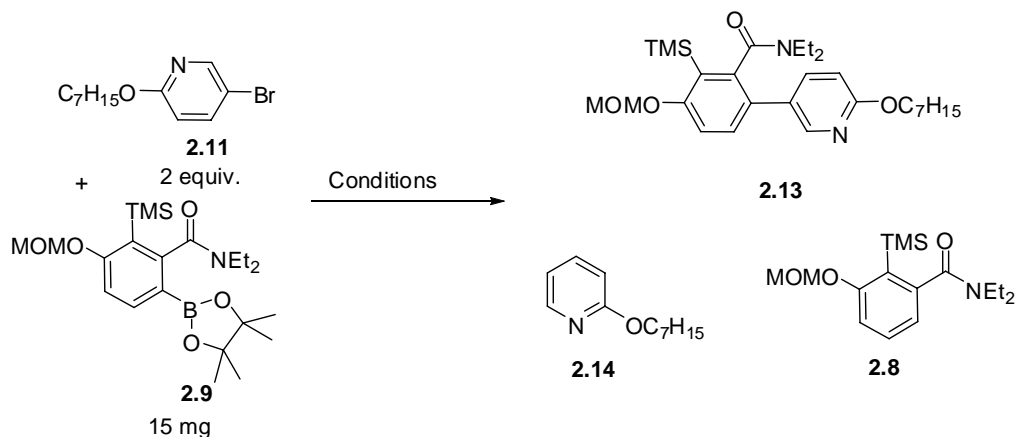
Scheme 2.6

With the coupling partners **2.11** and **2.9** in hand, standard Suzuki-Miyaura reaction conditions employing palladium tetrakis-triphenylphosphine (Pd(PPh₃)₄) as the Pd (0) catalyst, Na₂CO₃ as the base, and conditions of reflux in dimethoxyethane (DME) was applied. In the first attempt, the cross-coupling product **2.13** was isolated in only 27% yield with significant amount of **2.9** (23%) remaining but consumption of most of **2.11**. However, in two subsequent reactions, using a strictly controlled oxygen-free environment by vigorously degassing the solvent and base, product **2.13** was isolated in a higher but still disappointing yield of 41%.



Scheme 2.7

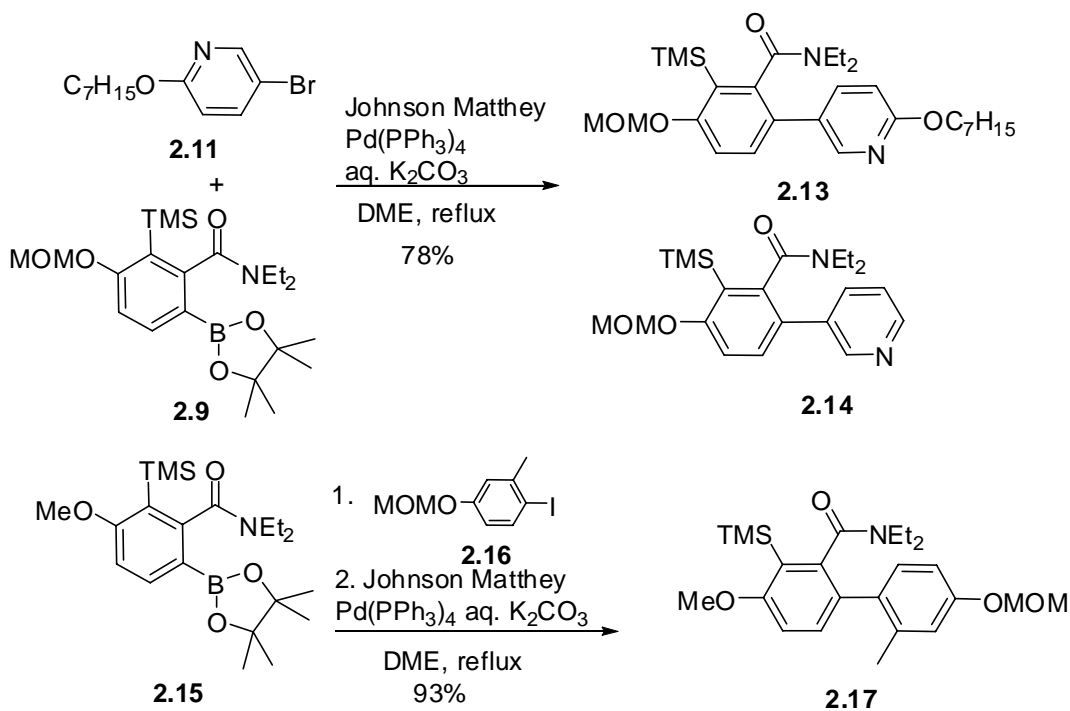
In an attempt to optimize conditions for the cross coupling of **2.9** with **2.11**, a reactor block screening process was carried out and the results are summarized in **Table 2.2**. However, as seen, disappointing results were obtained: only the conditions of Pd(OAc)₂ as catalyst and SPhos as ligand in a mixture of toluene and water afforded GC/MS detectable product **2.13** (3%).



Catalyst	Ligands	Base (equiv) /Solvent	GC-MS Result (% yld)				
			2.8	2.9	2.11	2.13	2.14
5% Pd(OAc) ₂	10% SPhos	1.3 K ₃ PO ₄ / tol: H ₂ O (10:1)	---	9	86	4	---
2.5% Pd ₂ (dba) ₃	5% SPhos	1.3 K ₃ PO ₄ / mesitylene	1	9	88	---	---
2.5% Pd ₂ (dba) ₃	5% PtBu ₃	2.3 KF / THF	---	30	50	---	---
5% Pd[PPh ₃] ₂ Cl ₂	-----	3 Na ₂ CO ₃ /Dioxane	1	5	85	---	1
5% Pd(OAc) ₂	5% DtBPF	1.3 K ₃ PO ₄ / Dioxane	---	---	100	---	---

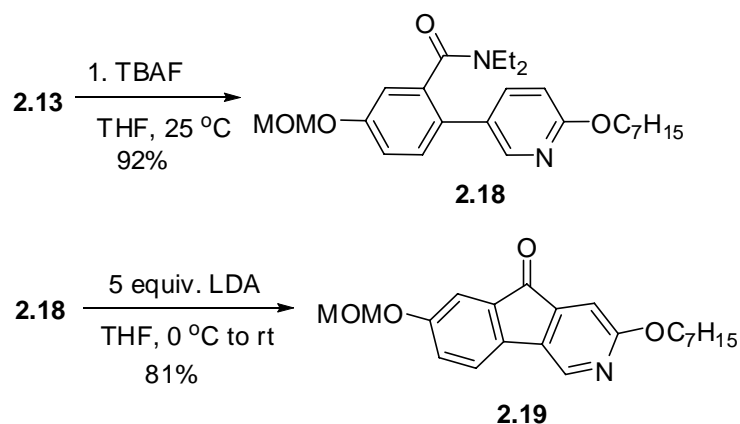
Table 2.2

At this point, the Suzuki-Miyaura cross-coupling reaction was repeated under the original, standard conditions. To our surprise, the desired product **2.13** was isolated in good yield (78%) together with a small amount of deheptoxyl cross coupling product **2.14**. Although this was a delightful result, there was no explanation to suggest the cause of the improvement except being due to the change in source of catalyst from Sigma-Aldrich to Johnson Matthey. Nevertheless, it can be deduced that the commercial source of $\text{Pd}(\text{PPh}_3)_4$ may not be reliable and $\text{Pd}(\text{PPh}_3)_4$ should be prepared by the literature procedure.²²¹ Repetition of the reaction twice using the same catalyst led to the formation of product **2.13** in a range of 67-78 % yields. Furthermore, a laboratory colleague, Wei Gan successfully and reproducibly used the Johnson Matthey $\text{Pd}(\text{PPh}_3)_4$ catalyst for the cross coupling reactions of **2.16** and **2.15** give **2.17** respectively in an excellent yields (93%) (Scheme 2.8).²²²



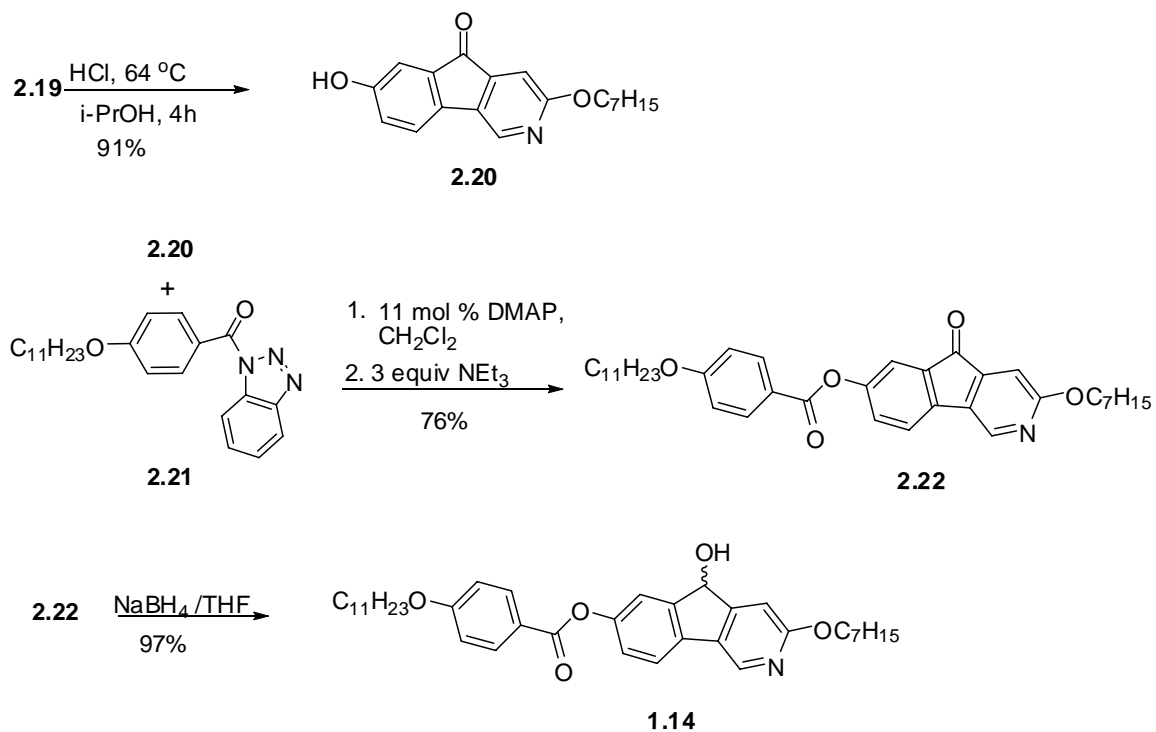
Scheme 2.8

With a reproducible procedure for the synthesis of **2.13** in hand, the synthesis of **1.14** was pursued. Thus, desilylation of **2.13** followed by treatment with LDA gave the fluorenone **2.19** (Scheme 2.9) in very good yield. LDA-mediated DreM of **2.18** was anticipated²⁰ to require a prolonged reaction time to achieve a high yield; however, TLC monitoring showed that it was complete within 1 h. Thus, contrary to previous practice,^{169,109} we suggest that excessive time is not required for an effective LDA-mediated DreM reaction. The short reaction procedure was also adapted for the synthesis of azabiaryls.¹¹⁸



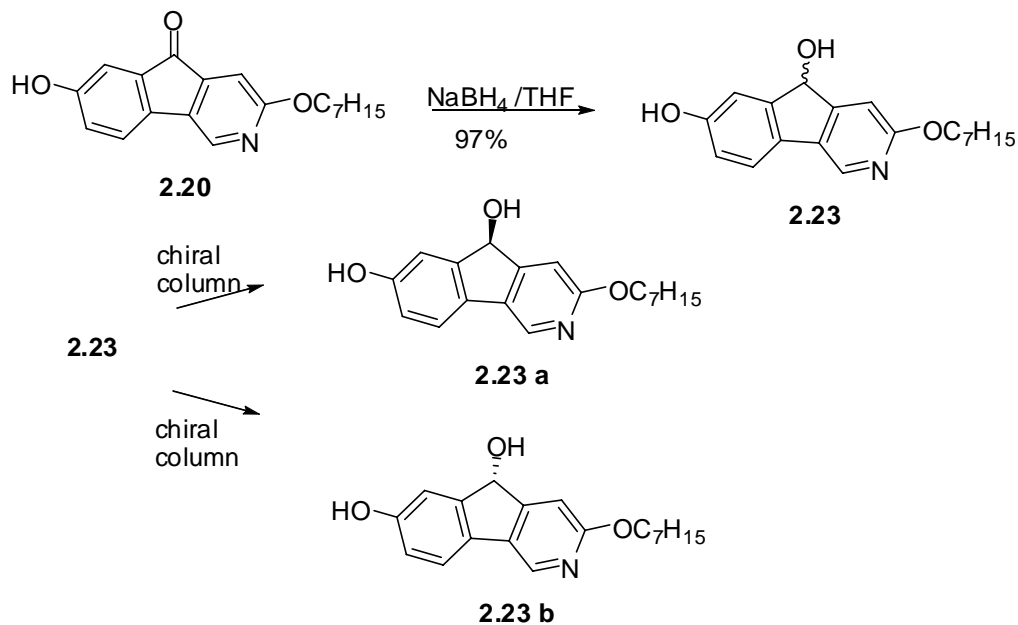
Scheme 2.9

As expected, selective MOM deprotection of the intermediate **2.19** without cleavage of the heptyloxy was achieved by treatment with hydrochloric acid to give **2.20**. Esterification of **2.20** using the benzotriazole method²²³ (**2.21**) furnished **2.22** which upon NaBH₄ reduction gave **1.14**. The LC properties of **2.22** and **1.14** are presented in Section 2.2.



Scheme 2.12

It was assumed that in order to obtain the two enantiomers of **1.14**, separation must be carried out at the diol **2.23** stage using an AS-Chiral column because the resemblance between the ester and the ether linkage of **1.14** would not provide sufficient difference for normal phase AS-Chiral column recognition. Fortunately and gratifyingly, separation of enantiomers **2.23 a** and **2.23 b** was achieved on the AS-Chiral column using a solvent ratio of 1:19 *i*PrOH : hexane with retention times of 69 min and 87 mins respectively. However, it seems life frequently has a taste of irony since both **1.14** and **2.23** were not stable in air and underwent rapid oxidation to give **2.22** and **2.20** respectively.



Scheme 2.13

2.2. Mesophase Characterization of 2.22 and 1.14

The mesophases formed by compounds **2.22** and **1.14** were characterized by polarized microscopy and differential scanning calorimetry (DSC). The mesophase properties are summarized in **Table 2.3**. The azafluorenone **2.22** forms a N phase, as shown by the Schlieren texture (**Figure 2.1**) with a temperature range of only 1 °K. Compound **2.22** forms a SmC phase as shown by the characteristic grey Schlieren texture (**Figure 2.2**), with a broader temperature range (99 °K). The azafluorenol **1.14** forms SmA phase (shown by the fan texture and homeotropic domain, **Figure 2.3**); the clearing point to isotropic phase at 178 °C was significantly higher than that of **2.22**. At 141 °C, the homeotropic domain turned into a Schlieren texture and the fan texture turned into a broken fan texture, which is characterization of SmA – SmC transition phase (**Figure 2.4**). The temperature range of the SmC phase formed by the azafluorenol **1.14** is less than that of **2.22**. The increase in temperature range of smectic phases for the

azafluorenol **1.14** is consistent with a stabilization by intermolecular hydrogen bonding between the hydroxyl group and aza group, as shown by the **Figure 1.21**.

Table 2.3. Mesophase properties data for **2.22**, **1.14**

Compound	Phase Sequence ^a
2.22	Cr_ 90 °C_SmC_159 °C_N_160 °C_I
1.14	Cr_ 85 °C_SmC_141 °C_SmA_178 °C_I ^b

^a Phase transition temperature in °C and (enthalpies of transition) in kJ/mol were measured on heating by differential scanning calorimetry at a rate of 5K/min. ^b Phase transition temperatures measured by polarized microscopy.

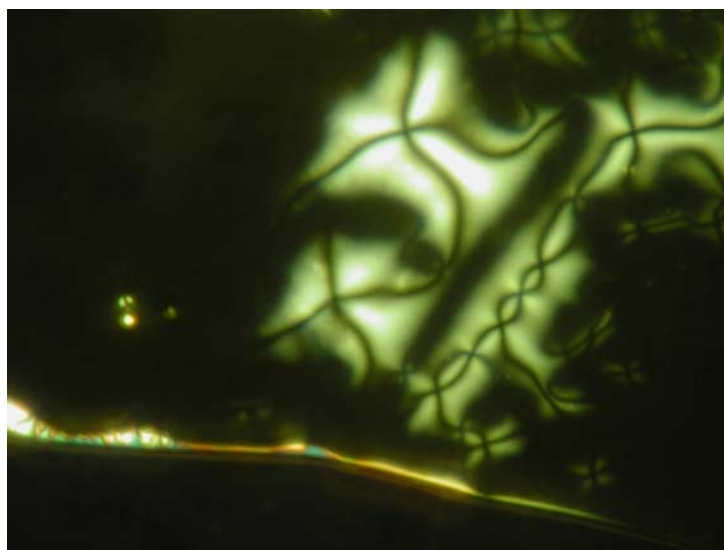


Figure 2.1. Photomicrograph of **2.22** in the N phase at 160 °C

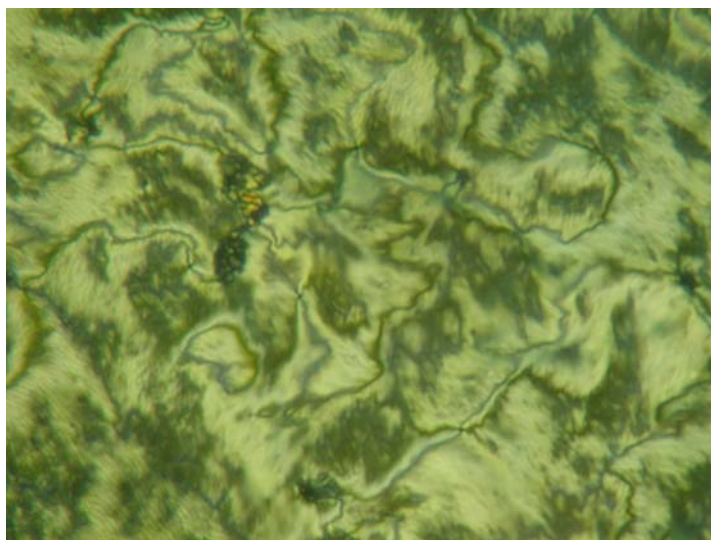


Figure 2.2. Photomicrograph of **2.22** in the SmC phase at 159 °C

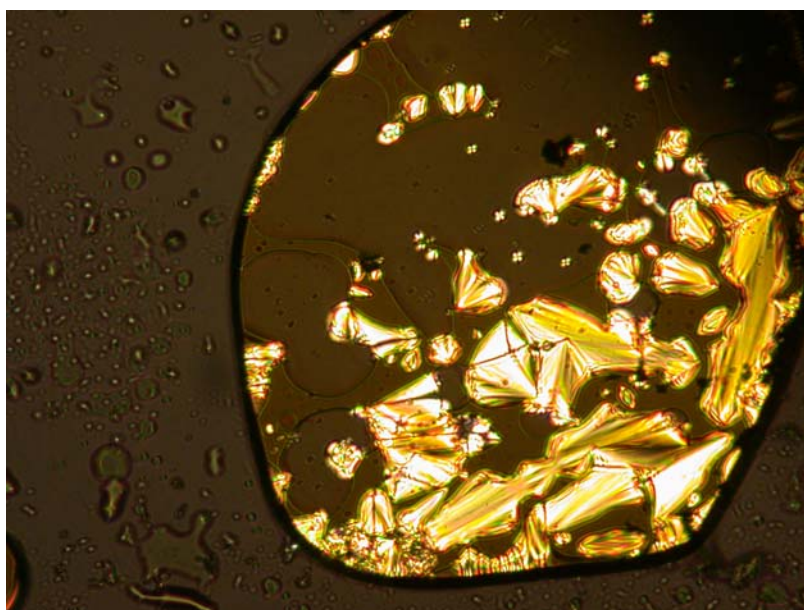


Figure 2.3. Photomicrograph of **1.14** in the SmA phase at 178 °C

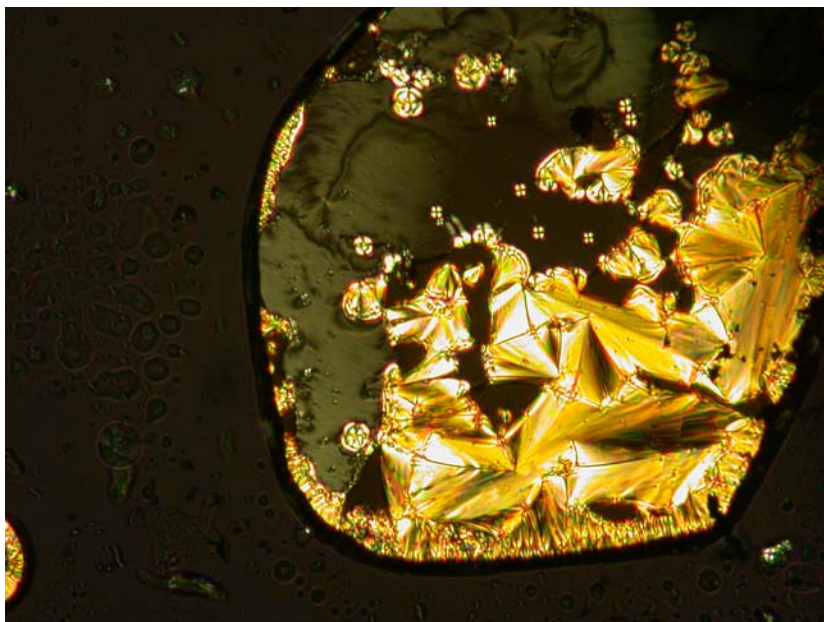


Figure 2.4. Photomicrograph of **1.14** in the SmC phase at 141 °C

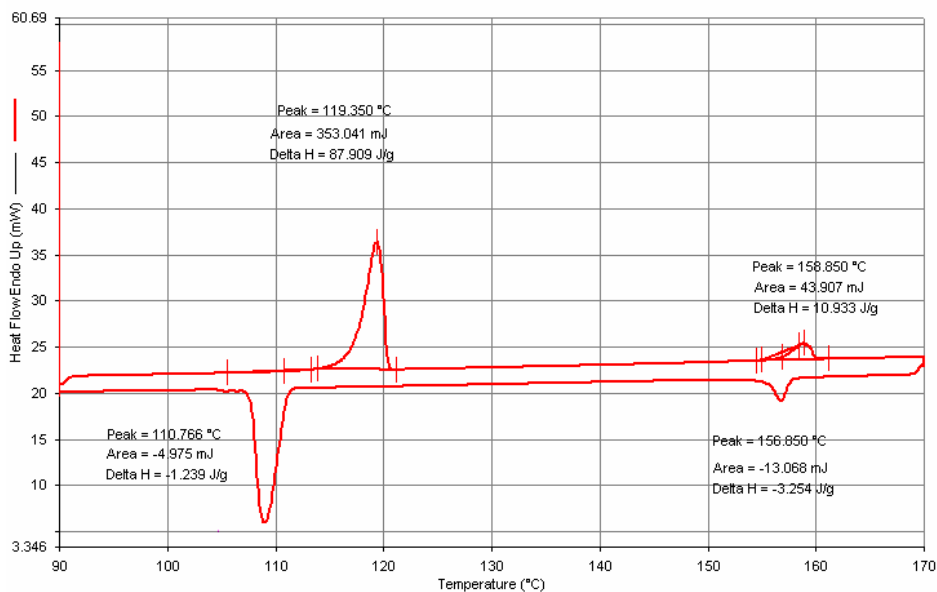


Figure 2.5. Differential Scanning Calorimetry of **2.22**.

CHAPTER 3 SUMMARY AND CONCLUSIONS

3.1. Summary

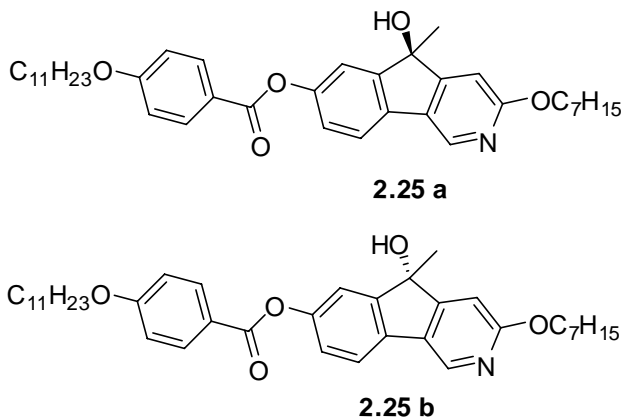
The synthesis of 3-aza-fluorenone and 3-aza-fluorenol SmC mesogens, **1.14** and **2.22**, by a combined directed *ortho* metalation – cross coupling approach has been

achieved. Synthesis of **1.14** and **2.22** was designed to incorporate the functionality to ensure a smooth Suzuki-Miyaura cross coupling reaction. This in turn promoted regioselectivity in the facile DreM which is a key step to form azafluorenone core. Initial LC characterization revealed the mesophases formed by these two mesogens **1.14** and **2.22** respectively. Large temperature range of Sm phase for the azafluorenone **1.14** is indicative of mesophase stabilization by intermolecular hydrogen bonding between the hydroxyl group and pyridine nitrogen.

3.2. Conclusions and Future Work

The larger temperature range of Sm phase observed for the azafluorenone **1.14** may be attributed to intermolecular hydrogen bonding between the hydroxyl group and pyridine. Since **1.14** is not a stable compound due to its ready oxidation to **2.22** in the open atmosphere, a structure activity relationship study of the effect of stronger hydrogen bond network (based on the previous fluorenone model)¹⁶ on polar order by introducing aza moiety with chirality in the core can not be concluded. The mesogen system needs to be structurally modified for making the azafluorenone core LC stable in the open atmosphere. By incorporating a C-9 methyl, the azafluorenone LC **2.25** (Scheme 3.1) should be resistant to oxidation even upon heating. Once **2.25** can be obtained as an enantiomerically pure, the resolving phase of **2.25** will be characterized by polarized microscopy, differential scanning calorimetry, and powder X-ray diffraction as well as the change of liquid crystal phases (SmA* \rightarrow SmC*) will also be examined as function of temperature. To determine the extent of hydrogen bonding in the SmC* phase formed by azafluorenone mesogen **2.25**, FT-IR spectroscopy will be used. Finally, spontaneous

polarization (P_s) and tilt angles (θ) will be measured as a function of temperature to verify which conformation of azafluorenol contributes significantly to P_s .



Scheme 3.1.

CHAPTER 4 EXPERIMENTAL SECTION

4.1. General Methods

^1H NMR (200, 300 and 400 MHz) and ^{13}C NMR (50, 75 and 100 MHz) spectra were recorded on Bruker AC-200, AC-300 and AV-400 instruments in CDCl_3 (unless otherwise indicated). The chemical shifts are reported in δ (ppm) relative to tetramethylsilane or CDCl_3 as internal standard. Low resolution mass spectra were recorded on a Micromass VG Quattro triple quadrupole mass spectrometer; peaks are reported as m/z (percent intensity relative to the base peak). High resolution mass spectra were recorded on a Micromass 70-250S double focusing mass spectrometer. Infrared spectra were recorded on a Bomem MB-100 FT-IR spectrometer as KBr pellets or neat on NaCl plates. Melting points were obtained using a Fisher Scientific hot stage apparatus and are uncorrected. Differential scanning calorimetry analyses were performed on a Perkin-Elmer or DSC-6 DSC-7 instrument with a scanning rate of 5

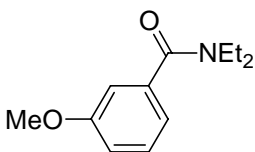
K/min. Texture analyses were performed using a Nikon Eclipse E600 POL polarized microscope fitted with a Linkam LTS 350 hot stage and TMS 93 temperature controller.

4.2. Materials

All dry solvents used were purified under an argon atmosphere according to Armarego²²⁴ or purchased from commercial sources. THF and Et₂O were freshly distilled from solven purification system by Innovative Technology., Inc., and CH₂Cl₂ and DMF (reduced pressure) were freshly distilled from CaH₂ or purchased from commercial sources, and toluene was freshly distilled from sodium metal. Diisopropylamine (DIPA) and *N,N,N',N'*-tetramethylethylenediamine (TMEDA) were distilled from CaH₂. *n*-Butyllithium (hexane solution) and *s*-butyllithium (hexane solution) were purchased from Aldrich Chemical Company and periodically titrated against *s*-butanol with *N*-benzylbenzamide or 1,10-phenanthroline as an indicator.²²⁵ Pd(PPh₃)₄ was purchased from Sigma Aldrich or free of charge from Johnson Mathey. All commodity chemicals were purchased from commercial sources and used without further purification. LDA was freshly prepared before use by stirring a 1:1 mixture of DIPA and *n*-BuLi in THF for 15 min at 0 °C.

4.3 Experimental Procedures

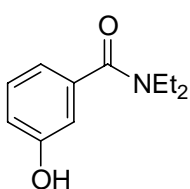
***N,N*-diethyl-3-methoxybenzamide (2.3).**²²⁶ To a dry flask containing 3-methoxybenzoic



acid (10.0 g, 66 mmol) was added SOCl₂ (47.8 mL, 10.0 equiv) and anhydrous DMF (5 mL, 0.10 equiv). The resulting solution was stirred for 1 h at 25 °C and concentrated *in vacuo*. Anhydrous toluene (50 mL) was added and the solution was concentrated *in vacuo*. This was

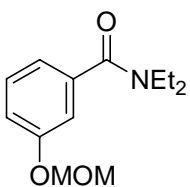
repeated three times. The residue was dissolved in anhydrous CH_2Cl_2 (300 mL) and cooled to $0\text{ }^\circ\text{C}$. To the resulting solution was added HNEt_2 (18 mL, 2.5 equiv) and the solution was allowed to warm to $25\text{ }^\circ\text{C}$ over 2 h, followed by stirring for a further 2 h. The mixture was diluted with H_2O (50 mL) and the whole was extracted with CH_2Cl_2 (50 mL \times 2). The combined organic extracts were washed with brine, dried (Na_2SO_4) and concentrated *in vacuo* to give a yellow oil. Vacuum distillation gave 12.9 g (94%) of **2.3** as a colourless oil: $^1\text{H NMR}$ (400 MHz, CDCl_3) δ ppm 7.30 (m, 1H), 6.92 (m, 3H), 3.82 (s, 3H), 3.51 (m, 2H), 3.24 (m, 2H), 1.16 (m, 6H). The $^1\text{H NMR}$ spectrum is in accord with that reported.¹⁹⁸

***N,N*-Diethyl-3-hydroxybenzamide (2.4).**²²⁷ To a solution of **2.3** (8.6 g, 41.3 mmol) in



anhydrous CH_2Cl_2 (295 mL) cooled to $-78\text{ }^\circ\text{C}$ under argon was added dropwise neat BBr_3 (9.8 mL, 2.5 equiv). The mixture was stirred for 30 min at $-78\text{ }^\circ\text{C}$, then allowed to warm to rt over 30 min. The reaction mixture was cooled to $0\text{ }^\circ\text{C}$, neutralized with satd aq Na_2CO_3 , and the whole was diluted with water and extracted with CH_2Cl_2 ($2 \times 150\text{ mL}$). The combined organic layers were extracted with 10% aq NaOH . The aqueous extract was neutralized with 2M aq HCl , the whole was extracted with CH_2Cl_2 ($\times 2$) and the combined organic extracts were dried (Na_2SO_4) and concentrated *in vacuo* to give 6.5g (82%) of **2.4** as a colourless solid: mp $81\text{--}82\text{ }^\circ\text{C}$ (EtOAc) [lit²²⁷ mp $84\text{ }^\circ\text{C}$ EtOAc]; $^1\text{H NMR}$ (400 MHz, CDCl_3) δ ppm 7.19 (s, 1H), 6.96 (s, 1H), 6.76 (m, 2H), 3.55 (m, 2H), 3.29 (m, 2H), 1.24 (s, 3H), 1.12 (s, 3H).

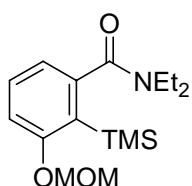
***N,N*-Diethyl-3-methoxymethoxybenzamide (2.5)** Under an Ar atmosphere, **2.4** (5.0 g,



25.9 mmol) was added dropwise into a suspension of NaH (60% in mineral oil, 1.55 g, 1.5 equiv) in anhydrous THF (215 mL), at $0\text{ }^\circ\text{C}$. The

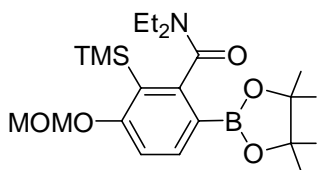
reaction mixture was stirred for 30 min and MOMCl (4.92 mL, 2.5 equiv) was added dropwise at 0 °C. The solution was allowed to warm to rt, then stirred for 30 min at rt and extracted with CH₂Cl₂ (2 × 50 mL). The combined organic extracts were dried (Na₂SO₄) and concentrated in vacuo to give a yellow oil. Purification by flash chromatography on silica gel (40% EtOAc/hexanes) gave 5.85 g (95%) of **2.5** as a colourless oil: ¹H NMR (400 MHz, CDCl₃) δ ppm 7.34 (dd, ³J = 8.0 Hz, ⁴J = 5.2 Hz, 1H), 7.07 (m, 2H), 7.02 (d, 2H), 5.20 (s, 2H), 3.55 (m, 2H), 3.49 (s, 3H), 3.31 (s, 2H), 1.31 (m, 6H).

***N,N*-Diethyl-3-methoxymethoxy-2-trimethylsilylbenzamide (2.6)** To a dry flask



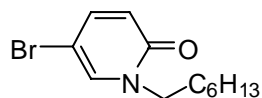
containing **2.5** (5.6 g, 24 mmol) in anhydrous THF (120 mL) cooled to -78 °C under argon were sequentially added dropwise TMSCl (5.1 mL, 1.7 equiv) and LDA (40.3 mL, 1.7 equiv as a 1 M solution in anhydrous THF). The mixture was allowed to warm to rt over 4-6 h without removing the bath. The mixture was diluted with saturated aq NH₄Cl, and the whole was concentrated and extracted with EtOAc (2 × 50 mL). The combined organic extracts were washed with brine, dried (Na₂SO₄) and concentrated to a yellow oil. Purification by flash chromatography on silica gel (15% EtOAc/hexanes) gave 6.8 g (92%) of **2.6** a colorless solid: mp 62-65 °C (hexane). ¹H NMR (400 MHz, CDCl₃) δ ppm 7.33 (t, J = 7.6 Hz, 1H), 7.09 (d, J = 8 Hz, 1H), 6.82 (d, J = 7.6 Hz, 1H), 5.20 (s, 2H), 3.67 (m, 1H), 3.50 (s, 3H), 3.44 (m, 1H), 3.29 (m, 2H), 1.29 (t, J = 7.2 Hz, 3H), 1.11 (t, J = 7.2 Hz, 3H), 0.30 (s, 9H). ¹³C NMR (100 MHz, CDCl₃) δ ppm 171.7, 162.8, 144.6, 130.5, 124.7, 119.8, 112.6, 94.2, 56.1, 43.4, 39.0, 13.7, 12.8, 0.6; MS (EI) m/z 310 (M⁺, 23), 294 (100), 278 (12), 250 (58); HRMS (EI) calcd for C₁₆H₂₇NO₃Si: 310.1838, found 310.1848.

2-*N,N*-Diethylcarbamoyl-4-methoxymethoxy-3-trimethylsilylphenylboronic acid



pinacol ester (2.9) To a dry flask containing **2.6** (3.09 g, 10 mmol) and TMEDA (3 mL, 2.0 equiv) in anhydrous Et₂O (178 mL) cooled to -5 °C under argon was added *s*-BuLi (1.00 M solution in hexane, 15 mL, 2.0 equiv). After the mixture was stirred at -5 °C for 2 h, anhydrous B(O^{*i*}Pr)₃ (4.6 mL, 2 equiv) was added rapidly and the mixture was allowed to warm to rt over 2 h. The mixture was diluted with satd aq NH₄Cl, concentrated and extracted with EtOAc (2 × 70 mL). The combined organic extracts were washed with brine and dried (MgSO₄). To this solution was added pinacol (3.6 g, 2.0 equiv), and the mixture was concentrated to a yellow oil *in vacuo*. Purification by flash chromatography on silica gel (10% EtOAc/hexanes) gave 3.6 g (82%) of **2.9** as a colourless solid: mp 89-90 °C (hexane); IR (KBr) ν_{\max} 1638 cm⁻¹; ¹H NMR (300 MHz, CDCl₃) δ ppm 7.87 (m, 1H), 7.05 (d, *J* = 8.4 Hz, 1H), 5.21 (s, 2H), 3.78 (m, 1H), 3.48 (s, 3H), 3.33 (m, 1H), 3.17 (q, *J* = 6.9 Hz, 2H), 1.24 (m, 15H), 1.05 (t, *J* = 6 Hz, 3H), 0.29 (s, 9H); ¹³C NMR (100 MHz, CDCl₃) δ ppm 171.3, 164.9, 150.0, 139.5, 124.1, 111.5, 94.0, 83.6, 56.3, 43.4, 39.5, 25.0, 24.7, 13.1, 12.5, 0.81; MS (EI) *m/z* 435 (M⁺, 24), 420 (79), 376 (21), 362 (68), 45 (100); HRMS (EI) calcd for C₂₂H₃₈BNO₄Si: 436.2691, found 436.2688.

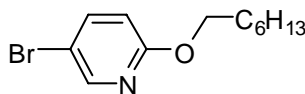
5-bromo-1-heptylpyridin-2(1H)-one (2.12) Under an Ar atmosphere, 5-bromopyridin-



2(1H)-one (1 g, 8.44 mmol) was added dropwise to a suspension of NaH (285 mg, 1.2 equiv 60% in hexane) in anhydrous THF (12 mL) at 0 °C. After the mixture was stirred for 1 h, 1-bromoheptane (2.7 mL, 3 equiv) was added, the ice bath was removed, and the mixture was allowed to warm to rt with stirring over 24 h. The reaction mixture was diluted with saturated aq. NH₄Cl

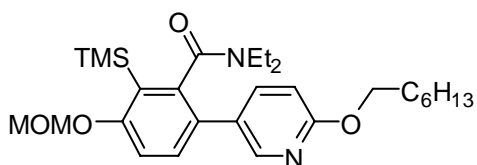
and extracted with CH_2Cl_2 (2×6 mL). The combined organic extract were dried (Na_2SO_4) and concentrated to a yellow oil. Purification by flash chromatography on silica gel (10% EtOAc/hexanes) gave 1.4 g of **2.12** (61%) as a yellow oil: ^1H NMR (400 MHz, CDCl_3) δ ppm 7.37 (d, $J = 3.2$ Hz, 1H), 7.32 (dd, $J^3 = 12.8$ Hz, $J^4 = 3.2$ Hz, 1H), 6.47 (d, $J = 12.8$ Hz, 1H), 3.88 (t, $J = 9.6$ Hz, 2H), 1.72 (m, 2H), 1.44 (m, 8H); 0.85 (m, 3H).

5-Bromo-2-heptyloxy pyridine (2.11) Under an Ar atmosphere, heptan-1-ol (4.7 mL, 4 equiv) was added dropwise to a suspension of NaH (1.35 g, 4 equiv 60% in hexane) in anhydrous THF (40 mL), at 0 °C.



After the mixture was stirred for 1.5 h, 2,5-dibromopyridine (2 g, 8.44 mmol) was added and the ice bath was removed. The mixture was allowed to warm to room temperature and stirred for 69 h. The reaction mixture was diluted with saturated aq. NH_4Cl and extracted with CH_2Cl_2 (2×20 mL). The combined organic extract were dried (Na_2SO_4) and concentrated to a yellow oil. Purification by flash chromatography on silica gel (10% EtOAc/hexanes) gave 2.1 g of **2.11** (92%) as a colourless oil: IR (KBr) ν_{max} 1583, 1452 cm^{-1} ; ^1H NMR (400 MHz, CDCl_3) δ ppm 8.20 (d, $J = 2$ Hz, 1H), 7.66 (dd, $^3J = 8.8$ Hz, $^4J = 2.8$ Hz, 1H), 6.67 (d, $J = 8.8$ Hz, 1H), 4.28 (t, $J = 6.8$ Hz, 2H), 1.81 (m, 3H), 1.46 (m, 8H); 0.93 (t, $J = 6.8$ Hz, 3H). ^{13}C NMR (100 MHz, CDCl_3) δ ppm 162.9, 147.4, 141.1, 112.8, 111.4, 66.6, 31.8, 29.1, 29.0, 26.0, 22.6, 14.1; MS (EI) m/z 287 ($(\text{M}+2)^+$, 2), 286 ($(\text{M}+1)^+$, 1), 285 (M^+ , 2), 173 (100), 145 (31); HRMS (EI) calcd for $\text{C}_{13}\text{H}_{20}\text{BrNO}$: 285.0728, found 285.0741.

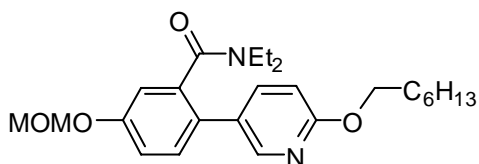
N,N-diethyl-6-(6-(heptyloxy)pyridin-3-yl)-3-(methoxymethoxy)-2-



(trimethylsilyl)benzamide (2.13) In a flask fitted with a reflux condenser under an Ar atmosphere,

containing a solution of **2.11** (0.10 g, 0.38 mmol) in anhydrous THF (5 mL) was added a solution of **2.9** (0.20 g, 1.2 equiv) in degassed DME (10 mL), Pd(PPh₃)₄ (46 mg, 0.10 equiv) and a 2 M aq solution of K₂CO₃ (1 mL, 5.0 equiv). The mixture was refluxed for 24 h, cooled, diluted with saturated aq NH₄Cl, and the whole was extracted with EtOAc (2 × 10 mL). The combined organic extracts were washed with brine, dried (Na₂SO₄) and concentrated *in vacuo* to give a brown oil. Purification by flash chromatography on silica gel (10% EtOAc/hexanes) gave 150 mg (78%) of **2.13** as a colourless oil: IR (KBr) ν_{\max} 1636 cm⁻¹; ¹H NMR (400 MHz, CDCl₃) δ ppm 8.11 (s, 1H), 7.71 (d, J = 8.4 Hz, 1H), 7.23 (d, J = 8.4 Hz, 1H), 7.15 (d, J = 8.8 Hz, 1H), 6.69 (d, J = 8.4 Hz, 1H), 5.21 (s, 2H), 4.29 (m, 2H), 3.81 (m, 1H), 3.50 (s, 3H), 3.00 (m, 1H), 2.78 (m, 2H), 1.80 (m, 2H), 1.43 (m, 9H), 0.89 (m, 3H); 0.88 (m, 3H), 0.86 (m, 3H). 0.30 (s, 9H). ¹³C NMR (100 MHz, CDCl₃) δ ppm 169.5, 163.2, 162.3, 146.6, 142.9, 140.1, 132.4, 129.5, 129.0, 128.5, 125.2, 112.7, 109.8, 94.2, 66.2, 56.2, 42.5, 38.1, 31.8, 31.6, 29.1, 28.9, 26.0, 22.6, 14.1, 12.9, 11.8, 1.0, 0.75, 0.48; MS (EI) m/z 501 (M⁺, 5), 485 (100), 370 (12); HRMS (EI) calcd for C₂₈H₄₄N₂O₄Si: 500.3070, found 500.3064.

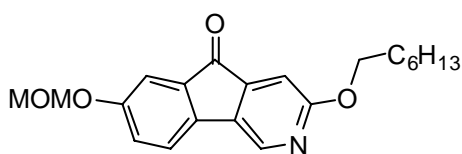
N,N-diethyl-2-(6-(heptyloxy)pyridin-3-yl)-5-(methoxymethoxy)benzamide (2.18)



To a solution of **2.13** (167 mg, 0.334 mmol) in anhydrous THF (4 mL) was added a 1M solution of TBAF in anhydrous THF (0.67 mL, 2.0 equiv). The mixture was stirred for 12 h at 25 °C, diluted with saturated aq NH₄Cl, and the whole was concentrated *in vacuo* and extracted with EtOAc (3 mL). The combined organic extracts were washed with brine, dried (Na₂SO₄) and concentrated to a brown oil. Purification by flash chromatography on silica gel (30% EtOAc/hexanes) gave

139 mg (97%) of **2.18** as a colourless oil: IR (KBr) ν_{\max} 1632 cm^{-1} ; ^1H NMR (400 MHz, CDCl_3) δ ppm 8.17 (s, 1H), 7.74 (dd, $^3J = 8.4$ Hz, $^4J = 2.4$ Hz, 1H), 7.29 (d, $J = 8.4$ Hz, 1H), 7.14 (dd, $^3J = 8.4$ Hz, $^4J = 2.4$ Hz, 1H), 7.06 (d, $J = 2.4$ Hz, 1H), 6.73 (d, $J = 8.8$ Hz, 1H), 5.25 (br. m. 2H), 4.32 (m, 2H), 3.75 (broad s, 1H), 3.50 (s, 3H), 3.04 (m, 2H), 2.80 (m, 1H), 1.83 (m, 3H), 1.48 (m, 8H), 0.99 (t, $J = 7.2$ Hz, 3H), 0.92 (m, 6H); ^{13}C NMR (100 MHz, CDCl_3) δ ppm 169.8, 163.4, 156.8, 146.1, 139.3, 137.6, 130.6, 128.4, 128.3, 116.9, 114.7, 110.3, 94.4, 66.3, 56.1, 42.4, 38.5, 31.8, 29.1, 26.0, 22.6, 14.2, 14.1, 13.5, 12.2; MS (EI) m/z 428 (M^+ , 51), 357 (100), 330 (51), 258 (32), 241 (20); HRMS (EI) calcd for $\text{C}_{25}\text{H}_{36}\text{N}_2\text{O}_4$: 428.2675, found 428.2684.

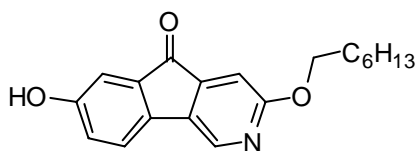
7-Methoxymethoxy-2-(2-octyloxy)-3-azafluoren-9-one (2.19) Under an Ar atmosphere,



a freshly prepared 1.0 M solution of LDA in anhydrous THF (1.47 mL, 5.0 equiv) was added dropwise to a solution of **2.18** (0.125 g, 0.293 mmol) in THF (8.8 mL) at 0 °C. After the mixture was stirred at rt for 1 h, saturated aq NH_4Cl solution was added and the mixture was extracted with Et_2O (2×10 mL). The combined organic extracts were washed with brine, dried (Na_2SO_4) and concentrated to furnish a red oil. Purification by flash chromatography on silica gel (5% EtOAc /hexanes) gave 85.3 mg (82%) of **2.19** as an orange solid: mp 92 - 94 °C (EtOAc); ^1H NMR (300 MHz, CDCl_3) δ ppm 8.23 (s, 1H), 7.48 (d, $J = 7.5$ Hz, 1H), 7.40 (d, $J = 2.4$ Hz, 1H), 7.21 (dd, $^3J = 8.1$ Hz, $^4J = 2.1$ Hz, 1H), 6.96 (s, 1H), 5.22 (s, 2H), 4.35 (t, $J = 6.9$ Hz, 2H), 3.51 (s, 3H), 1.85 (m, 2H), 1.51 (m, 11 H), 0.93 (m, 3H); ^{13}C NMR (75 MHz, CDCl_3) δ ppm 192.2, 164.7, 157.8, 144.6, 137.6, 137.3, 135.5, 130.1, 123.6, 121.4, 112.8, 107.1,

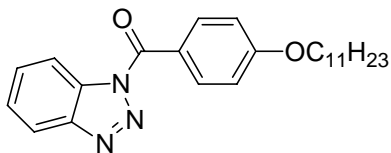
94.6, 67.2, 56.2, 31.8, 29.1, 29.0, 26.0, 22.6, 14.1; MS (EI) m/z 355 (M^+ , 63), 257 (100), 227 (48), 105 (76); HRMS (EI) calcd for $C_{21}H_{25}NO_4$: 355.1784, found 355.1778.

3-(Heptyloxy)-7-hydroxy-5H-indeno[1,2-c]pyridin-5-one (2.20) To a solution of **2.19**



(307 mg, 0.863 mmol) in *i*-PrOH (24 mL) was added 6 M aq HCl (0.40 mL, 2.75 equiv). After the mixture was stirred for four h at rt, it was diluted with water and the whole was extracted with CH_2Cl_2 (2×2 mL). The combined extracts were washed with brine, dried (Na_2SO_4) and concentrated to afford a red solid. Purification by flash chromatography on silica gel (10% EtOAc/hexanes) gave 243 mg (90%) of **2.20** as a dark red solid: mp 167-169 °C (CH_2Cl_2 /hexanes); 1H NMR (400 MHz, $CDCl_3$) δ ppm 8.21 (s, 1H), 7.44 (d, $J = 7.6$, 1H), 7.18 (s, 1H), 7.03 (d, $J = 6.4$ Hz, 1H), 6.96 (s, 1H), 4.35 (t, $J = 7.2$ Hz, 2H), 1.82 (m, 2H), 1.46 (m, 9H), 0.91 (m, 3H); ^{13}C NMR (100 MHz, $CDCl_3$) δ ppm 193.2, 165.8, 159.8, 146.1, 138.1, 136.8, 136.4, 132.2, 123.6, 123.1, 112.5, 107.2, 68.1, 33.0, 30.2, 30.1, 27.1, 23.7, 14.4; MS (EI) m/z 311 (M^+ , 4), 213 (100), 185 (6); HRMS (EI) calcd for $C_{19}H_{21}NO_3$: 311.1521, found 311.1507.

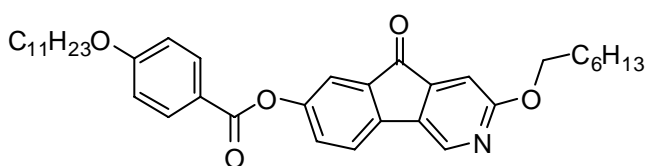
1-(4-Undecyloxybenzoyl)benzotriazole (2.21). A solution of 4-undecyloxybenzoic acid



(246 mg, 0.841 mmol), $SOCl_2$ (4 mL) and anhydrous DMF (0.13 mL) was stirred for 1 h at rt. The solution was concentrated *in vacuo*, anhydrous toluene (4 mL) was added and the solution was concentrated again; this procedure was repeated three times. The resulting residue was dissolved in CH_2Cl_2 (4 mL) and cooled to 0 °C. A solution of benzotriazole (120 mg, 1.2 equiv) and pyridine (0.136 mL, 2.0 equiv) in anhydrous THF (4 mL) was added dropwise. The mixture was allowed

to warm to rt and stirred for 4 h. The mixture was diluted with satd aq NH₄Cl and extracted with CH₂Cl₂ (2 × 10 mL). The combined extracts were dried (Na₂SO₄) and concentrated *in vacuo* to give a colourless solid. Purification by flash chromatography on silica gel (3% EtOAc/hexanes) gave 203 mg (62 %) of **2.21** as a colourless solid: ¹H NMR (400 MHz, CDCl₃) δ ppm 8.41 (d, J = 8 Hz, 1H), 8.32 (d, J = 8.8 Hz, 2H), 8.20 (d, J = 8 Hz, 1H), 7.73 (t, J = 7.2 Hz, 1H), 7.58 (t, J = 7.6 Hz, 1H), 7.08 (d, J = 8.8 Hz, 2H), 4.12 (t, J = 6.4 Hz, 2H), 1.88 (m, 2H), 1.54 (m, 2H), 1.30 (m, 16H), 0.92 (m, 3H). The ¹H NMR spectrum is in accord with that reported.²¹³

7-(Heptyloxy)-2-((undecyloxybenzoyl)oxy)-6-azafluoren-9-one (2.22) To a flask

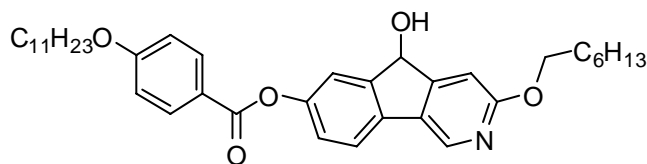


containing **2.20** (50 mg, 0.161 mmol), **2.21** (190 mg, 3 equiv) and DMAP (6 mg, 0.11 equiv) in anhydrous

CH₂Cl₂ (1 mL), was added Et₃N (5 mL) and the mixture was stirred for 4 h at rt. The solution was poured over into satd NH₄Cl and extracted with CH₂Cl₂ (2 × 5 mL). The combined organic extracts were dried (Na₂SO₄) and concentrated to give a yellow solid. Purification by flash chromatography on silica gel (10% EtOAc/hexanes) gave 65 mg (73%) of **2.22** as a yellow solid: (broad mp. range due to the exhibition of LC property; please see **Table 2.3**); IR (KBr) 1731, 1596 cm⁻¹; ¹H NMR (400 MHz, CDCl₃) δ ppm 8.33 (s, 1H), 8.16 (d, J = 8.4 Hz, 2H), 7.62 (d, J = 8.0 Hz, 1H), 7.56 (s, 1H), 7.39 (d, J = 8.0 Hz, 1H), 7.0 (m, 3H), 4.37 (t, J = 6.5 Hz, 2H), 4.08 (t, J = 6.3 Hz, 2H), 1.86 (m, 4H), 1.29 (m, 27H), 0.92 (m, 9H); ¹³C NMR (100 MHz, CDCl₃) δ ppm 189.7, 163.4, 162.9, 162.1, 149.6, 142.9, 139.4, 136.4, 133.6, 130.7, 127.8, 127.2, 119.5, 119.1, 117.4, 112.7, 105.5, 66.7, 65.7, 30.2, 30.1, 27.9, 27.88, 27.85, 27.6, 27.4, 27.3, 27.2, 24.3, 21.0, 20.9,

12.4, 12.39, 1.72; MS (EI) m/z 585.34 (M^+ , 3), 276 (100), 212 (81), 138 (26); HRMS (EI) calcd for $C_{37}H_{47}NO_5$: 585.3454, found 585.3457.

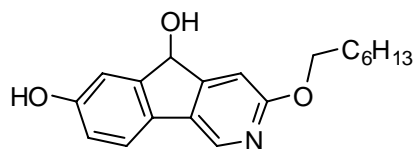
7-(Heptyloxy)-2-((undecyloxybenzoyl)oxy)-3-azafluoren-9-ol (1.14) To a solution of



2.22 (19 mg, 0.032 mmol) in 1:1 $Et_2O/iPrOH$ (5 mL) was added solid $NaBH_4$ (14 mg, 10 equiv). The

yellow solution was stirred for 5 min at rt, diluted with satd aqueous NH_4Cl and extracted with CH_2Cl_2 (3 mL \times 2). The combined organic extracts were dried (Na_2SO_4) and concentrated to give a colourless solid. Purification by flash chromatography on silica gel (10% $EtOAc$ /hexanes) gave 18 mg (97%) of **1.14** as a colourless solid: (broad mp range due to the exhibition of LC property; see **Table 2.3**, p 78); IR (KBr) ν_{max} 3394, 1727 cm^{-1} ; 1H NMR (400 MHz, $CDCl_3$) δ ppm 8.43 (s, 1H), 8.15 (d, $J = 8.8$ Hz, 2H), 7.67 (d, $J = 8$ Hz, 1H), 7.50 (s, 1H), 7.23 (d, $J = 1.6$ Hz, 1H), 7.09 (s, 1H), 6.99 (d, $J = 8.8$ Hz, 2H), 5.63 (s, 1H), 4.39 (t, $J = 6.4$ Hz, 2H), 4.07 (t, $J = 6.8$ Hz, 2H), 1.82 (m, 4H), 1.49 (m, 5H), 1.37 (m, 19H); 0.91 (m, 6H). Under open atmosphere, **1.14** was easily oxidized to **2.22** and thus the **1.14** was not fully characterized.

2-Hydroxy-7-(heptoxy)-3-azafluoren-9-ol (2.23). To a solution of **2.20** (88 mg, 0.27



mmol) in 1:1 $Et_2O/MeOH$ (5 mL) was added solid $NaBH_4$ (20 mg, 2.0 equiv). The yellow solution was stirred for 5 min at rt diluted with satd-aqueous NH_4Cl

and extracted with CH_2Cl_2 (2 \times 1 mL). The combined organic extracts were dried ($MgSO_4$) and concentrated to give a colourless solid which was easily oxidized under open atmosphere to **2.20** and thus **2.23** was not fully characterized.

REFERENCES

1. Zumdahl, S. S. *Chemical Principles*; D. C. Heath and Company: Lexington, MA, 1992.
2. Reinitzer, F. *Monatsch. Chem.* **1888**, 9, 421.
3. Lehman, O. *Z. Phys. Chem.* **1889**, 4, 462.
4. McMillan, W. L. *Phys. Rev. A: At. Mol. Opt. Phys.* **1973**, 8, 1921.
5. Wulff, A. *Phys. Rev. A: At. Mol. Opt. Phys.* **1975**, 11, 365.
6. Bartolino, R.; Doucet, J.; Durand, G. *Ann. Phys.* **1978**, 3, 389.
7. Clark, N. A.; Lagerwall, S. T. *Appl. Phys. Lett.* **1980**, 36, 899.
8. Walba, D. M.; Mallouck, T. E., Eds. *Advances in the Synthesis and Reactivity of Solids*; JAI Press: Greenwich, CT, 1991; Vol. 1, 173-235.
9. Walba, D. M.; Ros, M. B.; Clark, N. A.; Shao, R.; Johnson, K. M.; Robinson, M. G.; Liu, J. Y.; Doroski, D. *Mol. Cryst. Liq. Cryst.* **1991**, 198, 51.
10. Stegemeyer, H.; Meister, R.; Hoffmann, U.; Sprick, A.; Becker, A. *J. Mater. Chem.* **1995**, 5, 2183.
11. Lemieux, R. P. *Acc. Chem. Res.* **2001**, 34, 845.
12. Paleo, C. M.; Tsiourvas, D. *Angew. Chem. Int. Ed. Eng.* **1995**, 34, 1696.
13. Gray, G. W.; Hartley, J. B.; Ibbotson, A.; Jones, B. *J. Chem. Soc.* **1955**, 4359.
14. Ivanov, A. V.; Lyakhov, S. A.; Yarkova, M. Y.; Galatina, A. I.; Mazepa, A. V. *Russ. J. Gen. Chem.* **2002**, 72, 1435.
15. Takatoh, K.; Sakamoto, M. *Mol. Cryst. Liq. Cryst.* **1990**, 182B, 339.
16. McCubbin, J. A.; Tong, X.; Wang, R.; Zhao, Y.; Snieckus, V.; Lemieux, R. P. *J. Am. Chem. Soc.* **2004**, 126, 1161.
17. Taylor, R. *Electrophilic Aromatic Substitution*; John Wiley & Sons, 1990.
18. Esteves Pierre, M.; De, M. C. J. W.; Cardoso Sheila, P.; Barbosa Andre, G. H.; Laali Kenneth, K.; Rasul, G.; Prakash, G. K. S.; Olah George, A. *J. Am. Chem. Soc.* **2003**, 125, 4836.
19. Gschwend, H. W.; Rodriguez, H. R. *Org. React. (N.Y.)* **1979**, 26, 1.
20. Snieckus, V. *Chem. Rev.* **1990**, 90, 879.
21. Clayden, J. *The Chemistry of Organolithium Compounds*, Rappoport, Z.

Marek, I. ed.; John Wiley & Sons, UK, 2004.

22. Gilman, H.; Young, R. V. *J. Am. Chem. Soc.* **1934**, *56*, 1415.
23. Gilman, H.; Bebb, R. L. *J. Am. Chem. Soc.* **1939**, *61*, 109.
24. Halesa, A. F.; Schulz, D. N.; Tate, D. P.; Mochel, V. D. *Adv. Organomet. Chem.* **1980**, *18*, 55.
25. Sibi, M. P.; Snieckus, V. *J. Org. Chem.* **1983**, *48*, 1935.
26. Macklin, T. K.; Snieckus, V. *Org. Lett.* **2005**, *7*, 2519.
27. Whisler, M. C.; MacNeil, S. L.; Snieckus, V.; Beak, P. *Angew. Chem. Int. Ed.* **2004**, *43*, 2206.
28. Heck, R. F. *Synlett* **2006**, 2855.
29. Roberts, J. D. C., D. Y. *J. Am. Chem. Soc.* **1946**, *68*, 1658.
30. Morton, A. A. *J. Am. Chem. Soc.* **1947**, *69*, 969.
31. Beak, P.; Meyers, A. I. *Acc. Chem. Res.* **1986**, *19*, 356.
32. Hay, D. R.; Song, Z.; Smith, S. G.; Beak, P. *J. Am. Chem. Soc.* **1988**, *110*, 8145.
33. Collum, D. B. *Acc. Chem. Res.* **1992**, *25*, 448.
34. Bauer, W.; Schleyer, P. v. R. *J. Am. Chem. Soc.* **1989**, *111*, 7191.
35. Van Eikema Hommes, N. J. R.; Schleyer, P. v. R. *Angew. Chem.* **1992**, *104*, 768.
36. Saa, J. M.; Deya, P. M.; Suner, G. A.; Frontera, A. *J. Am. Chem. Soc.* **1992**, *114*, 9093.
37. Saa, J. M.; Morey, J.; Frontera, A.; Deya, P. M. *J. Am. Chem. Soc.* **1995**, *117*, 1105.
38. Anderson, D. R.; Faibish, N. C.; Beak, P. *J. Am. Chem. Soc.* **1999**, *121*, 7553.
39. de Visser, S. P.; de Koning, L. J.; van der Hart, W. J.; Nibbering, N. M. M. *Recl. Trav. Chim. Pays-Bas* **1995**, *114*, 267.
40. Buker, H. H.; Nibbering, N. M. M.; Espinosa, D.; Mongin, F.; Schlosser, M. *Tetrahedron Lett.* **1997**, *38*, 8519.
41. Kortüm, G.; Vogel, W.; Andrussow, K., Eds. *Dissoziationskonstanten organischer Säuren in wässriger Lösung*, Butterworths: Longdon, 1961.
42. Hall, G. E.; Piccolini, R.; Roberts, J. D. *J. Am. Chem. Soc.* **1955**, *77*, 4540.
43. Streitwieser, A.; Mares, F. *J. Am. Chem. Soc.* **1968**, *90*, 2444.

44. Chadwick, S. T.; Rennels, R. A.; Rutherford, J. L.; Collum, D. B. *J. Am. Chem. Soc.* **2000**, *122*, 8640.
45. Fuoss, R. M.; Kraus, C. A. *J. Am. Chem. Soc.* **1933**, *55*, 2387.
46. Shimano, M.; Meyers, A. I. *J. Am. Chem. Soc.* **1994**, *116*, 10815.
47. Nguyen, T.-H.; Chau Nguyet Trang, T.; Castanet, A.-S.; Nguyen Kim Phi, P.; Mortier, J. *Org Lett* **2005**, *7*, 2445.
48. Melvin, L. S. *Tetrahedron Lett.* **1981**, *22*, 3375.
49. Alessi, M.; Snieckus, V. *Unpublished results* **2006**.
50. Hartung, C. G.; Snieckus, V. *Modern Arene Chemistry* **2002**, 330.
51. Singh, K. J.; Collum, D. B. *J. Am. Chem. Soc.* **2006**, *128*, 13753.
52. Chadwick, S. T.; Ramirez, A.; Gupta, L.; Collum, D. B. *J. Am. Chem. Soc.* **2007**, *129*, 2259.
53. Sammakia, T.; Latham, H. A. *J. Org. Chem.* **1996**, *61*, 1629.
54. Gilman, H.; Langham, W.; Jacoby, A. L. *J. Am. Chem. Soc.* **1939**, *61*, 106.
55. Collum David, B.; McNeil, A., J.; Ramirez, A. *Angew. Chem. Int. Ed.* **2007**, *46*, 3002.
56. Corriu, R. J. P.; Mase, J. P. *J. Chem. Soc., Chem. Commun.* **1972**, 144.
57. Tamao, K.; Sumitani, K.; Kumada, M. *J. Am. Chem. Soc.* **1972**, *94*, 4374.
58. Baba, S.; Negishi, E. *J. Am. Chem. Soc.* **1976**, *98*, 6729.
59. Milstein, D.; Stille, J. K. *J. Am. Chem. Soc.* **1978**, *100*, 3636.
60. Hatanaka, Y.; Hiyama, T. *Synlett* **1991**, 845.
61. Hiyama, T.; Hatanaka, Y. *Pure Appl. Chem.* **1994**, *66*, 1471.
62. Miyaura, N.; Suzuki, A. *J. Chem. Soc., Chem. Commun.* **1979**, 866.
63. Kharasch, M. S.; Fields, E. K. *J. Am. Chem. Soc.* **1941**, *63*, 2316.
64. Negishi, E.; King, A. O.; Okukado, N. *J. Org. Chem.* **1977**, *42*, 1821.
65. Miyaura, N.; Suzuki, A. *Chem. Rev.* **1995**, *95*, 2457.
66. Miyaura, N.; Yamada, K.; Suzuki, A. *Tetrahedron Lett.* **1979**, 3437.
67. Batey, R. A.; Quach, T. D. *Tetrahedron Lett.* **2001**, *42*, 9099.
68. Milstein, D.; Stille, J. K. *J. Am. Chem. Soc.* **1979**, *101*, 4992.
69. Hatanaka, Y.; Hiyama, T. *Synlett* **1991**, 845.
70. Denmark, S. E.; Wehrli, D. *Org. Lett.* **2000**, *2*, 565.

71. Hirabayashi, K.; Kawashima, J.; Nishihara, Y.; Mori, A.; Hiyama, T. *Org. Lett.* **1999**, *1*, 299.
72. Stille, J. K.; Lau, K. S. Y. *Acc. Chem. Res.* **1977**, *10*, 434.
73. Kochi, J. K. *Organometallic Mechanisms and Catalysis*; Academic: New York, 1978.
74. Hegedus, L. S. *J. Organomet. Chem.* **1994**, *477*, 269.
75. Amatore, C.; Azzabi, M.; Jutand, A. *J. Am. Chem. Soc.* **1991**, *113*, 8375.
76. Hartwig, J. F.; Paul, F. *J. Am. Chem. Soc.* **1995**, *117*, 5373.
77. de Meijere, A.; Diederich, F.; Editors *Metal-Catalyzed Cross-Coupling Reactions, Second Completely Revised and Enlarged Edition; Volume 2*, 2004.
78. Fauvarque, J. F.; Pfluger, F.; Troupel, M. *J. Organomet. Chem.* **1981**, *208*, 419.
79. Reetz, M. T.; Lohmer, G.; Schwickardi, R. *Angew. Chemie. Int. Ed.* **1998**, *37*, 481.
80. Hegedus, L. S.; Schlosser, M., Eds. *Organometallics in Synthesis*; Wiley: New York, 1994.
81. Miyaura, N. *J. Organomet. Chem.* **2002**, *653*, 54.
82. Negishi, E. *Acc. Chem. Res.* **1982**, *15*, 340.
83. Haddach, M.; McCarthy, J. R. *Tetrahedron Lett.* **1999**, *40*, 3109.
84. Bumagin, N. A.; Korolev, D. N. *Tetrahedron Lett.* **1999**, *40*, 3057.
85. Miyaura, N.; Ishiyama, T.; Sasaki, M.; Ishikawa, M.; Satoh, A.; Suzuki, A. *J. Am. Chem. Soc.* **1989**, *111*, 314.
86. Kobayashi, Y.; Mizojiri, R. *Tetrahedron Lett.* **1996**, *37*, 8531.
87. Darses, S.; Genet, J.-P.; Brayer, J.-L.; Demoute, J.-P. *Tetrahedron Lett.* **1998**, *1997*, 4393.
88. Miyaura, N.; Yamada, K.; Suginome, H.; Suzuki, A. *J. Am. Chem. Soc.* **1985**, *107*, 972.
89. Murata, M.; Ishiyama, T.; Miyaura, N. *Unpublished results*.
90. Braga Ataulpa, A. C.; Morgon Nelson, H.; Ujaque, G.; Maseras, F. *J. Am. Chem. Soc.* **2005**, *127*, 9298.
91. Matos, K.; Soderquist, J. *J. Org. Chem.* **1998**, *63*, 461.
92. Suzuki, A. *Metal-catalyzed Cross-coupling Reactions*; Wiley-VCH: Weinheim, 1998 p49.

93. Stang, P. J.; Kowalski, M. H. *J. Am. Chem. Soc.* **1989**, *111*, 3356.
94. Ozawa, F.; Yamamoto, A. *Chem. Soc. Jpn.* **1987**, 773.
95. Brown, H. C.; Bhat, N. G.; Somayaji, V. *Organometallics* **1983**, *2*, 1311.
96. Hensel, V.; Shchlüter, A.-D. *Liebigs Ann. Recl.* **1997**, 303.
97. Li, W.; Nelson, D. P.; Jensen, M. S.; Hoerrner, R. S.; Cai, D.; Larsen, R. D.; Reider, P. J. *J. Org. Chem.* **2002**, *67*, 5394.
98. Parry, P. R.; Wang, C.; Batsanov, A. S.; Bryce, M. R.; Tarbit, B. *J. Org. Chem.* **2002**, *67*, 7541.
99. Ishiyama, T.; Murata, M.; Miyaura, N. *J. Org. Chem.* **1995**, *60*, 7508.
100. Ishiyama, T.; Ishida, K.; Miyaura, N. *Tetrahedron* **2001**, *57*, 9813.
101. Furstner, A.; Seidel, G. *Org. Lett.* **2002**, *4*, 541.
102. Ishiyama, T.; Takagi, J.; Ishida, K.; Miyaura, N.; Anastasi, N. R.; Hartwig, J. F. *J. Am. Chem. Soc.* **2002**, *124*, 390.
103. Ishiyama, T.; Takagi, J.; Hartwig John, F.; Miyaura, N. *Angew. Chem. Int. Ed.* **2002**, *41*, 3056.
104. Ishiyama, T.; Nobuta, Y.; Hartwig, J. F.; Miyaura, N. *Chem. Commun.* **2003**, 2924.
105. de Meijere, A. D., F., Ed. *Metal-Catalyzed Cross-Coupling Reactions Volume 1*; Wiley-VCH Verlag GmbH&Co. KGaA: Weinheim, 2004; Vol. 1.
106. Sharp, M. J.; Snieckus, V. *Tetrahedron Lett.* **1985**, 5997.
107. Anctil, E. J.-G.; Snieckus, V. *J. Organomet. Chem.* **2002**, *653*, 150.
108. Sattelkau, T.; Qandil, A. M.; Nichols, D. E. *Synthesis* **2001**, 262.
109. Fu, J. M.; Sharp, M. J.; Snieckus, V. *Tetrahedron Lett.* **1988**, *29*, 5459.
110. Wipf, P.; Jung, J.-K. *J. Org. Chem.* **2000**, *65*, 6319.
111. James, C. A.; Snieckus, V. *Tetrahedron Lett.* **1997**, *38*, 8149.
112. MacNeil, S. L.; FAMILONI, O. B.; Snieckus, V. *J. Org. Chem.* **2001**, *66*, 3662.
113. Myers, A. G.; Tom, N. J.; Fraley, M. E.; Cohen, S. B.; Madar, D. J. *J. Am. Chem. Soc.* **1997**, *119*, 6072.
114. Zhao, Z.; Snieckus, V. *Org. Lett.* **2005**, *7*, 2523.
115. Brown, H. C.; Bhat, N. G.; Srebnik, M. *Tetrahedron Lett.* **1988**, *29*, 2631.
116. Tokunaga, Y.; Ueno, H.; Shimomura, Y.; Seo, T. *Heterocycles* **2002**, *57*, 787.

117. Caron, S.; Hawkins, J. M. *J. Org. Chem.* **1998**, *63*, 2054.
118. Alessi, M.; Larkin, A. L.; Ogilvie, K. A.; Green, L. A.; Lai, S.; Lopez, S.; Snieckus, V. *J. Org. Chem.* **2007**, *72*, 1588.
119. Zhang, J.; Zhao, L.; Song, M.; Mak, T. C. W.; Wu, Y. *J. Organomet. Chem.* **2006**, *691*, 1301.
120. Leclerc, N.; Serieys, I.; Attias, A.-J. *Tetrahedron Lett.* **2003**, *44*, 5879.
121. Hodgson, P. B.; Salingue, F. H. *Tetrahedron Lett.* **2004**, *45*, 685.
122. Bouillon, A.; Lancelot, J.-C.; Sopkova-de Oliveira Santos, J.; Collot, V.; Bovy, P. R.; Rault, S. *Tetrahedron* **2003**, *59*, 10043.
123. Oh, C. H.; Lim, Y. M.; You, H. *Tetrahedron Lett.* **2002**, 4645.
124. Saito, S.; Sakai, M.; Miyaura, N. *Tetrahedron Lett.* **1996**, 2993.
125. Wolfe, J. P.; Singer, R. A.; Yang, B. H.; Buchwald Stephen, L. *J. Am. Chem. Soc.* **1999**, *121*, 9550.
126. Littke, A. F.; Fu, G. C. *Angew. Chem. Int. Ed.* **2002**, *41*, 4176.
127. Littke, A. F.; Dai, C.; Fu, G. C. *J. Am. Chem. Soc.* **2000**, *122*, 4020.
128. Barder, T., E.; Walker, S. D.; Martinelli, J. R.; Buchwald, S. L. *J. Am. Chem. Soc.* **2005**, *127*, 4685.
129. O'Brien, C. J.; Kantchev, E. A. B.; Valente, C.; Hadei, N.; Chass, G. A.; Lough, A.; Hopkinson, A. C.; Organ, M. G. *Chem. Eur. J.* **2006**, *12*, 4743.
130. Anderson, J. C.; Namli, H.; Roberts, C. A. *Tetrahedron* **1997**, *53*, 15123.
131. Watanabe, T.; Miyaura, N.; Suzuki, A. *Synlett* **1992**, 207.
132. Sabat, M.; Johnson, C. R. *Org Lett* **2000**, 1089.
133. Kimber, M. C.; Try, A. C.; Painter, M. M. *J. Org. Chem.* **2000**, 3042.
134. Kirchhoff, J. H.; Dai, C.; Fu, G. C. *Angew. Chem. Int. Ed.* **2002**, 1945.
135. Li, G. Y. *Angew. Chem. Int. Ed.* **2001**, 1513.
136. Hoye, T. R.; Chen, M.; Hoang, B.; Mi, L.; Priest, O. P. *J. Org. Chem.* **1999**, *64*, 7184.
137. Saito, S.; Kano, T.; Hatanaka, K.; Yamamoto, H. *J. Org. Chem.* **1997**, *62*, 5651.
138. Gronowitz, S.; Bobosik, V.; Lawitz, K. *Chem. Scripta* **1984**, 120.
139. Scheidel, M.-S.; Briehn, C. A.; Bäuerle, P. *J. Organomet. Chem.* **2002**, *653*, 200.

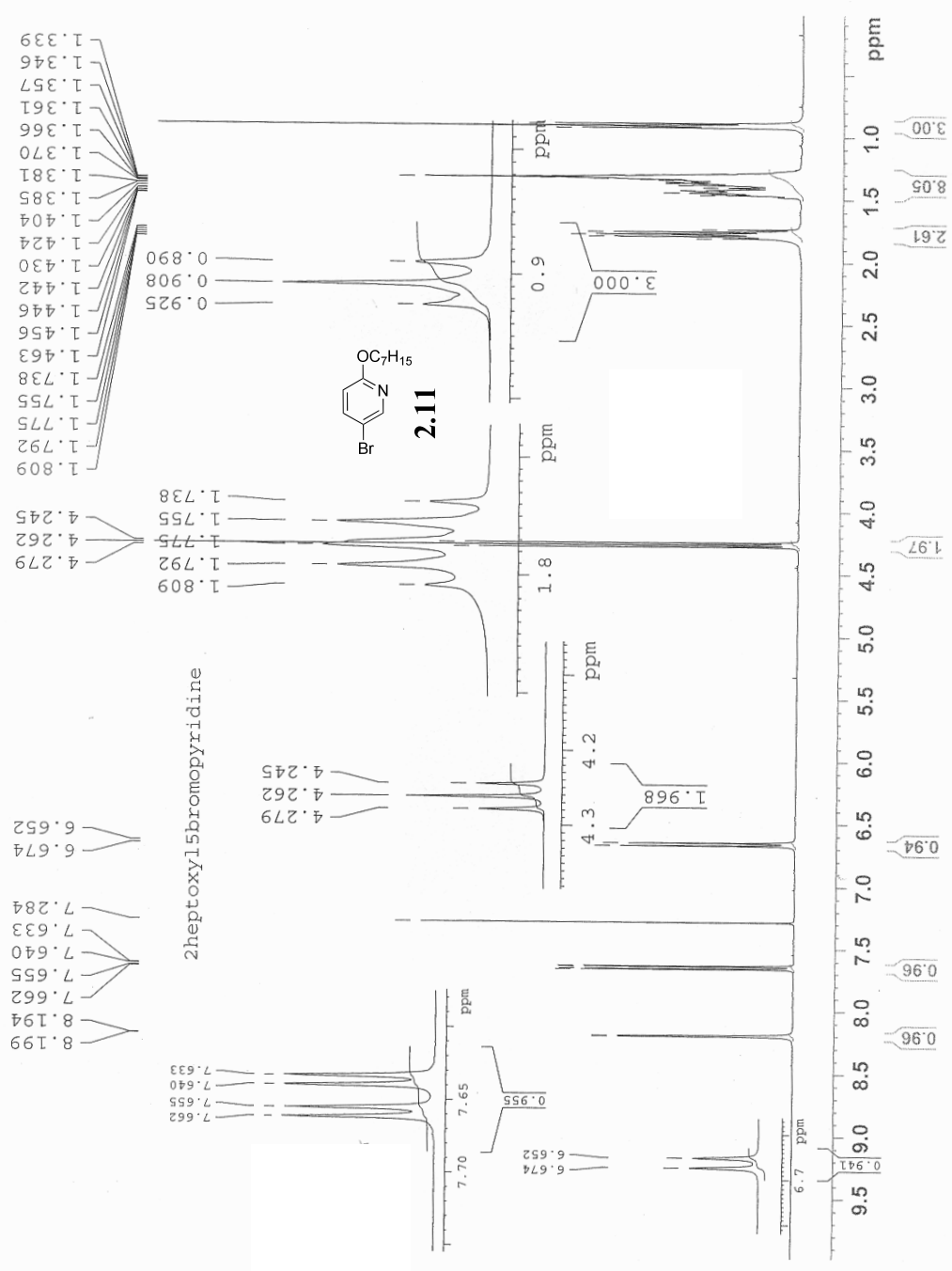
140. O'Neill, B. T.; Yohannes, D.; Bundesmann, M. W.; Arnold, E. P. *Org. Lett.* **2000**, 2, 4201.
141. Wright, S. W.; Hageman, D. L.; McClure, L. D. *J. Org. Chem.* **1994**, 6095.
142. Miyaura, N.; Yanagi, T.; Suzuki, A. *Synth. Commun.* **1981**, 11, 513.
143. Monovich, L. G.; Le Huerou, Y.; Roenn, M.; Molander, G. A. *J. Am. Chem. Soc.* **2000**, 122, 52.
144. Kamikawa, K.; Watanabe, T.; Uemura, M. *J. Org. Chem.* **1996**, 61, 1375.
145. Kelly, T. R.; Silva, R. A.; De Silva, H.; Jasmin, S.; Zhao, Y. *J. Am. Chem. Soc.* **2000**, 122, 6935.
146. Stavber, S.; Jereb, M.; Zupan, M. *Synlett* **1999**, 1375.
147. Groenendaal, L.; Frechet, J. M. J. *J. Org. Chem.* **1998**, 63, 5675.
148. Thompson, A. E.; Batsanov, A. S.; Bryce, M. R.; Saygili, N.; Parry, P. R.; Tarbit, B. *Tetrahedron* **2005**, 61, 5131.
149. Kawanaka, Y.; Ono, N.; Yoshida, Y.; Okamoto, S.; Sato, F. *J. Chem. Soc., Perkin Trans. 1* **1996**, 715.
150. Collot, V.; Bovy, P. R.; Rault, S. *Tetrahedron Lett.* **2000**, 41, 9053.
151. Sasaki, M.; Fuwa, H.; Ishikawa, M.; Tachibana, K. *Org. Lett.* **1999**, 1, 1075.
152. Saito, S.; Oh-tani, S.; Miyaura, N. *J. Org. Chem.* **1997**, 62, 8024.
153. Inada, K.; Miyaura, N. *Tetrahedron* **2000**, 56, 8657.
154. Urawa, Y.; Naka, H.; Miyazawa, M.; Souda, S.; Ogura, K. *J. Organomet. Chem.* **2002**, 653, 269.
155. Badone, D.; Baroni, M.; Cardamone, R.; Ielmini, A.; Guzzi, U. *J. Org. Chem.* **1997**, 62, 7170.
156. Baron, O.; Knochel, P. *Angew Chem Int Ed* **2005**, 44, 3133.
157. Kataoka, N.; Shelby, Q.; Stambuli, J. P.; Hartwig, J. F. *J. Org. Chem.* **2002**, 67, 5553.
158. Najera, C.; Gil-Molto, J.; Karlstroem, S. *Advanced Synthesis & Catalysis* **2004**, 346, 1798.
159. Grasa, G. A.; Viciu, M. S.; Huang, J.; Zhang, C.; Trudell, M. L.; Nolan, S. P. *Organometallics* **2002**, 21, 2866.
160. Zhang, C.; Huang, J.; Trudell, M. L.; Nolan, S. P. *J. Org. Chem.* **1999**, 64, 3804.

161. Littke, A. F.; Fu, G. C. *Angewandte Chemie International Edition* **1998**, *37*, 3387.
162. O'Neill, B. T.; Yohannes, D.; Bundesmann, M. W.; Arnold, E. P. *Org. Lett.* **2000**, *2*, 4201.
163. Chemler, S. R.; Danishefsky, S. J. *Org. Lett.* **2000**, *2*, 2695.
164. Pazos, Y.; De Lera, A. R. *Tetrahedron Lett.* **1999**, *40*, 8287.
165. Roush, W. R.; Sciotti, R. J. *J. Am. Chem. Soc.* **1998**, *120*, 7411.
166. Frohn, H. J.; Adonin, N. Y.; Bardin, V. V.; Starichenko, V. F. *Tetrahedron Lett.* **2002**, *43*, 8111.
167. Molander, G. A.; Bernardi, C. R. *J. Org. Chem.* **2002**, *67*, 8424.
168. Molander, G. A.; Rivero, M. R. *Org. Lett.* **2002**, *4*, 107.
169. Wang, W.; Snieckus, V. *J. Org. Chem.* **1992**, *57*, 424.
170. Fu, J.-M.; Zhao, B.-P.; Sharp, M. J.; Snieckus, V. *J. Org. Chem.* **1991**, *56*, 1683.
171. Fu, J. M.; Zhao, B. P.; Sharp, M. J.; Snieckus, V. *Can. J. Chem.* **1994**, *72*, 227.
172. Narasimhan, N. S.; Chandrachud, P. S.; Shete, N. R. *Tetrahedron* **1981**, *37*, 825.
173. Meyers, A. I. *Unpublished results*.
174. Sharp, M. J.; Taylor, N. J.; Snieckus, V. *Unpublished results*.
175. Tilly, D.; Samanta, S. S.; De, A.; Castanet, A.-S.; Mortier, J. *Org. Lett.* **2005**, *7*, 827.
176. Bouillon, A.; Lancelot, J.-C.; Collot, V.; Bovy, P. R.; Rault, S. *Tetrahedron Lett.* **2002**, *58*, 2885.
177. Bouillon, A.; Lancelot, J.-C.; Collot, V.; Bovy, P. R.; Rault, S. *Tetrahedron Lett.* **2002**, *58*, 3323.
178. Shiao, M.-J.; Peng, C.-J.; Wang, J.-S.; Ma, Y.-T. *J. Chin. Chem. Soc.* **1992**, *39*, 173.
179. James, C. A.; Coelho, A.; Snieckus, V. *Unpublished results*.
180. Chauder, B. A.; Kalinin, A. V.; Taylor, N. J.; Snieckus, V. *Angew. Chem. Int. Ed.* **1999**, *38*, 1435.
181. Cai, X.; Brown, S.; Hodson, P.; Snieckus, V. *Can. J. Chem.* **2004**, *82*, 195.
182. W. Krasodomski; M.K. Luczynski; J. Wilamowski, a. J.; Sepiol. *Tetrahedron* **2003**, *59*, 5677.
183. P. Hanson; P.W. Lovenich; S.C. Rowell; P.H. Walton; Timms., A. W. **1999**, *2*, 49.

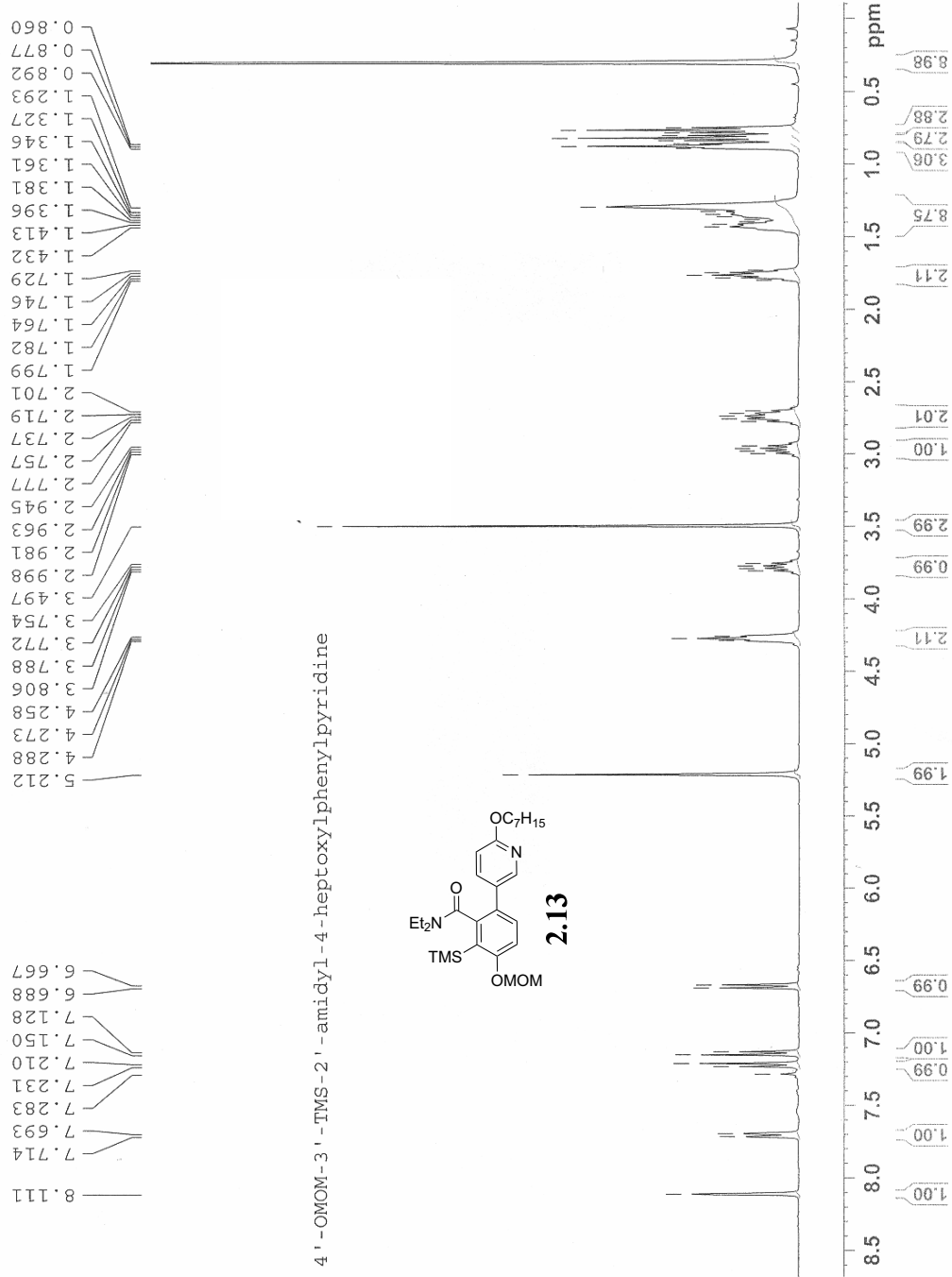
184. M.K. Lakshman; P.L. Kole; S. Chaturvedi; J.H. Saugier; H.J.C. Yeh; J.P. Glusker, H. L.; Carrell, A. K. K.; C.E. Afshar; W. Dashwood; G. Kenniston; ., W. M. B. *J. Am. Chem. Soc.* **2000**, *122*, 629.
185. Wei, G. *Unpublished resuts* **2007**.
186. Benesch, L.; Bury, P.; Guillaneux, D.; Houldsworth, S.; Wang, X.; Snieckus, V. *Tetrahedron Lett.* **1998**, *39*, 961.
187. M. Stiborova; E. Frei; A. Breuer, C. A. B.; H. H. Schmeiser. *Ex. Toxic. Pathol* **1999**, *51*, 421.
188. Wang, X.; Snieckus, V. *Tetrahedron Lett.* **1991**, *32*, 4883.
189. Beaulieu, F.; Snieckus, V. *J. Org. Chem.* **1994**, *59*, 6508.
190. FAMILONI, O. B.; Ionica, I.; Bower, J. F.; Snieckus, V. *Synlett* **1997**, 1081.
191. Gray, M.; Chapell, B. J.; Taylor, N. J.; Snieckus, V. *Angew. Chem., Int. Ed. Engl.* **1996**, *35*, 1558.
192. MacNeil, S. L.; Gray, M.; Briggs, L. E.; Li, J. J.; Snieckus, V. *Synlett* **1998**, 419.
193. Lohse, O.; Beutler, U.; Funfschilling, P.; Furet, P.; France, J.; Kaufmann, D.; Penn, G.; Zaugg, W. *Tetrahedron Lett.* **2001**, *42*, 385.
194. Tan, J. S.; Ciufolini, M. A. *Org. Lett.* **2006**, *8*, 4771.
195. Cai, X.; Snieckus, V. *Org. Lett.* **2004**, *6*, 2293.
196. Champoux, J. *J. Annu. Rev. Biochem.* **2001**, *70*, 369.
197. Gribble, G. W., Ed. *The Alkaloids*; Academic Press: New York, 1990; Vol. 39.
198. Koyama, J.; Morita, I.; Kobayashi, N.; Osakai, T.; Usuki, Y.; Taniguchi, M. *Bioorg. Med. Chem. Lett.* **2005**, *15*, 1079.
199. Hong, B.-C.; Hallur, M.; Liao, J.-H. *Synth. Commun.* **2006**, *36*, 1521.
200. McCubbin, A.; Snieckus, V.; Lemieux, R. *Liq. Cryst.* **2005**, *32*, 1195.
201. Kyba, E. P.; Liu, S. T.; Chockalingam, K.; Reddy, B. R. *J. Org. Chem.* **1988**, *53*, 3513.
202. Bowman, W. R.; Bridge, C. F.; Brookes, P.; Cloonan, M. O.; Leach, D. C. *J. Chem. Soc., Perkin Trans. I* **2002**, 58.
203. Katritzky, A. R.; Abdel-Fattah, A. A. A.; Tymoshenko, D. O.; Essawy, S. A. *Synthesis* **1999**, 2114.

204. Chen, J.; Deady, L. W.; Desneves, J.; Kaye, A. J.; Finlay, G. J.; Baguley, B. C.; Denny, W. A. *Bioorganic & Medicinal Chemistry* **2000**, *8*, 2461.
205. Tu, S.; Jiang, B.; Jia, R.; Zhang, J.; Zhang, Y. *Tetrahedron Lett.* **2007**, *48*, 1369.
206. Nitta, M.; Ohnuma, M.; Iino, Y. *J. Chem. Soc., Perkin Trans. 1* **1991**, 1115.
207. Padwa, A.; Heidelbaugh, T. M.; Kuethe, J. T. *J. Org. Chem.* **2000**, *65*, 2368.
208. Larock, R. C.; Tian, Q. *J. Org. Chem.* **2001**, *66*, 7372.
209. Campo, M. A.; Larock, R. C. *J. Org. Chem.* **2002**, *67*, 5616.
210. Shiao, M.-J.; Liu, K.-H.; Lin, P.-Y. *Heterocycles* **1993**, *36*, 507.
211. Alves, T.; De Oliveira, A. B.; Snieckus, V. *Tetrahedron Lett.* **1988**, *29*, 2135.
212. Rebstock, A.-S.; Mongin, F.; Trecourt, F.; Queguiner, G. *Tetrahedron* **2003**, *59*, 4973.
213. McCubbin, J. A. *PhD. Thesis* 2004.
214. Reed, J. N.; Snieckus, V. *Tetrahedron Lett.* **1983**, *24*, 3795.
215. Mills, R. J.; Snieckus, V. *J. Org. Chem.* **1989**, *54*, 4386.
216. Fraser, R. R.; Bresse, M.; Mansour, T. S. *J. Am. Chem. Soc.* **1983**, *105*, 7790.
217. Larkin, A. L. *MSc. Thesis, Queen's University* **2002**.
218. Comins, D. L.; Jianhua, G. *Tetrahedron Lett.* **1994**, *35*, 2819.
219. Hopkins, G. C.; Jonak, J. P.; Minnemeyer, H. J.; Tieckelmann, H. *J. Org. Chem.* **1967**, *32*, 4040.
220. Nakamura, T.; Kakinuma, H.; Umemiya, H.; Amada, H.; Miyata, N.; Taniguchi, K.; Bando, K.; Sato, M. *Bioorg. Med. Chem. Lett.* **2004**, *14*, 333.
221. Coulson, D. R. *Inorg. Synth.* **1972**, *13*, 121.
222. Gan, W.; Lemieux, R.; Snieckus, V. *Unpublished results* **2007**.
223. Hartley, C. S.; Lemieux, R. *Lab. Invest.* **2003**.
224. Armarego, W. L. F.; Chai, C. *Purification of Laboratory Chemicals, 5th Edition*, 2003.
225. Watson, S. C.; Eastham, J. F. *J. Organomet. Chem.* **1967**, *9*, 165.
226. Grammaticakis, P. *Bull. Soc. Chim. Fr.* **1964**, 924.
227. Coutuner, P. *Compte. Rendu.* **1936**, *202*, 1994.

400 MHz



400 MHz



400 MHz

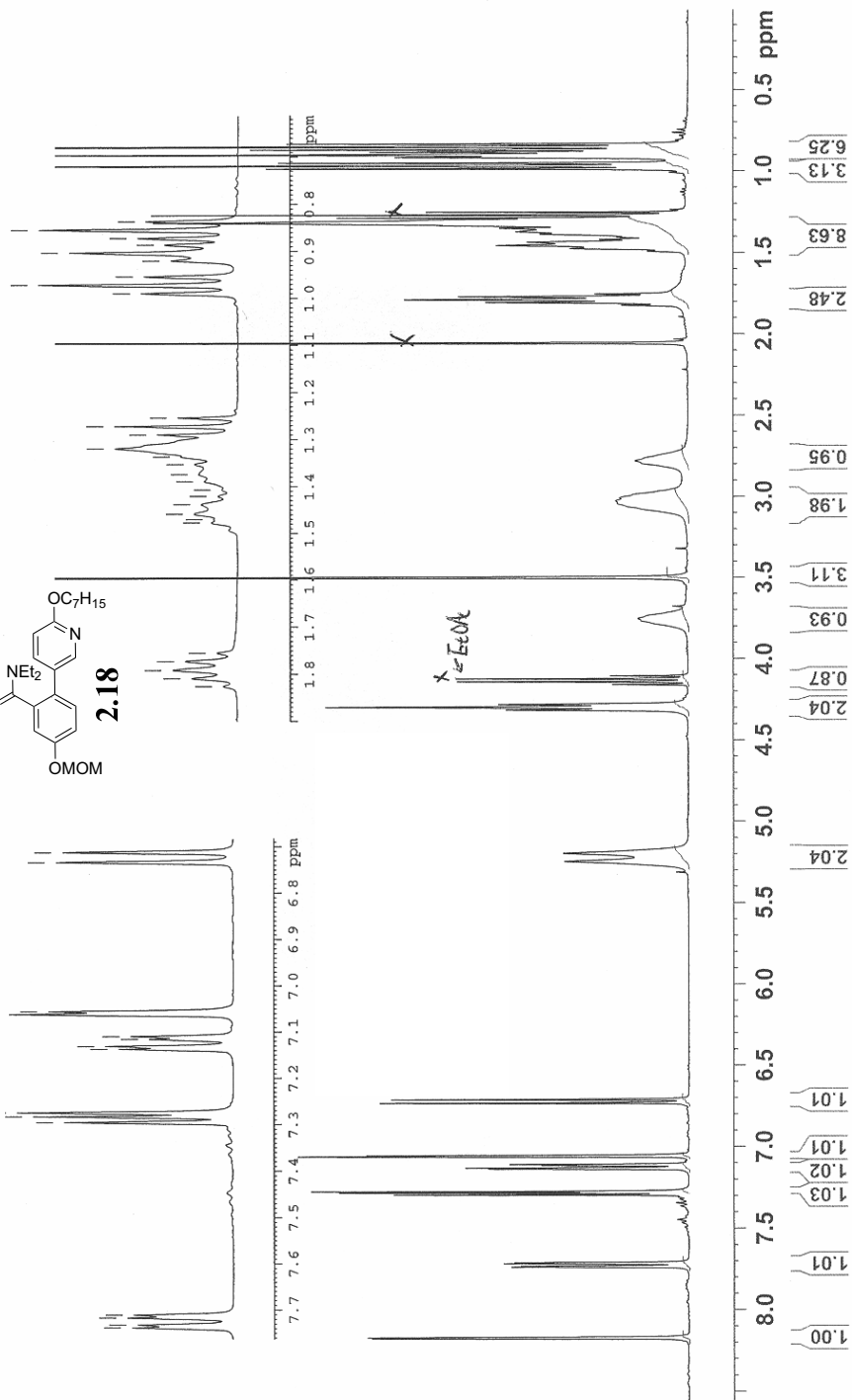
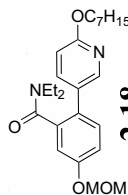
4'-OMOM-2-diethylamidy-4-heptoxyphenylpyridine

0.989
0.971
0.953
0.919
0.902
0.886
0.872
0.854
0.836

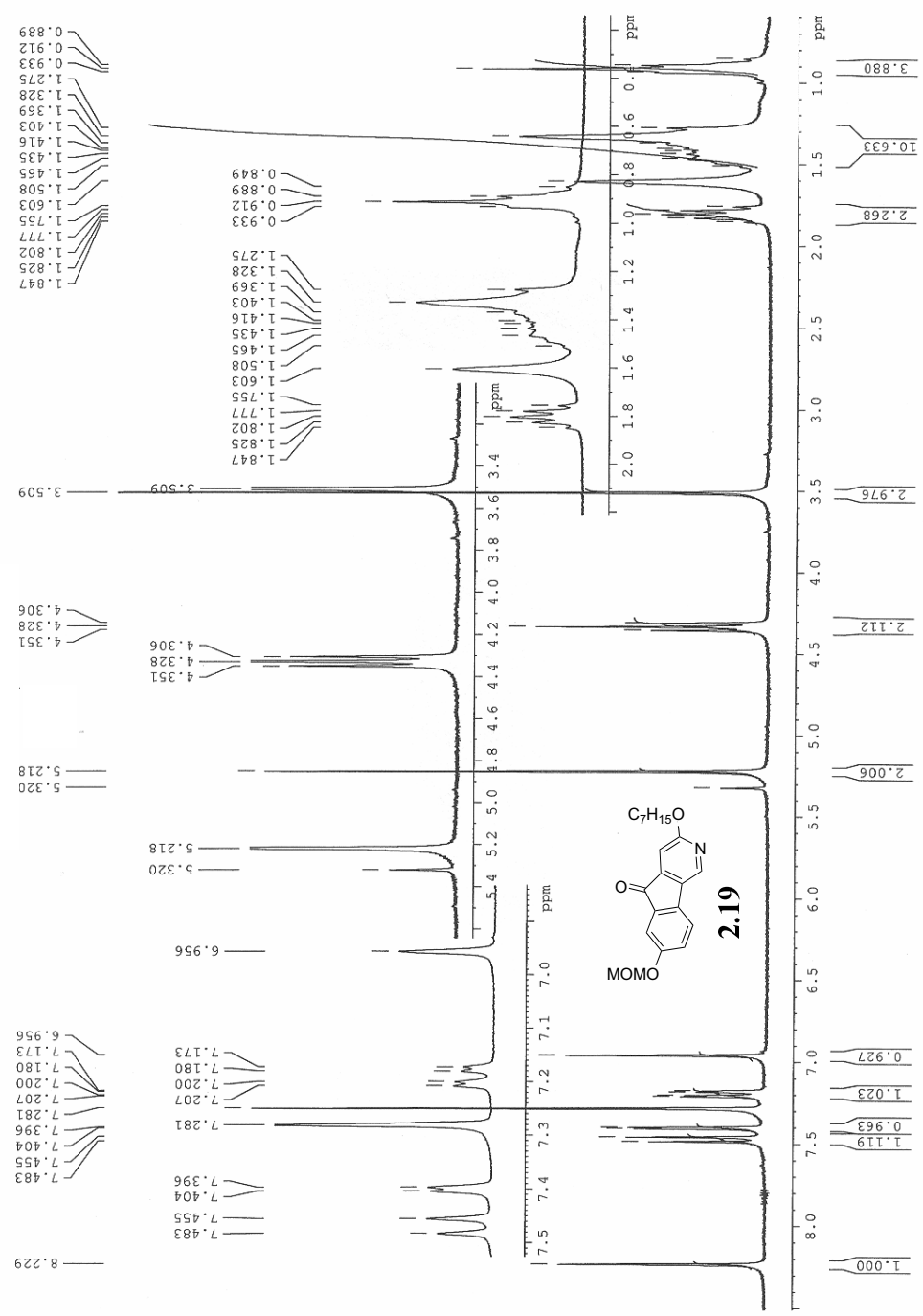
1.253
1.271
1.289
1.319
1.336
1.352
1.373
1.389
1.406
1.420
1.438
1.458
1.469
1.477

1.825
1.808
1.791
1.772
1.754

7.716
7.710
7.294
7.282
7.273
7.136
7.130
7.115
7.108
7.060
7.054
6.733
6.711

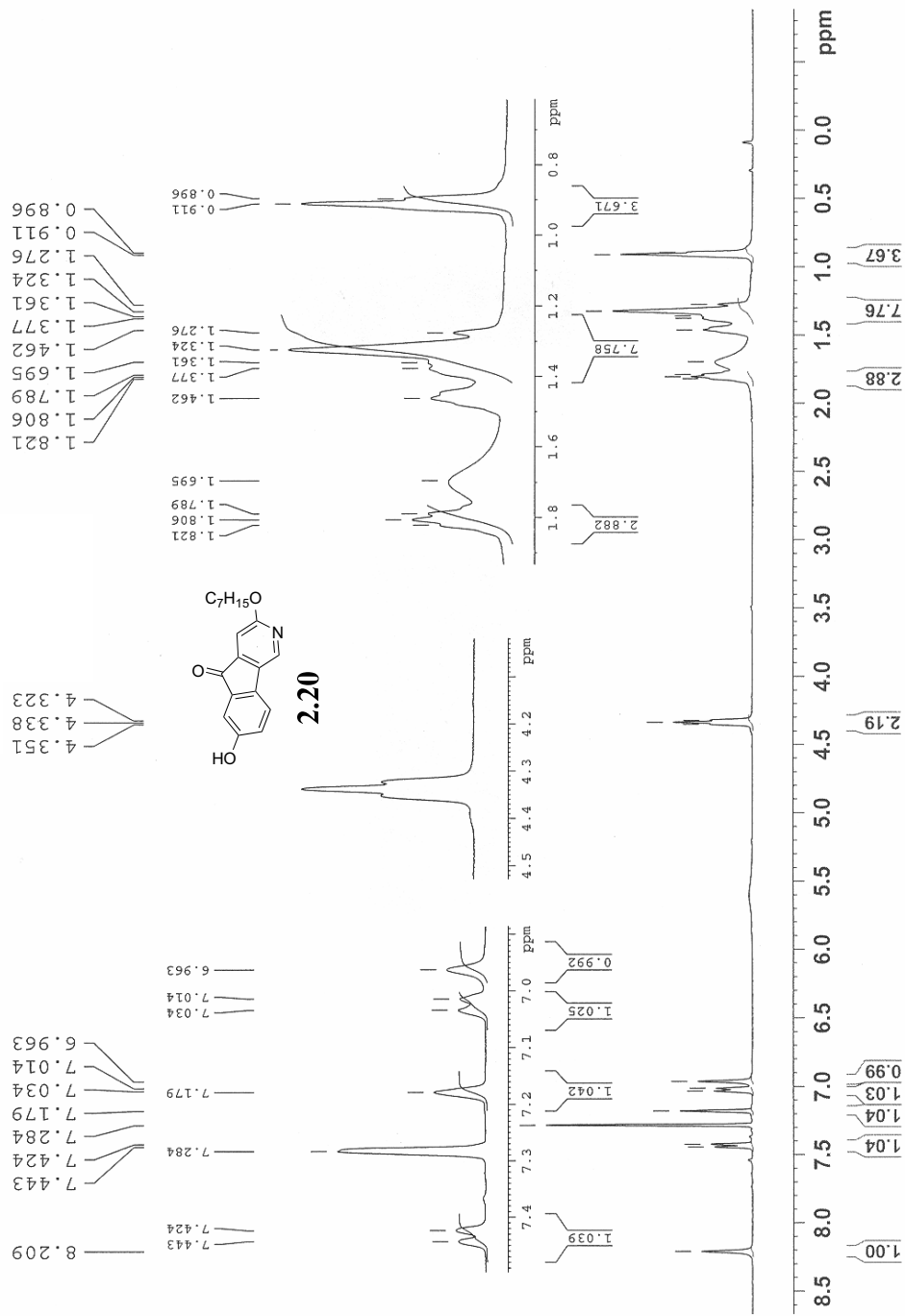


300 MHz

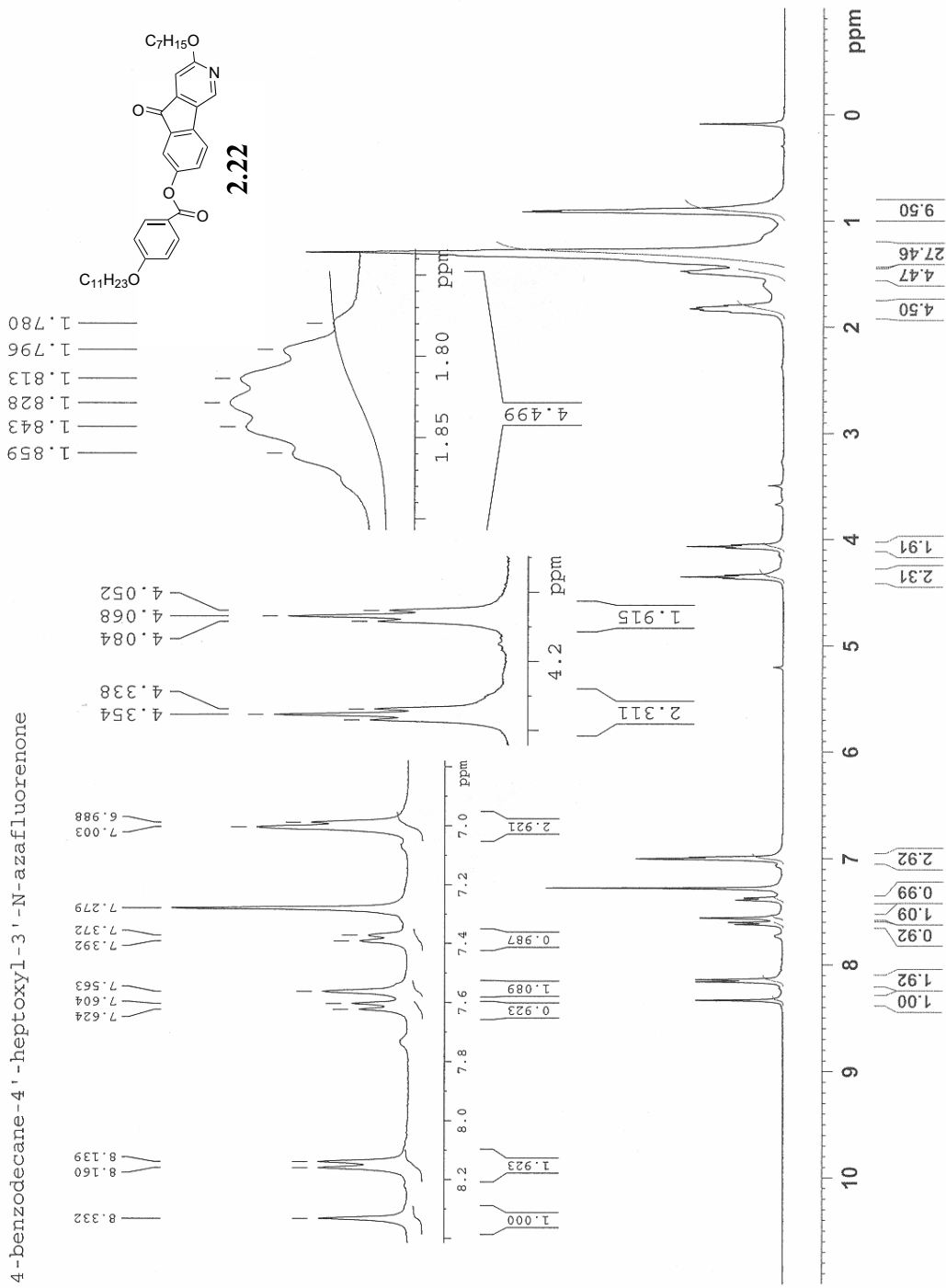


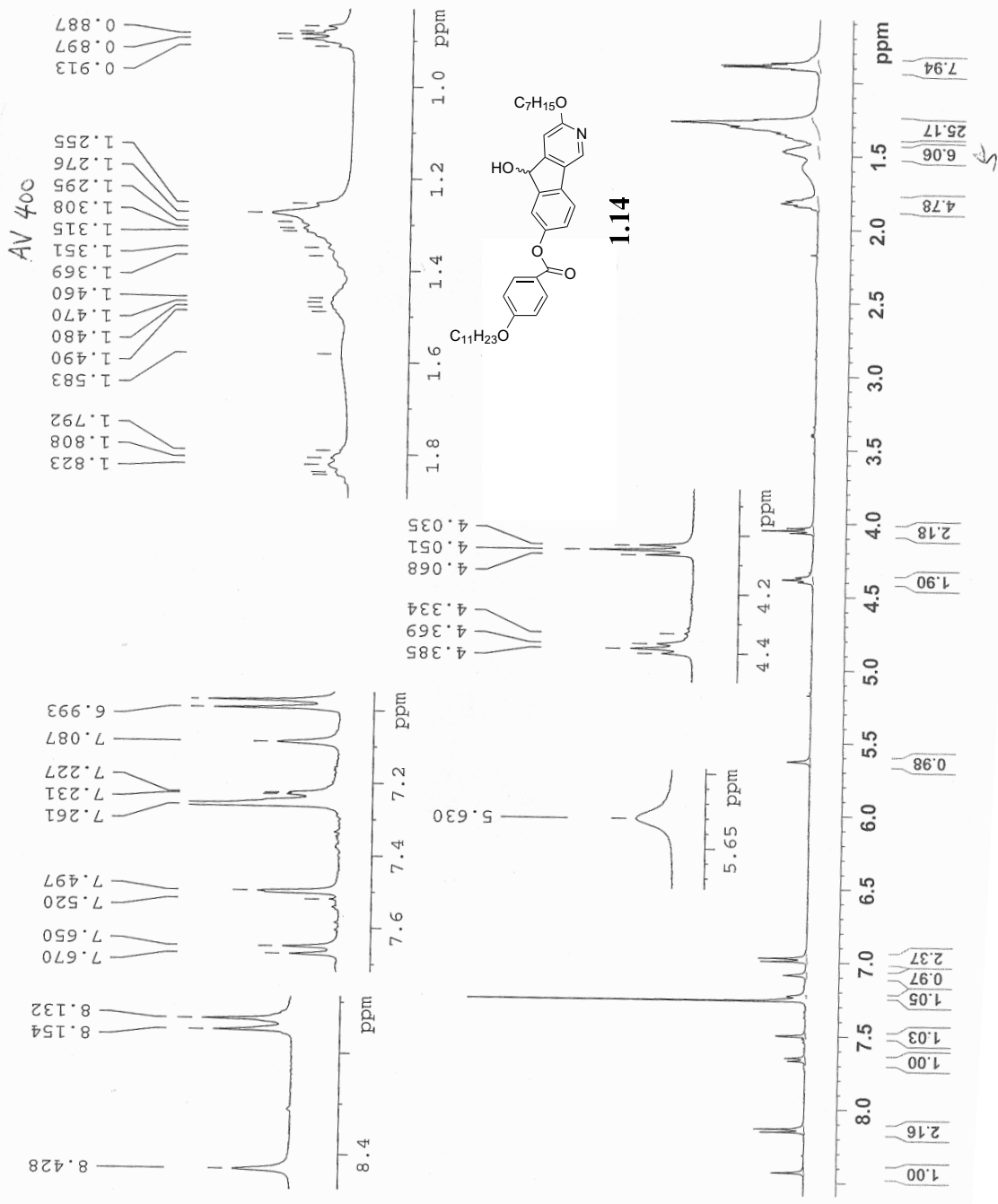
4-OH-3'-N-4'-heptoxylazafluorenone

AV 400

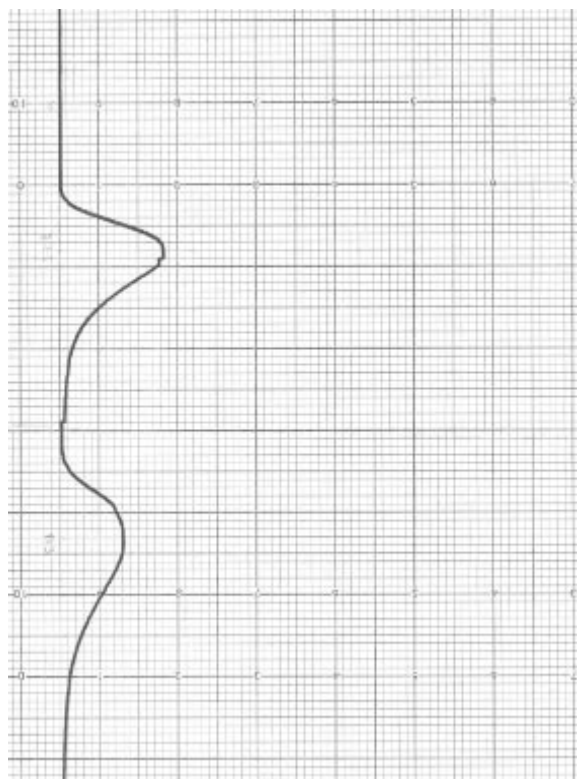


4-benzodecane-4'-heptoxyl-3'-N-azafluorenone





Appendix 2. HPLC Traces of 2.23



2.23